INFORMATION TO USERS

This manuscript has been reproduced from the microfilm master. UMI films the text directly from the original or copy submitted. Thus, some thesis and dissertation copies are in typewriter face, while others may be from any type of computer printer.

The quality of this reproduction is dependent upon the quality of the copy submitted. Broken or indistinct print, colored or poor quality illustrations and photographs, print bleedthrough, substandard margins, and improper alignment can adversely affect reproduction.

In the unlikely event that the author did not send UMI a complete manuscript and there are missing pages, these will be noted. Also, if unauthorized copyright material had to be removed, a note will indicate the deletion.

Oversize materials (e.g., maps, drawings, charts) are reproduced by sectioning the original, beginning at the upper left-hand corner and continuing from left to right in equal sections with small overlaps.

Photographs included in the original manuscript have been reproduced xerographically in this copy. Higher quality 6" x 9" black and white photographic prints are available for any photographs or illustrations appearing in this copy for an additional charge. Contact UMI directly to order.

Bell & Howell Information and Learning
300 North Zeeb Road, Ann Arbor, MI 48106-1346 USA
800-521-0600

UMI®

BIOCHEMICAL CHARACTERIZATION OF

YEAST CELL ADHESION PROTEINS

by

HUI ZHAO

A dissertation submitted to the Graduate Faculty in Biochemistry in partial fulfillment of the requirements for the degree of Doctor of Philosophy, The City University of New York.

2000

This manuscript has been read and accepted for the Graduate Faculty in Biochemistry in satisfaction of the dissertation requirement for the degree of Doctor of Philosophy.

Dec 9, 1999
Date

Chair of Examining Committee

December 17, 1999
Date

Executive Officer

Supervisory Committee

The City University of New York

BIOCHEMICAL CHARACTERIZATION OF YEAST CELL ADHESION PROTEINS

by

Hui Zhao

Advisor: Professor Peter N. Lipke

Studies in cell adhesion of lower organisms could provide information for understanding the more complex adhesion systems in higher organisms. In this work, sexual agglutination, the simplest yeast cell adhesion system, was the subject for studies of conformational properties of the cell adhesion molecule, α-agglutinin and its interaction with its binding ligand, a-agglutinin.

Circular dichroism (CD) and bioassays have been used to investigate the relationship between conformational and functional changes in α-agglutinin under different conditions. Parts of α-agglutinin reversibly switched conformation from β-sheet to α-helix under conditions in which protein inactivation was reversible (pH ≤ 8.5 or temperature ≤ 55°C). Model peptides derived from β-turn-β regions of α-agglutinin mimicked the behavior of the intact protein. Our results strongly implied that conformational switching occurred in some regions of the protein having high helical potential.

Real time interaction of the agglutinins has been characterized using isotopic labeling and Surface Plasmon Resonance ("SPR"). The interaction of the agglutinins had high affinity and a slow dissociation rate. The proteins became more structured upon binding. Kinetic and

CD studies suggested that conformational rearrangements of the agglutinins were involved in the high affinity interaction. Hydrophobic interactions at the interface of the protein complex stabilized the conformation of the proteins.

Point mutations in domain III of α-agglutinin reduced the secretion of α-agglutinin. Moreover, the mutated α-agglutinin was more sensitive to protease digestion. The purified mutated α-agglutinin, however, had similar structural and functional properties as that of wild type protein. Our results implied that the point mutations led to misfolding of α-agglutinin, so that the protein could not be secreted properly.

ACKNOWLEDGEMENTS

I would like to thank many people who have made this work successful.

First and foremost, I want to thank my advisor Dr. Peter Lipke for his scientific guidance and encouragement throughout the years working in his laboratory.

To my colleagues in the lab for their technical assistance and suggestions.

To Dr. Peter Kahn for his collaboration and useful advice throughout the course of this work.

To Dr. Janet Kurjan, Dr. Hans de Nobel and Jeremy Pike for providing invaluable suggestions.

To the members of my thesis committee: Dr. Laurel Eckhardt, Dr. Gary Quigley and Dr. Dan Eshel for their encouragement and advice.

To my parents, my sister and her family for their understanding, patience and support throughout the years.

Table of Contents

List of Tables

List of Figures

Chapter I

General Introduction

I. Mating Type Control and the Life Cycle of *Saccharomyces cerevisiae*

The yeast *Saccharomyces cerevisiae* has three cell types: two haploids (a and α) and one diploid (a/α) which play distinct roles in the life cycle. Determination of diploid or haploid cell type is controlled by a single mating type locus, *MAT*. Cells with the α allele (*MATα*) exhibit the phenotype of α cells; cells with **a** allele (*MAT**a***) exhibit the phenotype of **a** cells, and cells with both alleles (*MATa/α*) exhibit the a/α cell (diploid) phenotype. Each cell type expresses a set of their own genes: haploid **a** or α cell-specific genes are only expressed in *MATa* or *MATα* cells, respectively; while diploid a/α cell specific genes are expressed only in *MATa/α* cells (Cross et al., 1988). The *MAT* locus is a regulatory genes controlling cell division, mating and sporulation in the life cycle of *S. cerevisiae* (Hartwell et al., 1985). For example: *MATα* encodes two proteins: *MATα1* and *MATα2* (Herskowitz 1988). *MATα1* is a positive regulator of α-specific genes, allowing their expression only in α cells. *MATα2* is a negative regulator of a-specific genes, preventing their expression in α cells. The presence of *MATa/α* in diploid cells leads to the expression of diploid feature genes and the suppression of genes for haploid cells (Herskowitz 1988).

The life cycle of *S. cerevisiae* includes two main aspects: cell proliferation and cell type transitions between haploid and diploid cells. *Saccharomyces cerevisiae* buds asymmetrically to produce daughter cells (Drubin and Nelson 1996). Genotype and nutritional conditions determine the pattern of budding. *MATa* and *MATα* cells bud adjacent to the previous bud site in a axial budding pattern; *MATa/α* cells bud either near the previous bud site or at the opposite end of the cell in a bipolar budding pattern (Chant

and Pringle 1995). When yeast cells undergo pseudohyphal growth, they always bud from the same pole in a unipolar budding pattern (Kron et al., 1994).

Haploid **a** and α cells mate to produce diploid a/α cells (Figure 1). Each haploid cell type has its own specific genes for mating. For example: *STE3, STE13, MFα, MFα2 and Agα1* are α-specific genes in α cells and *STE2, STE6, STE14, STE16, MFA1, MFA2 and AGA2* are **a** specific genes in **a** cells (Nakayama 1988; Herskowitz 1989). When haploid cells of opposite mating type are close to each other, sex pheromones secreted by their mating partners arrest their cell cycle in G1 phase (Sprague et al., 1983; Herskowitz 1988). Specific genes for mating are turned on, which leads to formation of diploid cells (Herskowitz 1988). When diploid cells are under nutritional starvation, they undergo sporulation and form haploid **a** and α cells (Figure 1).

II. Sexual Agglutination is a Prelude for Mating

Sexual agglutination takes place before cell and nuclear fusion and is a prelude for mating. **a**- and α-Agglutinin are the complementary molecules responsible for sexual agglutination (Figure 2). Interaction of the agglutinins brings cells of opposite mating type into close apposition, which promotes stable cell-cell contact leads to cell fusion and increases mating efficiency (Weinstock and Ballou 1986; Lipke et al., 1989; Roy et al., 1991). The sexual agglutinability of each cell types is regulated by the sexual pheromones secreted by its mating partners (Terrance and Lipke 1981).

Sexual agglutination has been studied in four yeast species: *H. wingei, P. amethionina, S. kluyveri and S. cerevisiae*. It is highly species specific (Lipke & Kurjan 1992). Cells of one yeast species are unable to agglutinate with cells of another species. Such a situation is an analogous to many cellular adhesion events, such as binding of

Figure 1. Life Cycle of *S.cerevisiae*. Haploid **a** and α cells (*MATa* and *MATα*) mate to form diploid (*MATa/α*) cells. When diploid cells are starved, they undergo meiosis to form haploid a and α cells spores. All three types of cells proliferate to produce their daughter cells by mitotic cell division.

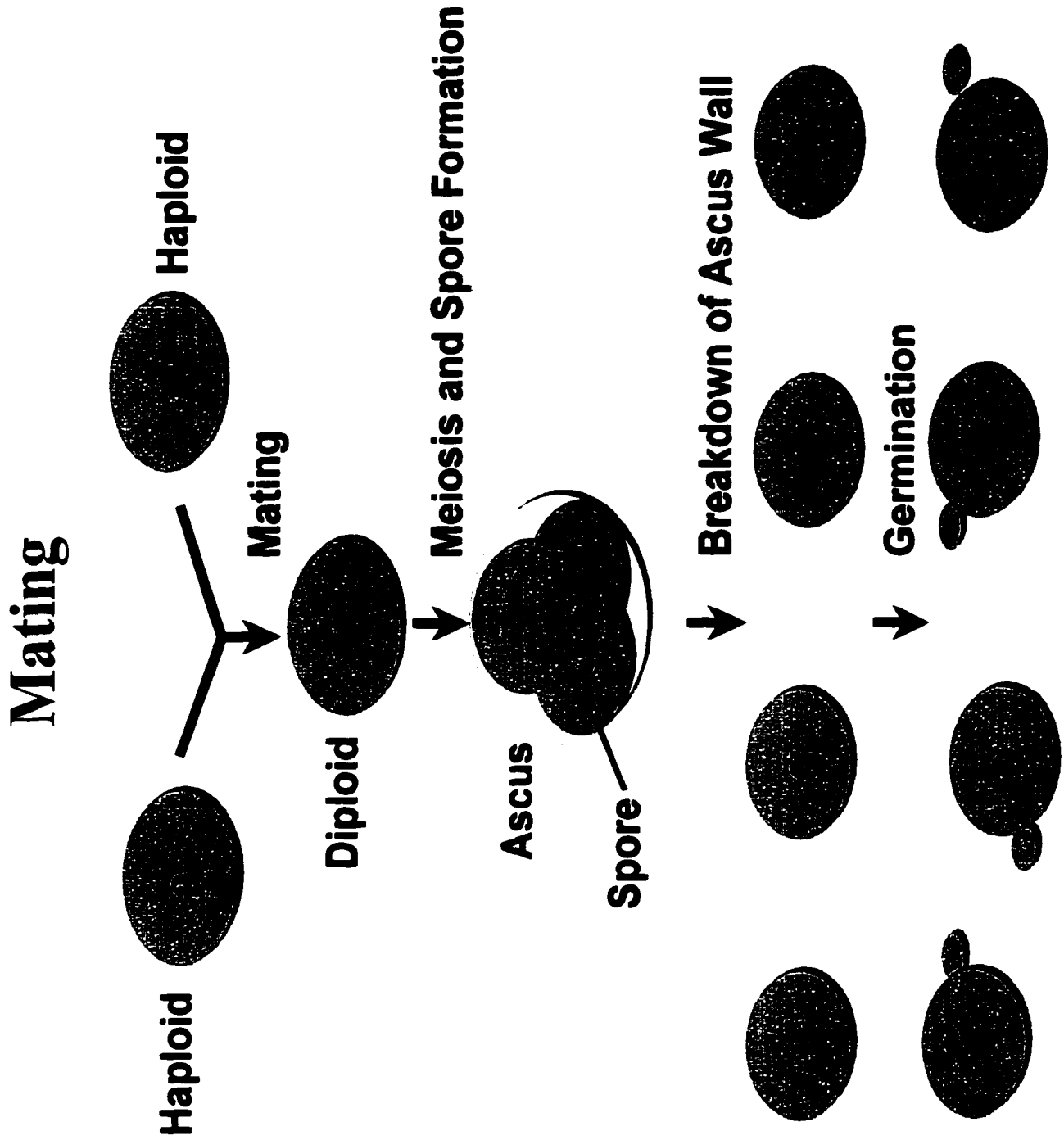

Figure 2. Sexual Agglutination in Budding Yeast. The interaction of a and α-agglutinin, expressed on the surface of haploid **a** and α cells is called sexual agglutination. a-Agglutinin is highly glycosylated, consisting of two subunits attached by two disulfide bonds. The small subunit Aga2p is the adhesive domain and the anchorage subunit Aga1p mediates cell surface anchorage of the protein on the cell wall (Lipke and Kurjan 1992). α-Agglutinin is a highly N- and O-glycosylated single polypeptide. The N-terminal half of the protein is responsible for its adhering to a-agglutinin and its C-terminal is responsible for its anchorage on the cell wall (Reprint from Lipke and Kurjan 1992).

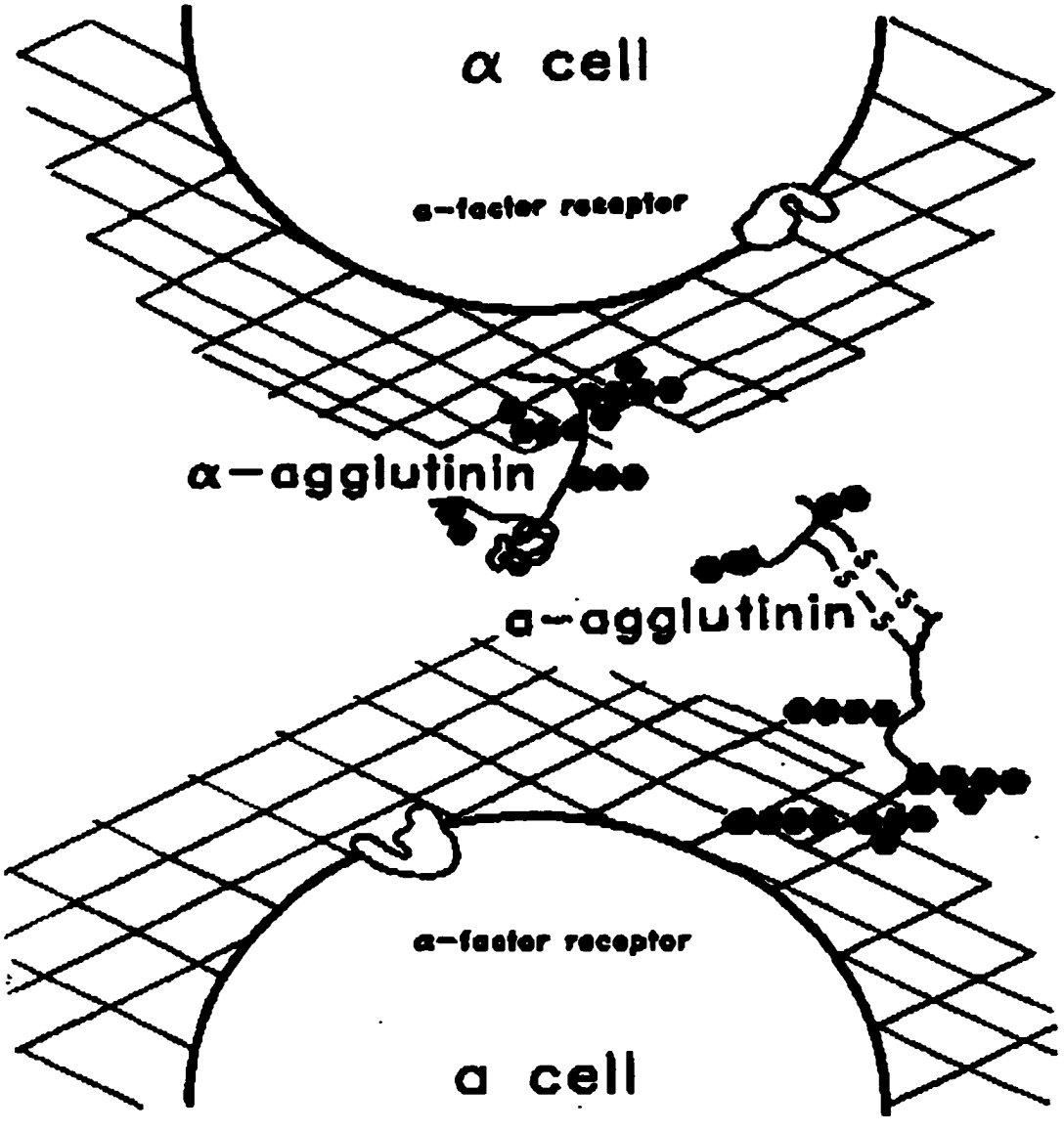

bacteria, viruses, and other pathogens to their cellular hosts; binding of pollen to the plant stigma; and binding of sperm to unfertilized eggs (e.g., sea urchin, abalone, Xenopus and mammals) during fertilization (Wassarman 1999). Like the agglutinins in sexual agglutination, corresponding complementary cell adhesion molecules on the cell surfaces are involved in each of these cell adhesion events.

III. Sexual Agglutination is a Simple Cell Adhesion System

i. Cell Adhesion in General

Cell adhesion was first identified in sponges in 1907 (Wilson 1907). Since then, cell adhesion has been found to be critical for cellular function and organism survival. It is seen in processes such as: inflammation, cell growth, proliferation, gene regulation, differentiation, apoptosis and migration (Juliano and Haskill 1993; Ruosahti and Reed 1994; Gumbiner 1996).

Cell adhesion systems have similar structural and functional roles throughout the eukaryote kingdom. In 1957, Moscona first found mammals and birds share similar molecular characteristics and binding sites for cell adhesion (Moscona 1957). Later, more cell adhesion molecules in higher eukaryotes were found to share structural and functional similarities to lower organisms. However, structural flexibility of each individual cell adhesion molecules determines the specific binding characteristics of the proteins.

Cell adhesions in higher organism are mediated by multiple systems. Study of cell adhesion in lower organisms could provide information for understanding the complexity of the adhering systems in higher organisms. For example: *Drosophila melanogaster* is one of the model systems to study cell adhesion. This system contains major classes of

cell adhesion molecules including Notch/Delta, immmunoglobulin homologs, fasciclin IV, Fasciclin I, Leucine-rich repeat proteins (LRRS), cadherins, integrins, etc (Corbin et al., 1991). *C. elegans* has simpler cell adhesion systems than *Drosophila*. In this system, adhesions of the neighboring cells are required for the determination of cell fate. Sexual agglutination in *S. cerevisiae*, a unicellular eukaryote, could be the simplest model cell adhesion system for both fungi and mammals. For example: α-agglutinin is a member of the immmunoglobulin superfamily (Figure 3). It has sequence similarities to cell adhesion molecules in the *ALS* family in yeast *Candida albicans* (Figure 4) and other members in the Ig superfamily, which is one of the major classes of cell adhesion molecules in mammalian systems.

ii. Structural Characteristics of Cell Adhesion Molecules

Cell adhesion molecules are usually glycoproteins that mediate cell-cell and cell-extracellular matrix recognition at the extracellular surface (Gumbiner 1996). Most cell adhesion molecules have similar conformations in their adhesive domains. For example: the adhesive domains of cadherin, Immonogolublin like, fibronectin type III and EGF are predominantly β-sheet structures. The common motif involved in cell adhesion is the Greek key barrel structure containing one or two anti-parallel β sandwiches (Vaughn and Bjorkman 1996).

Ig-like domains are a major class of Greek key barrel domains. They have sequence similarities to the variable or constant domain of antibodies containing seven to nine anti-parallel β strands (Williams and Barclay 1988). The anti-parallel β sheets form a 3-D β-barrel. Ig-like domains are stabilized by hydrophobic core and disulfide bonds

Figure 3. Structural Composition of α-Agglutinin. The N-terminus of α-agglutinin has three sequential Ig domains with N-glycosylation site indicated. Hydrophobic interactions and indicated disulfide bonds stabilize the domains. The C-terminal part of the protein is Ser- and Thr- rich and highly N- and O-glycosylated as indicated (Reprint from Chen et al., 1995).

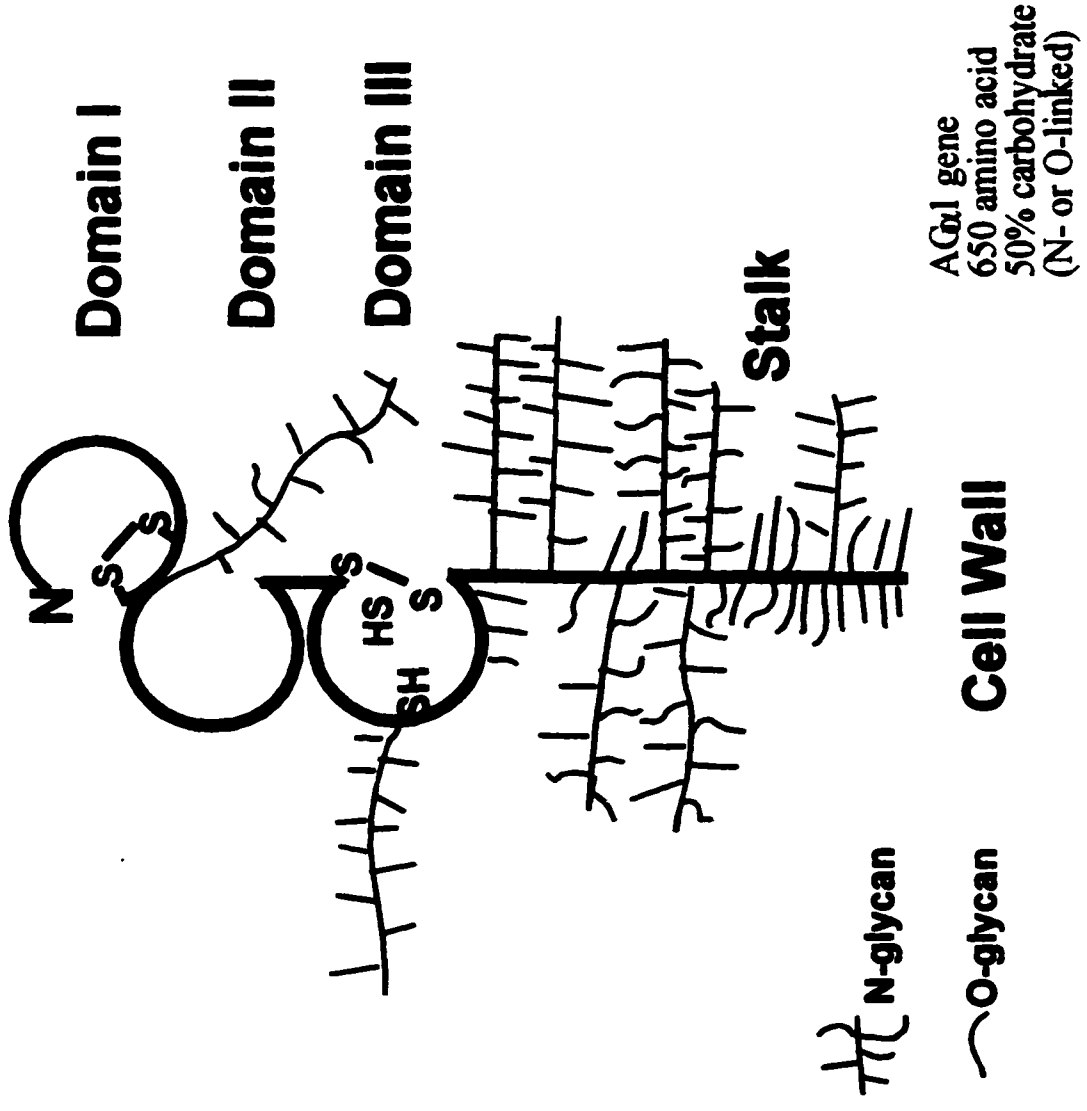

Figure 4. Sequence Alignment of AGα1^{350} to ALS1. AGα1^{350} was aligned with the N-terminal 350 amino acids of ALS1 using the GCG Bestfit program. BestFit is a program in the Wisconsin Sequence Analysis Package (TM) for identifying the best region of similarity between two sequences whose relationship is unknown. The paired output file from this program displays sequence similarity by printing one of three characters between similar sequence symbols: a straight line (|), a colon (:), or a period (.). Straight lines are put between symbols that are the same, colons are put between symbols whose comparison value is greater than or equal to 0.50, and periods are put between symbols whose comparison value is greater than or equal to 0.10. AGα1^{350} and ALS1 have 25.5% identity and 49.8% similarity. Potential O-glycosylation (♦) and N-glycosylation sites (*) in AGα1^{350} are marked.

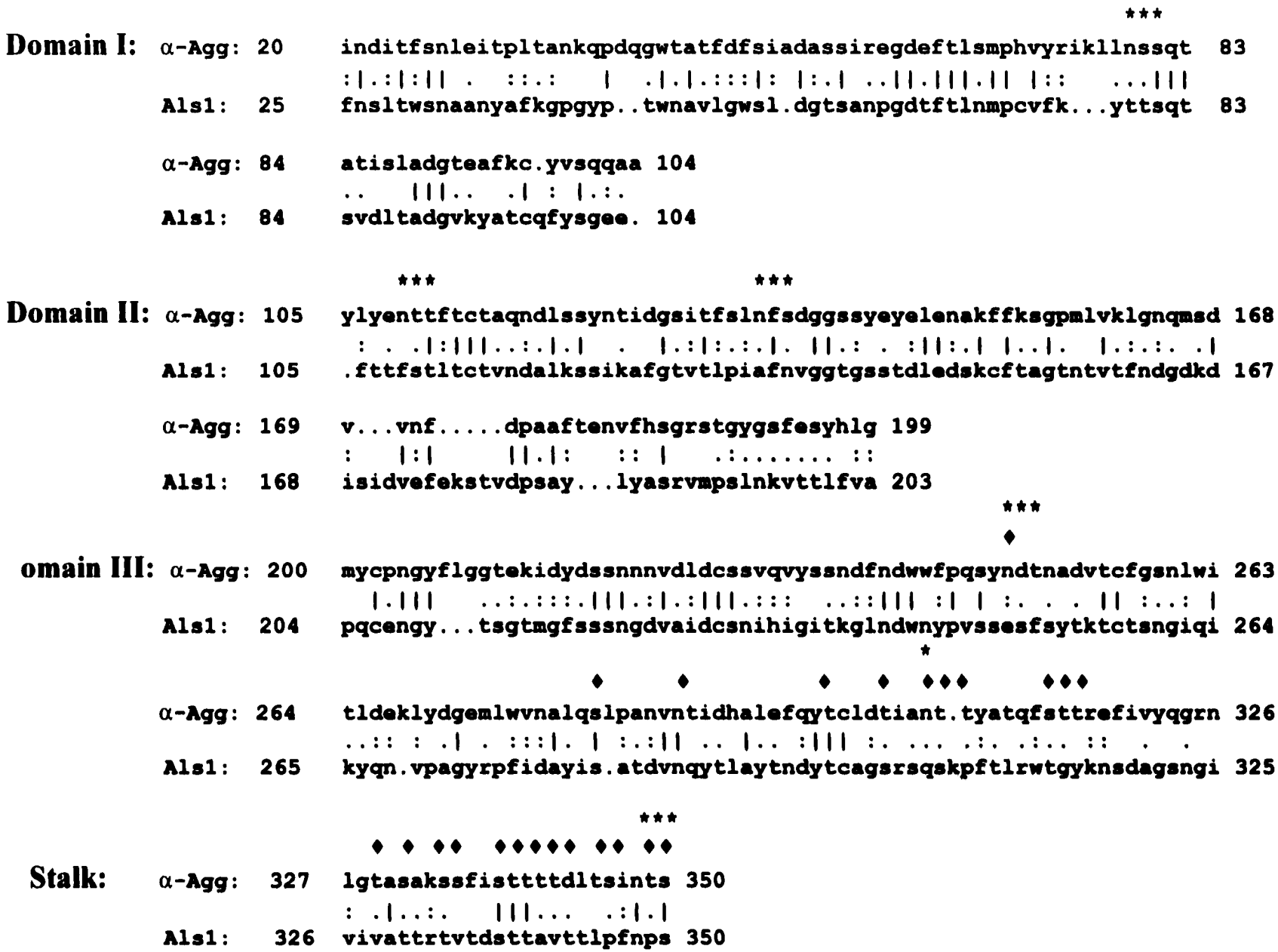

(Williams and Barclay 1988). They are divided into two major sets: Ig C-like and Ig V-like domains (Bork et al., 1994).

Ig C-like domains contain seven β strands arranged into two anti-parallel β-sheets: one consists of strands A, B, E and D, and the other one consists of strands G, F and C (Figure 5). Ig V-like domains contain nine β strands (Figure 5). The folding of Ig V-like domains is similar to the Ig C-like domains, except two more β strands, C' and C", are added in the extended GFC sheet.

The central portion of each β-sheet, the B, E and C, F β-strands, forms the structurally conserved core of the Ig fold. The edge of the sheets is conformationally flexible and the non-central strands can be shifted structurally between different sheets within the domains (Bork et al., 1994). This flexibility allows molecules on different cells to adopt the specific conformation required for specific adhesive binding (Recny et al., 1990; Politou et al., 1994; Huber et al., 1994). Therefore, even though Ig-like domains in cell adhesion molecules share conserved conformational features, they have functional diversities. They can bind to ligands varying from small peptides to hormones, or giant proteins with different binding modes (van der Merwe and Barclay 1996).

iii. Functionally Related Structural Characteristics of Cell Adhesion Molecules

Cell adhesion molecules have functional diversity. Interaction of cell adhesion molecules could be homophilic or heterophilic protein-protein interactions or protein-carbohydrate interactions. Structural changes of the cell adhesion molecules are often related to their functional properties (Dustin and Springer 1989; Shapiro et al., 1995; Jones 1996)

Figure 5. 2D and 3D Topology Diagrams of Ig Domains. Ig constant domain (Ig C) consists of seven anti-parallel β strands (A, B, C, D, E, F, G) which form a sandwich of two β sheets (Sheet I: A-B-E-D (2D: thick arrow; 3D: front); Sheet II: G-F-C (2D: thin arrow; 3D: back). Ig variable domain (Ig V) contains two additional strands (C' and C") between strands C and D compared to that of Ig C domain (Sheet I: A-B-E-D (2D: thick arrow; 3D: front); Sheet II: G-F-C-C'-C" (2D: thin arrow; 3D: back) (Vaughn and Bjorkman 1996).

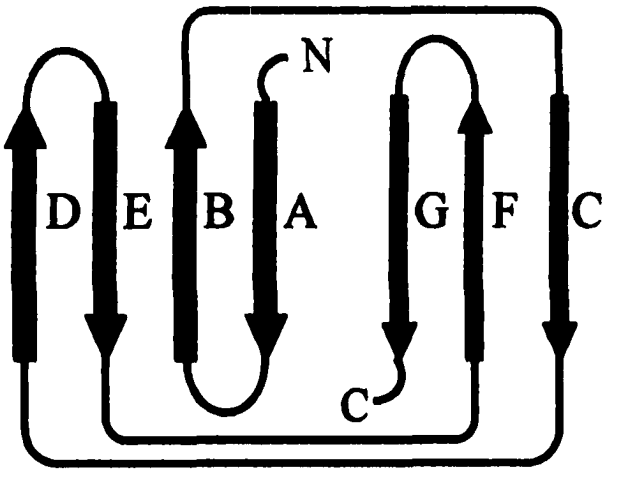

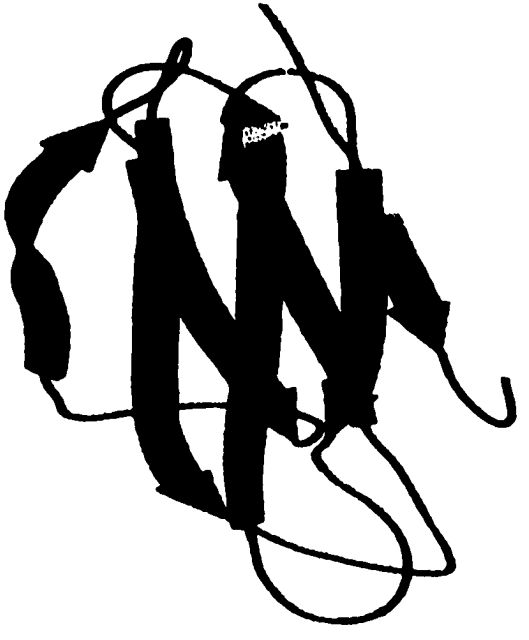

Ig C Domain

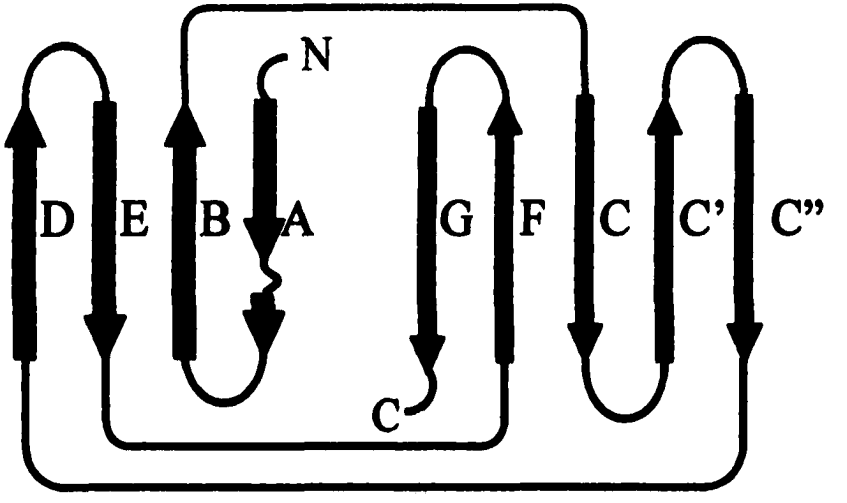

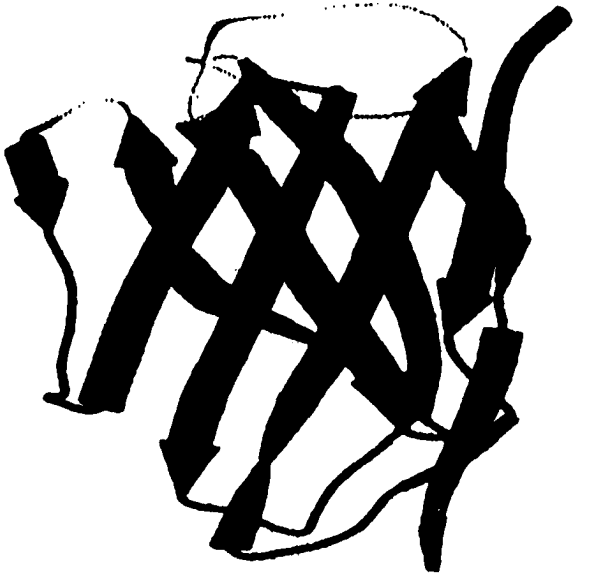

Ig V Domain

a. Homophilic Protein-Protein Interactions

e.g. Cadherins

Cadherins are transmembrane Ca^{2+}-dependent homophilic adhesion molecules (Takeichi 1991). Cadherins are responsible for maintenance of the junctions between similar cells in tissues. Cell-cell adhesion is mediated through the N-terminal domain of the cadherins (Nose et al., 1990). It contains five similar extracellular domains EC1 to EC5 (Gumbiner 1996). X-ray crystallographic studies in N-cadherin showed that EC1 domain forms a dimer, in which the monomers are oriented in parallel with their adhesive binding surface pointing outward from the plasma membrane (Shapiro et al., 1995; Nagar et al., 1996). The monomer units of EC1 domains interact with each other in an antiparallel way, using their adhesive binding surfaces and forming a β-barrel structure (Shapiro et al., 1995). A putative interface of the interaction was suggested to have both hydrophobic and polar/charged character that mimics the interface of the interaction of immunoglobulin domains with one another in the Ig superfamily (Jones 1996).

b. Heterophilic Protein-Protein Interactions

e.g. Integrins and Integrin Ligands

Binding of the integrins to various cell surface receptors and extracellular matrix ligands is a major class of heterophilic protein-protein interaction in cell adhesion systems (Humphries 1996). Upon binding to soluble fibrinogen, the integrin αIIbβ3 is converted to a high affinity binding state (Ginsberg et al., 1992; Ekblom and Timpl 1996). The conformational changes of the integrin induced by ligand binding in this case are critical for its adhesive activity (Gumbiner 1996). Binding of a T-cell receptor can

also modulate the binding affinity of the integrin, leukocyte function associated antigen-1 (LFA-1), to its receptors such as ICAM-1 or ICAM-2 (intercellular cell adhesion molecule). Binding of ICAM-1 can further induce conformational changes of LFA-1 (Dustin and Springer 1989; Cabanas et al., 1993). The adhesive binding site of the protein is located in the C-terminal of LFA-1 based on X-ray crystallographic study (Qu and Leahy 1995).

A tripeptide, arginine-glycine-aspartic acid (RGD), is a common integrin ligand binding motif (Ruoslahti and Pierschbacher 1987; Main et al., 1992). For example, the integrin binding ligand type III module of fibronectin has a Greek key barrel structure, whose RGD motif, located at the apex of the loop connecting F and G β strands, mediates adhesion (Krammer et al., 1999). Straightening of the RGD-loop into a more linear fluctuating conformation by unfolding reduces the accessibility of the loop to the surface bound integrins, and therefore decreases the affinity and selectivity of binding (Krammer et al., 1999).

c. Protein-Carbohydrate Interactions

The selectins are important in lymphocyte and neutrophil interaction with vascular endothelium (Jones 1996). The selectins are adhesion molecules that bind to carbohydrates. There are not yet any direct structural data on the binding of selectins to carbohydrates. The selectins binds carbohydrates with low affinity and have very fast on and off rates (Alon et al., 1995).

IV. Functionally Related Conformational Changes of the proteins

Many mechanisms for protein function require conformational changes. For example: conformational changes in the amyloid and prion proteins are involved in

diseases such as scrapie, bovine spongiform encephalitis, and, possibly Creutzfeld-Jacob and Alzheimer's diseases (Prusiner 1991). Heparin-induced conformational changes in microtubule-associated protein tau expose new phosphorylation sites in tau, which could also cause Alzheimer's diseases (Paudel and Li 1999). Conformational changes in viral fusion proteins are essential in promoting fusion of the virus and the target cell membranes. For example: Binding of CD4 glycoprotein to the HIV exterior envelop protein gp120 induces conformational changes in gp120 next to its binding site, which initiates a fusion of the viral and cellular membranes (Kwong et al., 1998).

i. High Affinity Interactions vs Conformational Changes

a. High Affinity Interactions

High affinity interactions are those characterized by having K_D of 10^{-8} M to 10^{-10} M. For example, integrins bind antibodies with K_D of 10^{-10} M (Barbas et al., 1993), Tumor Necrosis Factor (OX40) binds to activated mouse T cells with K_D of 2-4 $X10^{-10}$ M (Al-Shamkhani et al., 1997), α-platelet-derived growth factor receptor (α-PDGFR) binds to platelet-derived growth factor with K_D of 7 X 10^{-9} M (Mahadevan et al., 1995), while HIV core protein p24 binds to its antibody with K_D of 2 X 10^{-8} M (Glaser and Hausdorf 1996). Chaperonin binds to its substrate protein with K_D of 10^{-9} M (Murai et al., 1995). Proteinase binds to proteinase-inhibitor with K_D of 3.1 X 10^{-9} (Yang et al., 1994). Decorin, a component of the extracellular matrix of many tissues, binds to the complement component C1q with a K_D of 5 X 10^{-8} M (Ramamurthy et al., 1996), while SH2 domains of Src and Lck bind to a variety of phosphopeptides in the signal transduction pathway with K_D of 3.7 X 10^{-9} M (Payne et al., 1993).

b. Protein Conformational Changes Result in High Affinity Interactions

High affinity interactions are often related to conformational changes of the proteins. For example, the binding of the RDG binding motif in fibrinogen induces formation of a high affinity fibrinogen-binding state in integrins (Phillips et al., 1991; Du et al., 1991). Binding of ICAM-1 induces conformational change of LFA, which results in a high affinity interaction of LFA with ICAM-1 (Dustin and Springer 1989; Cabanas et al., 1993). IGF-I induced conformational changes in both growth factor and growth factor-I receptor results in high affinity interactions of the proteins (Jansson et al., 1997). When an integral plasma membrane protein, CD36, binds to thrombospondin (TSP) triggers a conformational change in TSP to expose a high affinity binding site, which results in a high affinity interaction (Leung et al 1992). A slow structural rearrangement next to the binding site of HIVp24 results in high affinity interaction between HIV core protein p24 and its antibody (Glaser and Hausdorf 1996). A major conformational rearrangement occurs in IgE upon binding to its high affinity receptor in allergic reactions (Sechi et al., 1996).

ii. Conformational changes at the Interfaces of Binding Complexes

Conformational changes on complex formation have been studied using 39 pairs of structures of protein complexes and unbound equivalents, averaged over interface and non-interface regions and for individual residues by molecular modeling (Betts and Sternberg 1999). Movements of main chains and side chains in the interface are closely related to the complex formation. However, movements of exposed non-interface residues are caused by flexibility and disorder (Betts and Sternberg 1999).

Larsen et al. compared protein-protein interaction interfaces among 136 homodimeric proteins available from the Protein Data Bank. Hydrophilicity of these interfaces is variable. One-third of them are stabilized by a hydrophobic core with a large hydrohobic piece surrounded by a circle of polar interactions (Larsen et al., 1998). However, the remaining two-thirds have mixed hydrophilic and hydrophobic character, with small hydrophobic pieces, polar interactions and water molecules scattered over the entire interface area (Larsen et al., 1998). High affinity protein-protein interactions, such as protease-substrate and antibody-antigen, depend on a good fit of the hydrophobic interface, where the proteins adopts precise shapes complementary to each other (Koshland and Neet 1968; Rini et al., 1992). Such complementarity maximizes the contribution of van der Waals contacts, which are energetically favorable (Creighton 1993). However, low affinity interactions with micromolar K_D, such as: CD2 to CD58 (LFA-3), often have poor shape complementarity at interfaces and are stabilized by hydrogen bond formed from side chains and salt links of charged amino acid (Wang et al., 1999; Ikemizu et al., 1999).

iii. Transition from Unstructured to Structured Conformation upon Binding

Conformationally unstructured regions in proteins are regions which are not tightly packed and are highly mobile (Dunker et al., 1998). These unstructured regions mediate binding diversity of the proteins and play important roles in molecular recognition by becoming structured upon ligand binding (Anderson et al., 1979, Frankel and Kim. 1991; Spolar and Record 1994; Zhang and Tanake 1995; Weinreb et al., 1996; Daughdrill et al., 1997). Well characterized unstructured to structured transitions upon

Unstructured to structured conformational transitions enable alternative packing arrangements of binding partners, which lead to high affinity interactions (Dunker et al., 1998). These transitions have significant kinetic implications by controlling on and off rates. Proteins that have higher flexibility could have faster dynamic searches for the appropriate orientation (Dunker et al., 1998).

V. Characteristics of the Sexual Agglutinins

As mentioned earlier, **a**- and α-agglutinin are cell wall glycoproteins responsible for sexual agglutination. Deglycosylation of α-agglutinin with Endo H does not affect the binding activity or agglutination ability of the protein (Terrance et al., 1987). The N-terminals of the proteins are synthesized with secretion signals, which are removed during the maturation process (Hauser and Tanner 1989). The agglutinins are transported to the cell surface via a secretory pathway (Figure 6). The C-terminal regions of the proteins are rich in Ser/Thr and contain a hydrophobic anchorage domains for the attachment of glycosyl phosphatidylinositol (GPI) anchors (Hauser and Tanner 1989; Wojciechowicz et al., 1989; Roy et al., 1991; Lipke and Kurjan; Lu et al., 1995). The agglutinins are synthesized and glycosylated in the endoplasmic reticulum (ER) and transported to the cell membrane via a GPI anchor. GPI anchoring is a transient stage during transportation of the agglutinins from the cell membrane to the cell wall, where the cell wall glycans anchor the proteins (Figure 6) (Lipke and Kurjan 1992; Van Berkel et al., 1994; Lu et al., 1994).

"Figure 6. A model of Transportation of the Agglutinins to Cell Wall. After translation, the agglutinins are translocated into the endoplamic reticulumum (ER), where the secretion signal is cleaved and protein glycosylation occurs. The C-terminal hydrophobic sequence is then cleaved and the GPI anchor is attached. The agglutinin is transported through the secretory pathway bound to the GPI anchor, with further glycosylation occurring in the Golgi complex. The agglutinins are then transferred from the GPI anchor to cell wall glycans. The mature agglutinin is anchored to the glycan with its binding domain exposed at the cell surface "(Quoted from Lipke and Kurjan 1992).

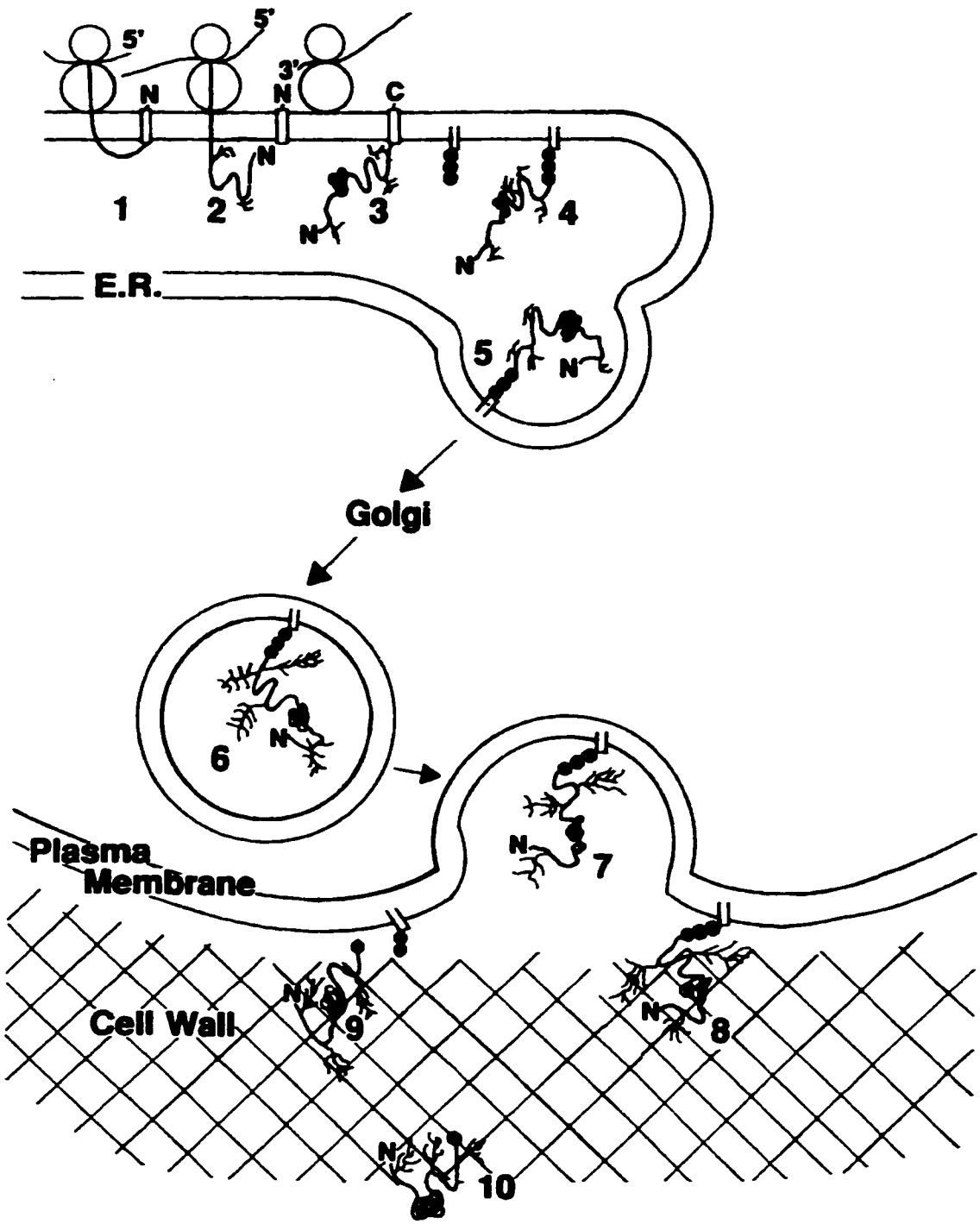

i. Characteristics of α-Agglutinin

α-Agglutinin is a 650 residue single polypeptide encoded by the *AGα1* gene (Figure 3) (Hauser and Tanner 1989; Lipke et al., 1989). It is a highly glycosylated protein with 12 potential N-glycosylation sites (Chen et al., 1995). The N-terminal half of the protein contains its adhesive domain for its binding ligand, a-agglutinin, and the C-terminal half contains the surface anchorage domain with over 50 % Ser and Thr (Lipke et al., 1989; Wojciechowicz et al., 1993; Lu et al., 1995; Chen et al., 1995). A truncated form of α-agglutinin containing N-terminal 350 amino acids is rich in β-sheet and fully active in binding to a-agglutinin (Wojciechowicz et al., 1993; Chen et al., 1995).

α-Agglutinin is a member in Ig superfamily. Sequence alignments between α-agglutinin and members of the immunoglobulin superfamily show that there are three Ig like domains in the N-terminal half of α-agglutinin (Lipke et al., 1995). Each of these three domains contains seven or nine β strands forming two anti-parallel β sheets.

Domain III is essential for ligand binding because a truncated form of α-agglutinin terminated at amino acid 278, which lacks part of domain III, lacks adhesive activity (Cappellaro et al., 1991; de Nobel et al., 1996). His 292 within the E-F loop of domain III is essential for α-agglutinin activity. Treatment by histdyl modifying reagent DEPC (diethylpyrocarbonate) and mutation of His 292 abolished the binding activity of the protein (Cappellaro et al., 1991; De Nobel et al., 1996). A putative binding site containing His 292 and residues in close proximity to His 292 was identified based on the site specific mutagenesis (Figure 7) (Cappellaro et al., 1991; de Nobel et al., 1996).). The three dimensional model of domain III shows that the essential residues for binding are clustered at one end of the β barrel of the domain, which resembles the ligand binding

Figure 7. Structural Model of Domain III of α-Agglutinin with A Putative Binding Site Highlighted. The three dimensional model of domain III of α-agglutinin was constructed by homology modeling based on known IgV fold. A putative binding site were highlighted with residues for which mutations reduced binding activity (Reprint from de Nobel et al., 1996).

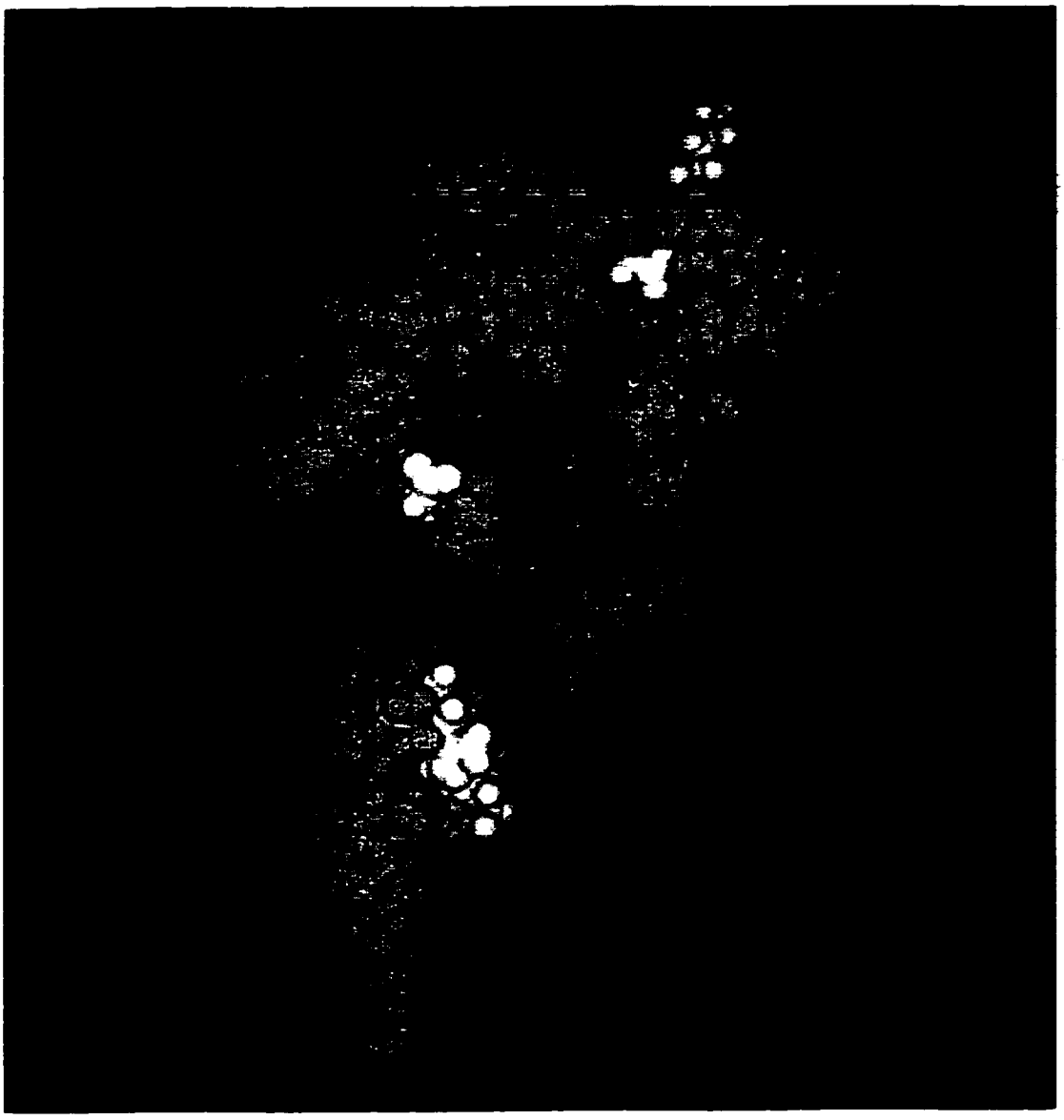

site of the human growth hormone receptor (hGHbp) (Bass et al., 1991, Lipke et al., 1995).

Like other members of the Ig superfamily, more than one domain of α-agglutinin is required for ligand binding (Colman et al., 1987; Clayton et al., 1989; Fleury et al., 1991; Holness et al., 1995). Partial deletions of domain I and part of domain II inactivate the protein (Wojciechowicz et al., 1993; Chen et al., 1995).

ii. Characteristics of a-Agglutinin

a-Agglutinin is a highly O-glycosylated protein consisting of two disulfide-linked subunits, the anchorage subunit (Aga1p) (Roy et al., 1991) and the adhesive subunit (Aga2p) (Cappellaro et al., 1991) (Figure 2). The anchorage subunit (Aga1p) is a 725 amino acid protein, encoded by the *AGA1* gene (Roy et al., 1991). The role of Aga1p is to mediate cell surface localization of a-agglutinin and to link the adhesive subunit Aga2p to the cell surface via disulfide bonds. The C-terminal hydrophobic sequence of Aga1p is responsible for the cell surface localization and subsequent attachment of a-agglutinin to the cell wall (Roy et al., 1991). *AGA1* mRNA is, however, not **a**-cell-specific and can be expressed in both hapolid **a** and α cells (Roy et al., 1991; de Nobel et al., 1995).

The adhesive subunit (Aga2p) is a small polypeptide of 69 amino acids encoded by *AGA2* gene. It has an apparent molecular weight of 22 kDa on SDS gels (Cappellaro et al., 1991). Aga2p is responsible for the binding of a-agglutinin to α-agglutinin. It is linked to the cell surface via two disulfide bridges (Cys7 and Cys50) to the anchorage subunit (Aga1p). The binding site of a-agglutinin to α-agglutinin is located at the C-terminal part of Aga2p (Cappellaro et al., 1994). The C-terminal 10 amino acids

(GSPINTQYVF) of a-agglutinin are active in binding in the nanomolar concentration range (Cappellaro et al., 1994).

iii. Interaction of the Agglutinins

Interaction of radioactive labeled α-agglutinin to **a** cells was previously studied by Terrance et. (Terrance et al., 1987). They speculate that ^{125}I- α-agglutinin bound to **a** cells in three modes: non-specific binding, like binding to α-cells, specific weak interaction, and tight interaction. The weak interaction was reversible by washing with bound and free α-agglutinin in kinetic equilibrium. The tight interaction was irreversible with a high affinity binding constant. Bound α-agglutinin could be dissociated only by treatment with denaturing reagents such as high pH (Lipke et al., 1987). However, it can not be ruled out that the weak interaction is an artifact from the partially active α-agglutinin fragment (Terrance et al., 1987). Whether the specific interaction of the agglutinins has two-states still need to be verified.

VI. Conditions Required for Sexual Agglutination in *S. cerevisiae*

Cells of opposite mating type exhibit maximal binding across similar ranges of ionic strength, pH, and temperatures (Terrance and Lipke 1981). For example, the optimal pH for agglutination is between 5.0 and 6.0. When the pH goes up to pH 8.5 or goes down to pH 3.5, the cells lose their binding ability gradually. Agglutination is also temperature dependent (Terrance and Lipke 1981). Agglutination occurs at temperatures between 12°C and 40°C. Less activity is seen above 55°C and below 10°C (Terrance and Lipke 1981). However, the controversial results from Yamaguchi's group shows that the agglutination substances are heat stable and the agglutinins are active even after 5-minute autoclaving or 3-minute boiling (Yamaguchi et al., 1982; Yamaguchi et al., 1984).

Therefore, *S. cerevisiae* cells have the ability to agglutinate at a broad range of pH and temperatures.

VII. Comparison of *ALS* Proteins in *C. albicans* with α-Agglutinin in *S. cerevisiae*

Cell adhesion molecules in the *ALS* family in the yeast *Candida albicans* are homologues of α-agglutinin in *S. cerevisae*. *C. albicans* is pathogenic, adhering to mammalian epithelial cells. Since *C. albicans* species do not mate, the *ALS* family does not encode a mating agglutinin. The *ALS* family is expressed upon hyphal formation, a form that is pathogenic and more adhesive than the single cell form (Calderone and Braun 1991).

Infectious organisms such as viruses, parasites and yeasts infect human cells by means of adhesion molecules. *C. albicans* is a fungus that exists in a diverse range of associations with human or animal hosts. It can survive in the host without obvious symptoms, and under appropriate circumstances, can cause disease that varies in site and severity (Hoyer et al., 1998). The pathogenicity of the fungus is correlated with its adherence. Adherent strains are more virulent than those with a less adhesive nature (Calderone and Braun 1991). Little is known about adhesion of *C. albicans* to its host cells. Several molecules in *ALS* family that are involved in adhesive interactions have been identified (Calderone and Braun 1991; Hoyer et al., 1995; Chaffin et al., 1998). It is the *ALS* family which mediates adhesion of *C. albicans* to mammalian cells (Fu et al., 1998; Gaur and Klotz 1997). For example, expression of *ALA1/ALS5* or *ALS1* in *S. cerevisiae* can mediate adhesion of non-adherent *S. cerevisiae* to mammalian epithelial and endothelial cells (Gaur and Klotz 1997; Fu et al., 1998).

Little is known about the structure and function of these adhesion molecules in the ALS family. However, *ALS* sequences have significant similarity to *AGα1*, especially in the N-terminal part of the proteins (Hoyer et al., 1995; Hoyer et al., 1998). Within this region, α-agglutinin contains three Ig domains, which are required for adhesion to a-agglutinin (Wojciechowicz et al., 1993; Lipke et al., 1995; Chen et al., 1995).

Three domains of the N-terminal of α-agglutinin^{350} were aligned with the same regions in *ALS1* protein. The results showed that the sequences in all three domains of the two proteins had about 50 % similarity and 25% identity (Figure 4). Therefore, the study of conformation of α-agglutinin and the interaction of the agglutinins will not only reveal interesting aspects of mechanism of cell adhesion in general but also provide a model for investigating the adherence of *ALS* proteins from pathogenic *C. albicans* to host cells.

VIII. Aim of this Thesis Research

In this work, the conformation of α-agglutinin under different environmental conditions which might be correlated with the specific adhesion properties in yeast *S. cerevisiae* has been studied. Secondly, the interaction of the agglutinins using isotopic labeling and Surface Plasmon Resonance techniques has been characterized. Thirdly, the effect of point mutations in domain III of α-agglutinin on the conformation of α-agglutinin and the interaction of the agglutinins has also been investigated.

Chapter II

Environmentally Induced Reversible Conformational Switching of Cell Adhesion Molecule, α-Agglutinin

Introduction

α-Agglutinin is a glycoprotein expressed on the cell surface of mating type α cells in *Saccharomyces cerevisiae.* It is involved in mediating cellular adhesion during mating between haploid α and **a** cells through an interaction with its glycoprotein ligand, **a**-agglutinin (Terrance and Lipke1981; Lipke et al., 1989; Hauser and Tanner 1989; Lipke and Kurjan 1992). The C-terminal half of α-agglutinin anchors the protein to the cell wall (Wojciechowicz et al., 1993; Lu et al., 1994; Lu et al., 1995; Kapteyn et al., 1996), and the N-terminal half contains the binding site for **a**-agglutinin (Wojciechowicz et al., 1993; Chen et al., 1995; de Nobel et al., 1996).

α-Agglutinin has structural and sequence properties typical of members of the Ig superfamily, including disulfide-bonded Cys residues in Ig-like sequence motifs (Wojciechowicz et al., 1993; Lipke et al., 1995; Chen et al., 1995; Lipke et al., 1995; Grigorescu et al., in preparation). An N-terminal fragment, α-agglutinin$^{20\text{-}351}$, is a β-sheet rich protein with full binding activity (Wojciechowicz et al., 1993; Chen et al., 1995). Based on secondary structure studies and structural models, it has three tandem Ig-like domains (Chen et al., 1995; de Nobel et al., 1996; Lipke et al., 1995; Grigorescu et al., in preparation). Domain III of α-agglutinin is known to be essential for function, because truncation of the *AGα1* gene at amino acid 278 eliminates the proposed E, F and G strands in domain III of α-agglutinin$^{20\text{-}351}$ and all of its binding activity (Wojciechowicz et al., 1993). Chemical modification and site-specific mutagenesis have identified residues in Domain III that are necessary for the binding of α-agglutinin$^{20\text{-}351}$ to **a**-agglutinin (Cappellaro et al., 1991; Wojciechowicz et al., 1993; de Nobel et al., 1996). Domains I

and II may also be essential for α-agglutinin to function: partial deletions of domain I or domain II of α-agglutinin$^{20\text{-}351}$ inactivate the protein, and domain III alone has no measurable activity (Wojciechowicz 1990).

The Ig superfamily contains diverse molecules, including immunoglobulins and their receptors, MHC antigens, T-cell receptors, growth factor receptors, neural adhesion molecules, and tumor antigens (Williams and Barclay 1988). The molecules are composed of β-sandwich domains, with interior hydrophobic cores often stabilized by disulfide bonds (Amzel and Poljak 1979; Manning and Woody 1987; Williams and Barclay 1988; Williams et al., 1989; Baldwin et al., 1993). Most of them are maximally active at pH values near 7.0 and temperatures near 37°C, the mammalian homeostatic conditions. In contrast, α-agglutinin is active at pH 5-6. At higher or lower pH, the binding activity of α-agglutinin decreases gradually, and there is no detectable activity at pH below 3.0 or above 9.0 (Terrance and Lipke 1981). α-Agglutinin is active at temperatures between 15°C and 40°C, but the activity is reduced at 10°C, and is lost within 10 minutes at 55°C (Terrance and Lipke 1981). Controversially, Yamaguchi showed that α-agglutinin is stable and still active even after 5 minutes of autoclaving (Yamaguchi et al., 1982; Yamaguchi et al., 1984). The broad range of conditions for stability may reflect its role as a cell wall protein of a single celled organism that may be exposed to a variety of extracellular conditions.

In this study, the role of pH, temperature, disulfide bonds and core interactions within the domains in the maintenance of the conformation of α-agglutinin were studied. The relationship between conformation and binding activity under different environmental conditions was also investigated. There was reversible conformational switching of significant parts of α-agglutinin from β-sheet to α-helix under conditions in which protein

inactivation was reversible. In order to understand the basis of the conformational switching and to determine the factors stabilizing the protein, we synthesized peptides of specific sequences found in α-agglutinin and studied their secondary structural characteristics. Although conformational switching has been seen in a number of other systems (Prusiner 1991; Carr and Kim 1993; Bullough et al., 1994; Chan et al., 1997; Weissenhorn et al., 1997; Tan and Richmond 1998; Jackson et al., 1999), its manifestations in α-agglutinin are unusual.

Materials and Methods

Overexpression and Purification of α-Agglutinin$^{20-351}$: Yeast strain Lα21 (*MATα ade2-1 his3-11,15 leu2-3,112 trp1-1 ura3-2 can1-100 agα1-3*) containing pPGK-Agα1^{351} constitutively expresses and secretes α-agglutinin$^{20-351}$, which is fully active (Wojciechowicz et al., 1993; Chen et al., 1995). Cell culture supernatant (4 L) was concentrated to 50 ml through a "Millipore" filtration apparatus with a membrane having a 30 kDa molecular weight cutoff. Concentrated supernatant was dialyzed against 4 L of 30 mM sodium acetate buffer, pH 5.5 at 4°C overnight and then chromatographed on DEAE-Sephadex A25 at 25°C. Partially purified α-agglutinin$^{20-351}$ was eluted with 350 mM sodium chloride in 30 mM sodium acetate, pH 5.5. The sample was dialyzed at 4°C, lyophilized, re-suspended in 30mM sodium acetate, pH 5.5, 0.01% SDS and 1 mM EDTA, and partially deglycosylated by endoglycosidase H. The deglycosylated protein was further purified at 25°C by a Bio-Gel P-60 size exclusion column equilibrated in 30 mM sodium acetate, pH 5.5 (Chen et al., 1995). α-Agglutinin$^{20-351}$ had an apparent molecular weight of 45 kDa on Coomassie Blue stained SDS gels and was of 99% purity by scanning densitometry (Molecular Dynamics). Each preparation produced 0.2-0.4 mg of α-agglutinin$^{20-351}$.

Agglutination Assay: *S. cerevisiae* wild-type haploid strains X2180-1A (*MATa SUC2 mal mel gal2 CUP1*) and X2180-1B (*MATα SUC2 mal mel gal2 CUP1*), obtained from the Yeast Genetics Stock Center (Berkeley, Calif.), were used for bioassays. **a** cells and α cells were grown separately in minimal medium to 2×10^7 cells per ml and **a** cells were treated with the sex pheromone α-factor as described (Terrance and Lipke 1981). These cells were harvested and washed in 100mM sodium acetate at pH 5.5 at 25°C. α-Agglutinin was incubated with **a** cells on a rotary shaker at 25°C for 90 minutes, and α cells were then

added. Cells were centrifuged at 900rpm/min for 5 minutes and re-suspended by stirring with a 7- by 90 mm paddle at 1000rpm for 4 seconds. The suspensions were left for 20 minutes to allow settling of the aggregates. OD_{660nm} of the samples were then measured. All samples were run in triplicate. The agglutination index (AI) was defined as: $AI=1-(2 \times A^{a+\alpha}) / (A^{a} + A^{\alpha})$ where A is the mean optical desity of the samples containing the cell types indicated by the superscript. The activity of α-agglutinin was determined by its ability to inhibit the agglutinability of **a** cells (Terrance and Lipke 1981).

pH Treatment of α-Agglutinin$^{20-351}$: Purified α-agglutinin$^{20-351}$ (0.2 mg/ml) was dialyzed against 100 mM sodium phosphate buffer at pH 1.5, 2.5, 7.5 and 8.5; 30 mM sodium acetate at pH 3.5 and 5.5; or 100 mM CAPS at pH 9.5 and 10.5 at 4°C overnight. α-Agglutinin$^{20-351}$ in buffers with different pH was reconstituted to pH 5.5 by dialyzing against 30 mM sodium acetate at pH 5.5.

Endoprotease Arg-C Digestion of α-Agglutinin$^{20-351}$: Digestion of α-agglutinin$^{20-351}$ (0.2 mg/ml) with mouse endoprotease Arg-C (Boehringer-Mannheim) was performed in 100 mM NH_4HCO_3 buffer at pH 7.8. The ratio of protease to substrate was 1:100. The digestion buffer was removed by centrifugation through Microcon filters with 10 kDa molecular weight cut off. The protein retained on the membrane was then suspended in 30 mM sodium acetate at pH 5.5. In order to isolate fragments of α-agglutinin$^{20-351}$, a Bio-Gel P-30 size exclusion column equilibrated with 100 mM sodium phosphate buffer at pH 7.8 was used. The isolated 30 kDa fragment of α-agglutinin was washed on Microcon filters as above and resuspended in 30 mM sodium acetate at pH 5.5 also as above, before measuring CD and agglutination activity.

Reduction of Disulfide Bonds of α-Agglutinin$^{20-351}$: α-Agglutinin$^{20-351}$ (0.2 mg/ml) was treated with 10 mM dithiothreitol (DTT) in 100 mM sodium phosphate, pH 7.0 at 37°C for 30 minutes. The DTT-containing buffer was then washed away by centrifugation through Microcon filters as above. α-Agglutinin$^{20-351}$ retained on the membrane was suspended in 30 mM sodium acetate at pH 5.5 for CD and agglutination assay.

Synthesis and Purification of Peptides: Peptides were synthesized by the solid phase method using fluorenylmethoxycarbonyl chemistry on an Applied Biosystems automated model 432A peptide synthesizer. The peptide-resins were treated with 80 % trifluoroacetic acid (TFA) / 5 % water / 5 % ethanedithiol / 10 % thioanisole at room temperature for 2 hours. The cleaved and deprotected peptides were then precipitated and washed in cold methyl t-butyl ether and collected by centrifugation at 25°C.

Purification of the peptides was achieved by reverse-phase HPLC on a C-18 column (21.4 × 250 mm) using 0.1% TFA as buffer A and 70 % acetonitrile in 0.1% TFA as buffer B. A linear gradient between 0% and 100% buffer B in buffer A was used at a flow rate of 5 ml/min over a period of 60 minutes. The elution profile was monitored at 215 nm. The purified peptides were lyophilized and re-dissolved in deionized water at 25°C and stored at 4°C.

Circular Dichroism Spectroscopy: Far UV CD spectra were recorded on a Jasco J-710 spectropolarimeter in quartz, thermo-regulated cuvettes (HELLMA) with 0.1 cm and 0.05 cm path lengths. Each spectrum represents the average of 10 scans taken at 0.5 nm intervals from 250 to 200 nm for the protein and 250 to 190 nm for the peptides. The spectra were corrected by subtraction of the appropriate buffer baseline spectra and smoothed by the Jasco Series 700 software. Each experiment was repeated three times. For conversion of

molar ellipticity from the observed ellipticity for α-agglutinin$^{20-351}$, a mean residue weight of 111.77 was used. The concentrations of protein and peptides were obtained from UV absorption at 280 nm by using extinction coefficients of 51,850 for the protein, and 2560 and 1280 for peptides I and II respectively. The coefficients were calculated from the amino acid compositions of the protein and peptides as being more accurate than methods based on quantitation of small amounts of protein (Gill and von Hippel 1989).

A different CD analysis method was used from the previous report (Chen et al., 1995): all CD data presented here were analyzed by the self-consistent method with the SELCON program (Sreerama and Woody 1993; Sreerama and Woody 1994), which uses a database of 33 reference proteins as standards. This program provides better estimates of conformation from CD, especially for proteins with poor spectra at wavelengths lower than 200 nm (Greenfield 1996). The spectra of α-agglutinin$^{20-351}$ are noisy in this region, perhaps due to the presence of residual glycosylation and the need to use carboxylate buffers. The error bars shown are the standard deviations of the mean estimates for each secondary structure element for all data sets in the final iteration.

The secondary structure estimates for six independent experiments carried out over the course of the year, using two different preparations of α-agglutinin$^{20-351}$ were averaged. The CD spectra were taken in 30 mM sodium acetate buffer, pH 5.5 at 25°C. The means and standard deviations of the secondary structure contents were: α-helix, 2.2% ± 1.3%; β-sheet, 45.0% ± 1.3%; turn 16.1% ± 3.3%; and other structures, 37.3% ± 2.9%. When turn and other structures were summed before averaging, the value was 53.4% ± 1.3%. These values for standard deviations imply standard errors of the mean of 0.6% or less, and 95% confidence limits of ±1.3% or less.

Results

Effect of pH on Conformation and Binding Activity of α-Agglutinin$^{20-351}$: Because the binding activity of α-agglutinin to a cells is pH-dependent (Terrance and Lipke 1981), the secondary structure of α-agglutinin$^{20-351}$ was studied at different pH values. The CD spectrum of α-agglutinin$^{20-351}$ at pH 5.5 showed a positive band below 200 nm, a positive shoulder at 204 nm and a negative maximum at 217 nm, which is a typical β-sheet spectrum. At pH 8.5, the spectrum showed several differences (Figure 8A). The secondary structure analysis was consistent with a decrease in β-sheet from 48% ± 2.5% at pH 5.5 to 30.6 % ± 1.1% at pH 8.5 and increases in α-helix content from 0.7% ± 2.0% to 18% ± 0.6% and in aperiodic structure from 36.4% ± 2.3% to 40.5% ± 1.0% (insert in Figure 8A). With the change in its secondary structure, the binding activity of α-agglutinin$^{20-351}$ decreased by about 90% at pH 8.5. However, restoration of the pH from 8.5 to 5.5 followed by incubation at 25°C for 30 minutes restored the CD spectrum of α-agglutinin$^{20-351}$ to its original shape with essentially complete recovery of the original β-sheet content (Figure 8A). In addition, at least 70% of the binding activity was recovered. At pH 9.5 or higher, α-agglutinin$^{20-351}$ showed irreversible loss of its binding activity and irreversible changes in the CD spectrum (not shown).

In contrast to the effect of high pH, the CD spectrum of α-agglutinin$^{20-351}$ at pH 3.5 still showed a typical β-sheet profile with slightly broadened bandwidth around the negative peak at 217 nm (Figure 8B), even though the protein had no detectable activity. Secondary structure analysis indicated that there were only minor changes in the secondary structure content (inset in Figure 8B). About 95% of binding activity was regained

Figure 8. Effect of pH on Far-UV CD of α-Agglutinin$^{20\text{-}351}$. A, Exposure to basic pH: Spectra were taken at 25°C in 30 mM sodium acetate, pH 5.5 (———); or 100 mM sodium phosphate, pH 8.5 (– – –). The spectrum of the reconstituted sample pH (8.5 ➡ 5.5), which had been pre-incubated in 100 mM sodium phosphate at pH 8.5 for 2 hours followed by 30 mM sodium acetate at pH 5.5 for 30 minutes, was measured at 25°C in 30 mM sodium acetate, pH 5.5 (·····). **Inset:** Secondary structure content calculated by curve fitting: ▭, β-sheet; ■, α-helix and ▨, aperiodic structures. Error bars: see text. All spectra contained about 16% turn (not shown). **B.** Exposure to low pH: Spectra were measured at 25°C in 30 mM sodium acetate, pH 5.5 (———); 30 mM sodium acetate, pH 3.5 (·····); or 100mM sodium phosphate, pH 1.5 (– – –). **Inset:** Secondary structure content calculated by curve fitting, bars as in A.

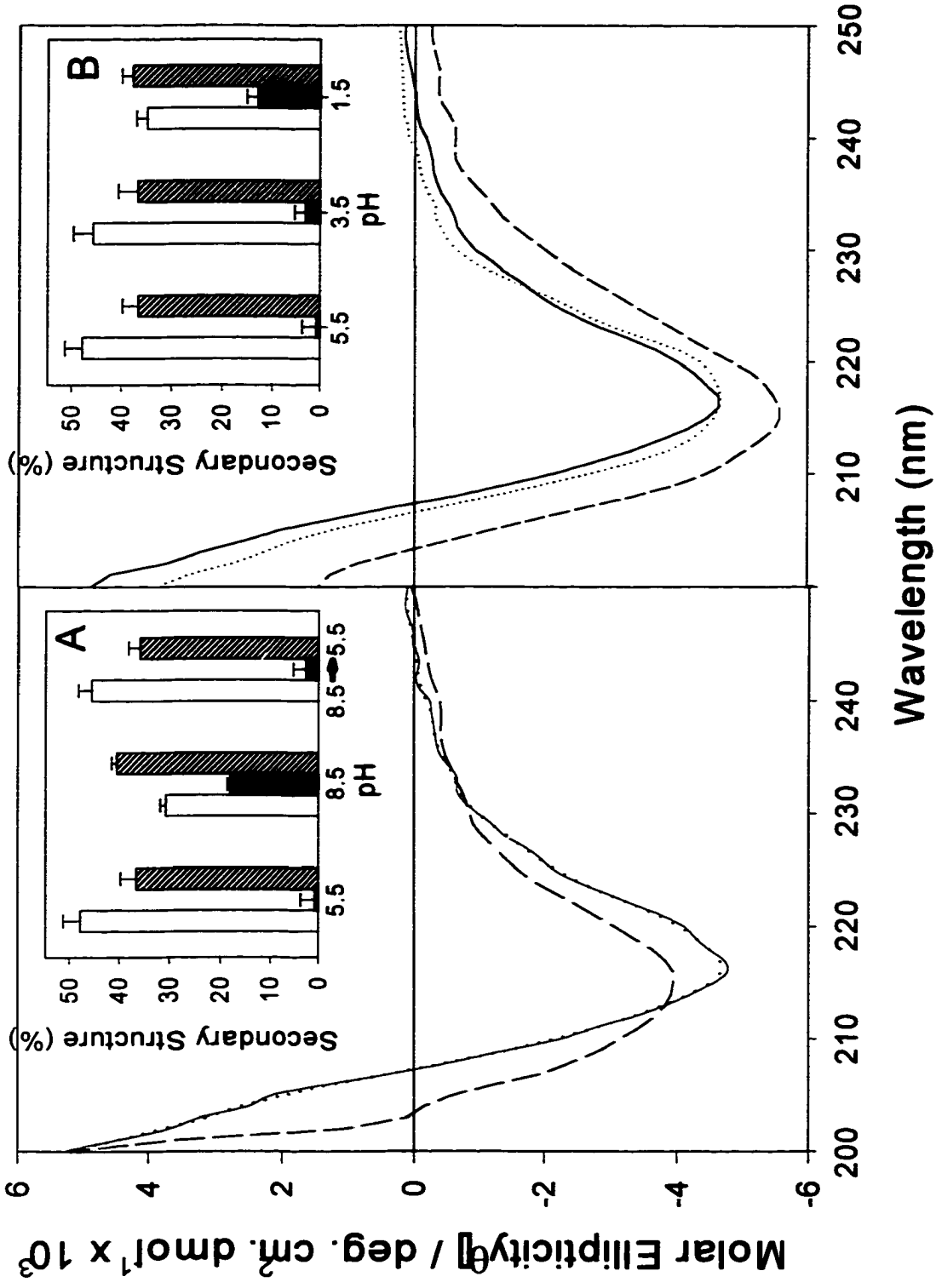

immediately after the protein was restored to pH 5.5. The CD spectra at pH 2.5 (not shown) and pH 1.5 (Figure 8B) showed a broader and more intense negative peak with a slight shift to lower wavelength and a decrease in the positive intensity near 200 nm compared to pH 5.5 (Figure 8B). More interestingly, at pH 1.5, α-agglutinin$^{20\text{-}351}$ still contained a considerable amount of β-sheet (insert in Figure 8B), and 30% of its binding activity was regained after 2 hours of incubation at pH 5.5 (not shown). Therefore, α-agglutinin$^{20\text{-}351}$ was extremely stable at low pH, and the conformational changes were partially reversible even after exposure to pH 1.5.

Effect of Temperature on Conformation and Binding Activity of α-Agglutinin$^{20\text{-}351}$: The binding activity of α-agglutinin is temperature-dependent (Terrance and Lipke 1981; Yamaguchi et al., 1982; Yamaguchi et al., 1984; Lipke et al., 1987). α-Agglutinin$^{20\text{-}351}$ was heated gradually from 25°C to 75°C in a thermo-regulated cuvette, and CD spectra were obtained after successive rises in temperature of 10°C. Each 10°C rise in temperature took half an hour, the protein being equilibrated at the new temperature for 20 minutes before acquisition of the spectra. The spectra showed little change at temperatures between 25°C and 45°C. Obvious change was seen at 55°C. There were further changes at 65°C (Figure 9) and 75°C (not shown).

Secondary structure analysis estimated that from 25°C to 45°C, the β-sheet content decreased only slightly, with minor increases of α-helix and random structure. At temperatures of 55°C and 65°C, there was more loss of β-sheet with a concomitant rise in α-helix and random structure (inset in Figure 9). At 75°C, around 50% of original β-sheet content was lost (not shown).

Figure 9. Effect of Temperature on Far-UV CD of α-Agglutinin [20-351]. Samples were equilibrated at various temperatures for 20 minutes and spectra were measured in 30mM sodium acetate, pH 5.5, at ——, 25°C, 35°C and 45°C; ·····, 55°C; or – – –, 65°C. **Inset:** Secondary structure content at different temperatures calculated by curve fitting: 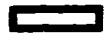 , β-sheet;  , α-helix and , aperiodic structures. Error bars: see text. All spectra contained about 16% turn (not shown).

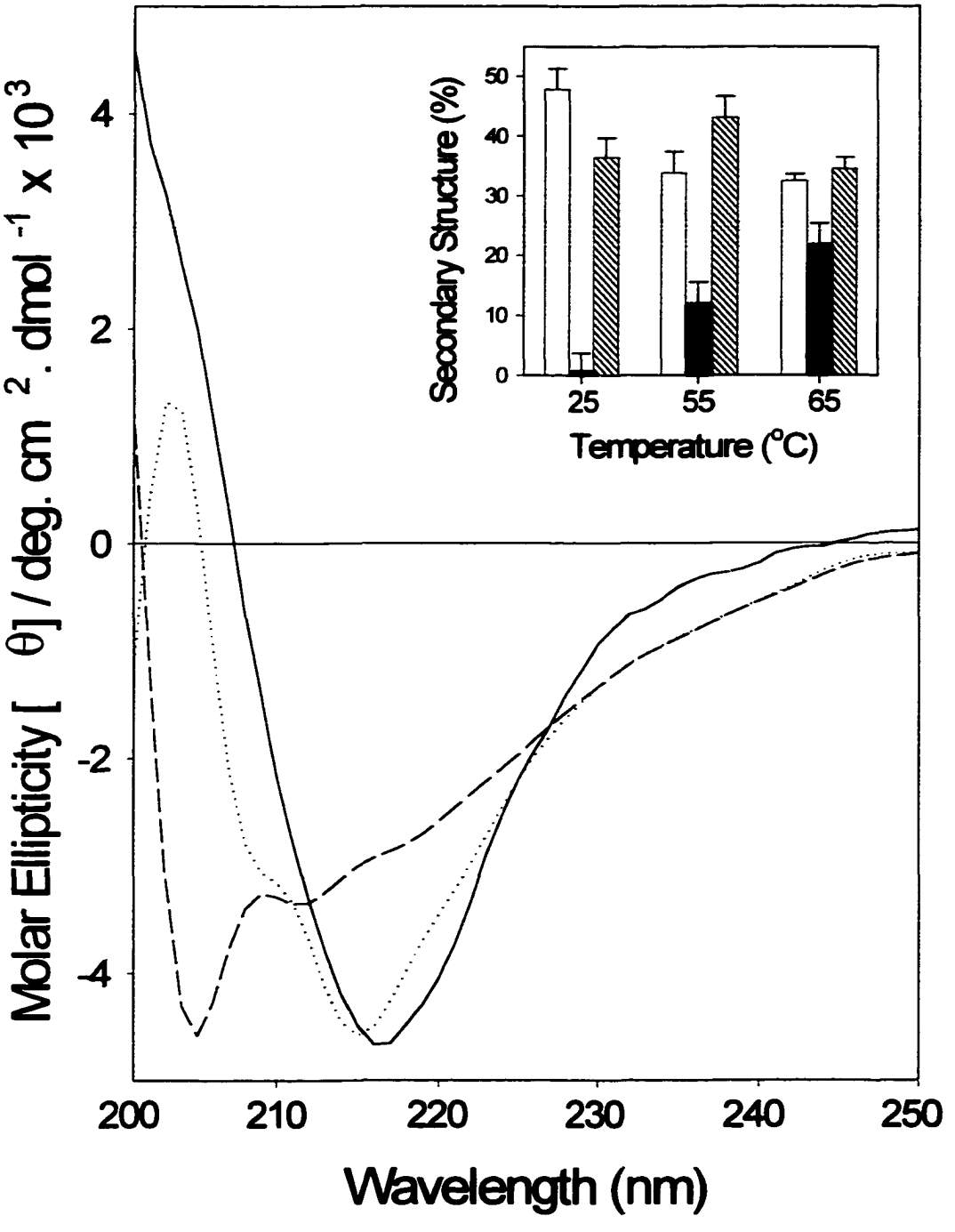

The binding activity of α-agglutinin$^{20-351}$ was measured after heating the samples at temperatures from 25°C to 75°C for 30 minutes, followed by 2 hour-incubation at 25°C. α-Agglutinin$^{20-351}$ was fully active after treatment below 45°C. Fifty percent of its binding activity remained after 55°C treatment, while 10% was retained after treatment at 65°C. There was almost no measurable activity left at 75°C (Figure 10A). Because the above assays incorporated a 2 hour recovery incubation at 25°C, the binding activity was tested at 25°C immediately after a 30 minute incubation at 55°C. Only about 10% of the binding activity remained (Figure 10B). Therefore, α-agglutinin$^{20-351}$ lost about 90 % of its binding activity at 55°C, half of the activity being regained upon a subsequent 2 hour incubation at 25°C. Because the bioassay requires a 90 minute incubation, more accurate kinetics of recovery could not be determined.

These results were surprising, because of a previous use of a 5 minute autoclaving step for the isolation of α-agglutinin (Yamaguchi et al., 1982; Yamaguchi et al., 1984). CD spectra of α-agglutinin$^{20-351}$ were therefore taken at 25°C immediately after heating at 100°C for 5 minutes and after 2 hours incubation at 25°C following the 100°C step. The brief heating induced only a small change in the CD spectrum and secondary structure content of the protein (Figure 11). These changes were reversed by a subsequent 2 hour incubation at 25°C (not shown).

Effect of Endoprotease Arg-C Digestion on Conformation and Binding Activity of α-Agglutinin$^{20-351}$: α-Agglutinin$^{20-351}$ is inactivated by endoprotease Arg-C, which cleaves at Lys^{154} in domain II (Chen et al., 1995). This digestion yields a large peptide with an apparent size of 30 kDa containing half of domain II and all of domain III, and a smaller peptide of about 20 kDa which includes domain I and part of domain II (Wojciechowicz

Figure 10. Effect of Heating on Specific Activity of α-Agglutinin$^{20\text{-}351}$. Specific activity was determined at 25°C in 100 mM sodium acetate at pH 5.5. **A,** α-Agglutinin samples were incubated at various temperatures for 30 minutes and then incubated at 25°C for 2 hours before assay. **B,** In a separate experiment: Specific activity of samples was measured immediately after 30 minute incubations at 25°C (first bar); 55°C (second bar); and after 30 minutes incubation at 55°C followed by a 2 hour incubation at 25°C (last bar).

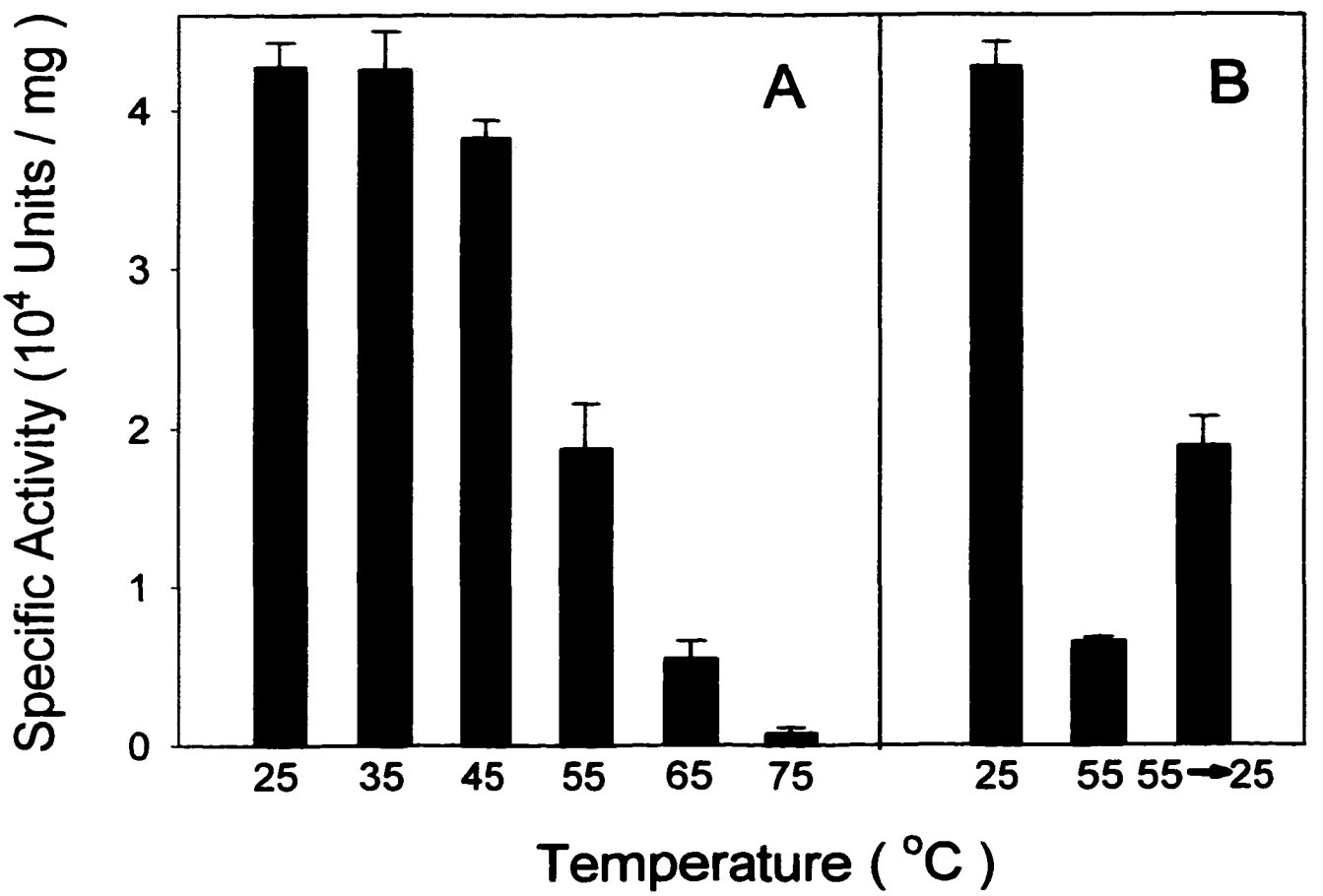

1990; Chen et al., 1995). The protein was digested at pH 7.8 and reconstituted at pH 5.5 for 30 minutes. Attempts to separate the major products of Arg-C proteolysis at pH 5.5 by gel filtration, ion exchange, or lectin affinity chromatography failed. Therefore, the digestion products remained bound to each other at this pH. However, the fragments were separated at pH 7.8 by gel filtration on Bio-Gel P-30. The CD spectrum of the larger fragment showed β-sheet conformation and a relatively higher proportion of random structure but with significant differences from that of the intact and cleaved but unseparated forms of α-agglutinin$^{20\text{-}351}$ (data not shown).

Role of Disulfide Bonds in Conformation and Binding Activity of α-Agglutinin$^{20\text{-}351}$: α-Agglutinin$^{20\text{-}351}$ contains disulfide bonds between Cys^{97}-Cys^{114} in domain I and Cys^{202}-Cys^{300} in domain III (Chen et al., 1995; Lipke et al., 1995; Grigorescu et al., in preparation). To determine their roles in maintaining the structure of the protein, it was treated with 10 mM dithiothreitol in 100 mM sodium phosphate at pH 7.0 for 30 minutes at 37°C. The DTT-treated sample was then reconstituted at pH 5.5 in fresh buffer without DTT at 25°C. This treatment inactivated α-agglutinin$^{20\text{-}351}$ (Chen et al., 1995), but induced only a small change in its CD spectrum (Figure 11). However, when the DTT-treated sample was heated at 100°C for 5 minutes, there were substantial changes in its CD spectrum, consistent with loss of 60% of the β-sheet and an increase in helical and random structure content (Figure 11).

Effect of pH on Conformation of Small Peptide Derivatives of α-Agglutinin: The studies described above and by Chen et al. (Chen et al., 1995) have shown that α-agglutinin has a typical β-sheet conformation with little helical content under native conditions. However, under other conditions, α-helices appear at the expense of β-sheets

Figure 11. Effect of DTT and Brief Heat Treatment at 100°C on Far-UV CD of α-Agglutinin$^{20-351}$. Spectra were taken at 25°C in 30 mM sodium acetate, pH 5.5; without any treatment (———); with 10 mM DTT treatment (·····); with heat treatment at 100°C for 5 minutes (– – –); or DTT treatment plus heat treatment at 100°C for 5 minutes (– · – ·). **Inset:** Secondary structure content calculated by curve fitting:  , β-sheet; 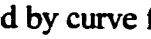 , α-helix and  , aperiodic structures. Error bars: see text. All spectra contained about 16% turn (not shown).

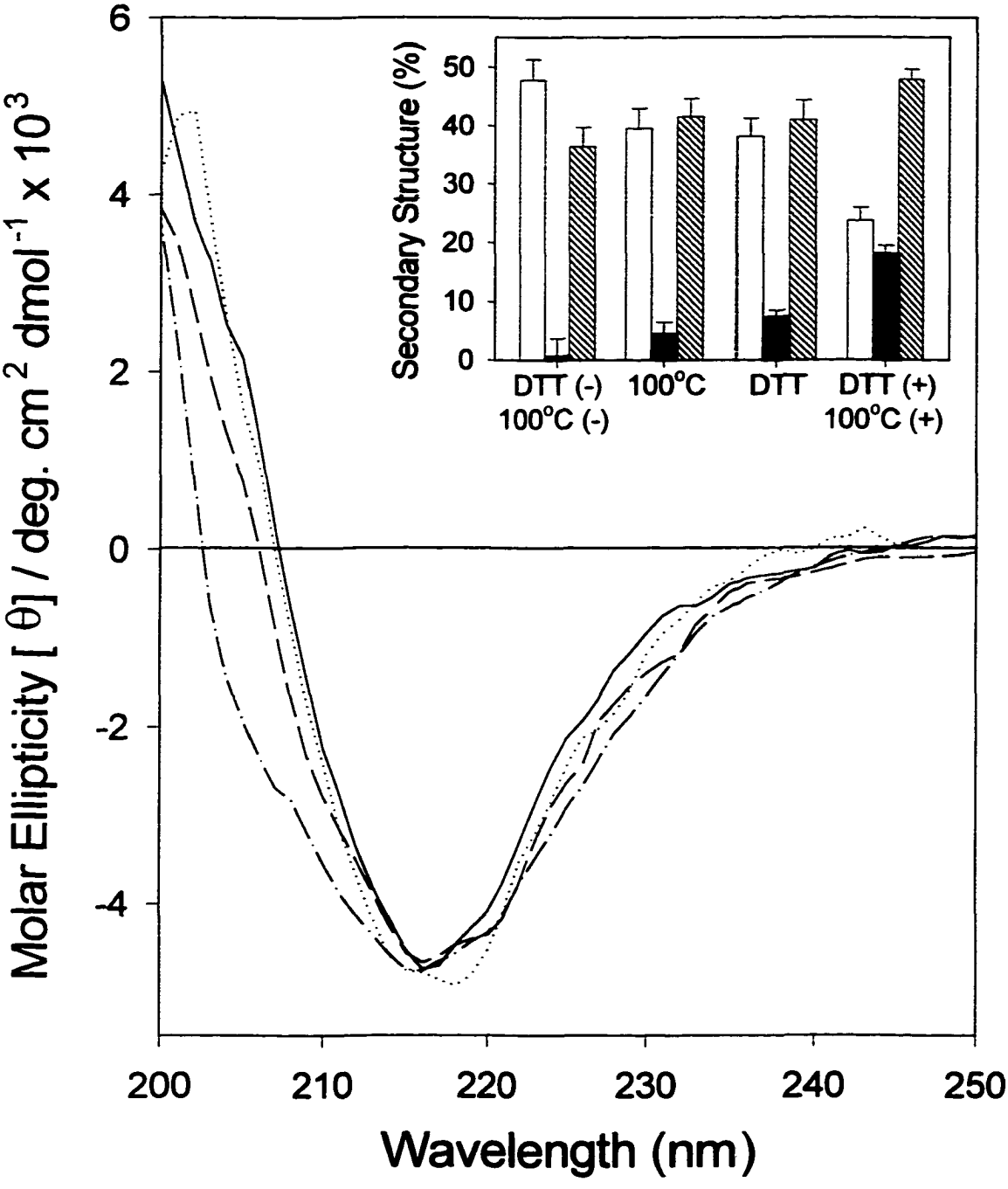

(Figures. 8, 9, 11). To investigate the idea that structural switching from β-sheet to α-helix may have occurred in specific regions in the protein, we synthesized two peptides, one derived from α-agglutinin domain II and the other from domain III (Figure 12). These peptides correspond to regions predicted to have high potential to form α-helices. However, because native α-agglutinin$^{20\text{-}351}$ has only 2.2% ± 1.3% α-helix (3-11 residues), regions of the protein containing these peptides are not likely to be helical in the native structure. In the modeled structures, these regions have β-loop-β structures (Lipke et al., 1995; Grigorescu et al., in preparation; Figure 12). Since the conformation of short peptides is unstable in aqueous solution, we examined the effect of Trifluoroethanol (TFE) on the conformation of the peptides derived from sequences of α-agglutinin$^{20\text{-}351}$. TFE stabilizes helices in peptides with propensities to form such structures (Lau et al., 1984; Sonnichsen et al., 1992; Shiraki et al., 1995; Hamada et al., 1995; Najbar et al., 1997). TFE has also been shown to stabilize β-sheets in peptides with appropriate sequences (Toniolo et al., 1979; Lu et al., 1984; Martenson et al., 1985; Yang et al., 1994; Wang et al., 1995; Najbar et al., 1997). The far-UV CD spectrum of peptide I, derived from domain II of α-agglutinin, displayed remarkable pH and TFE dependence (Figure 13). At pH values less than 3, the spectra were similar to one another, and were similar to those at pH greater than 8 (not shown). At each pH, however, addition of TFE changed the spectrum toward α-helix with characteristic negative ellipticity near 208 and 222 nm (Woody 1985). Addition of TFE at pH 3 caused a smooth two state transition with an isodichroic point at 203 nm. In the absence of TFE, the spectrum at this pH is typical of random coil with a negative peak a little above 200nm (Woody 1985; Yang et al., 1986). The spectra showed increasing helical characteristics

Figure 12. Three Dimensional Orientation and Helical Propensity of Two Peptides Derived from the Proposed β-Strands Regions of α-Agglutinin[20-351]. A, Homology model of domains II and III of α-agglutinin, with Peptide I (C-C' strand region of domain II) shown in cyan and Peptide II (E-F strand region of Domain III) shown in yellow. **B,** Sequence and secondary structure predictions of Peptides I and II. β-strands in the model are over-lined and sequence positions are indicated above every tenth residue. Garnier-Robson helical prediction state for residues in proteins with >20 % helix are shown as (+), and residues predicted to be helical even in proteins with very low helical content are underlined (±). Chou-Fasman helical potential (- - - -) and β-strand potential (———) are also shown.

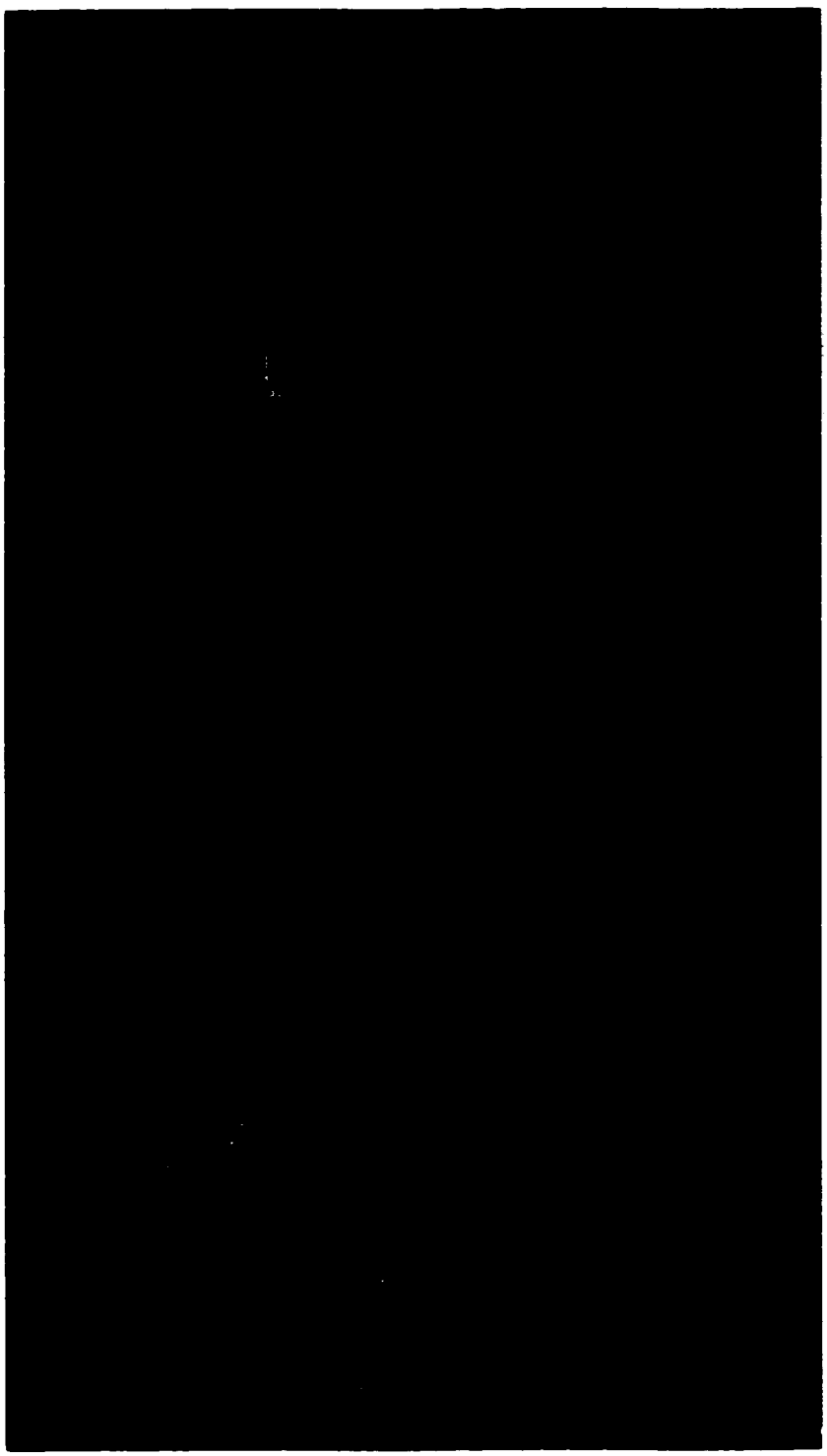

A

B

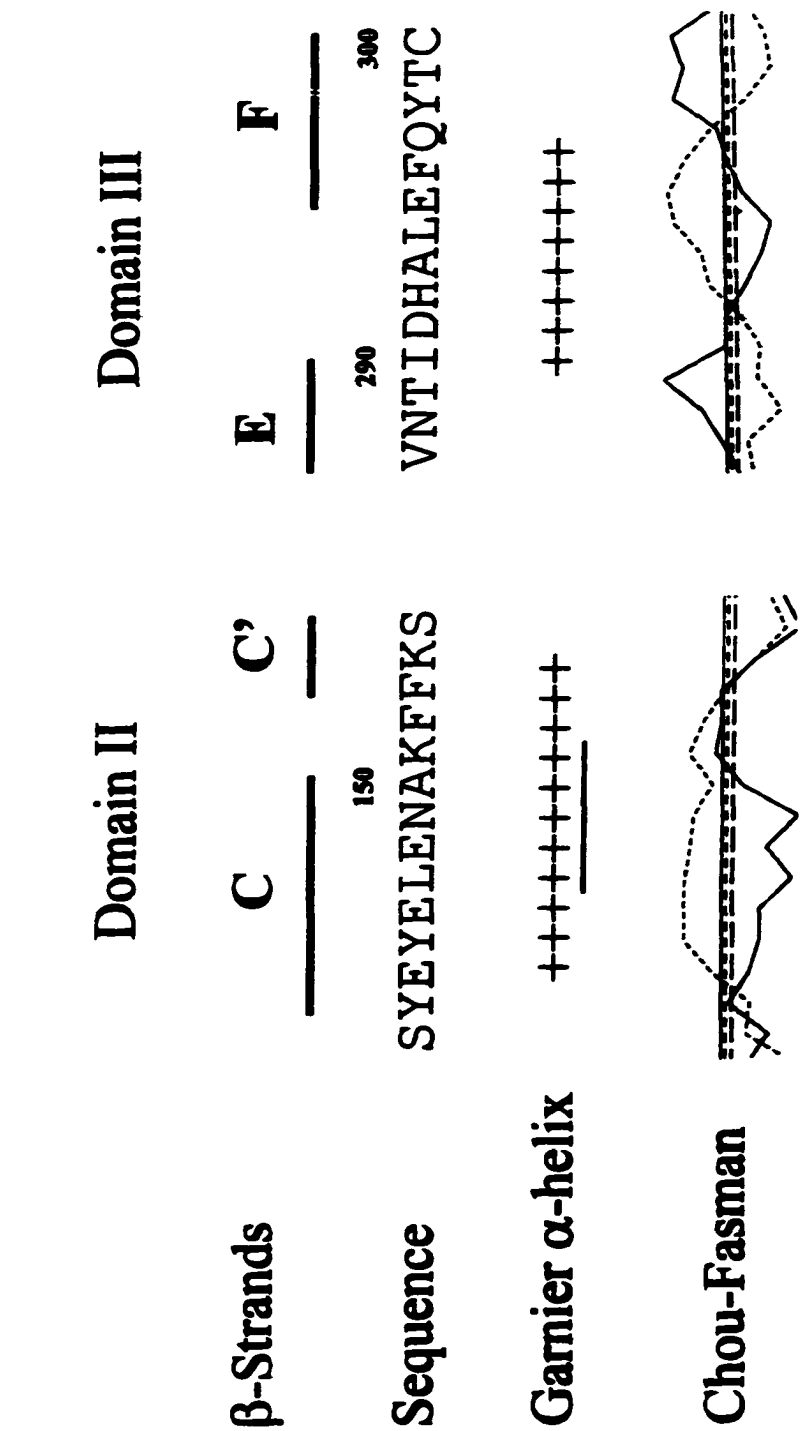

Figure 13. Effect of TFE on Far-UV CD of Peptide I at Different pH values. Spectra were measured in 10 mM sodium phosphate at pH from 2 to 10 in ——, 10% TFE; ·····, 20 % TFE; — — —, 40 % TFE or — ·· — ··, 60 % TFE. The spectra below pH 3 were similar to one another, as were those above 8. The spectra at pH 3, 5 and 7 are shown.

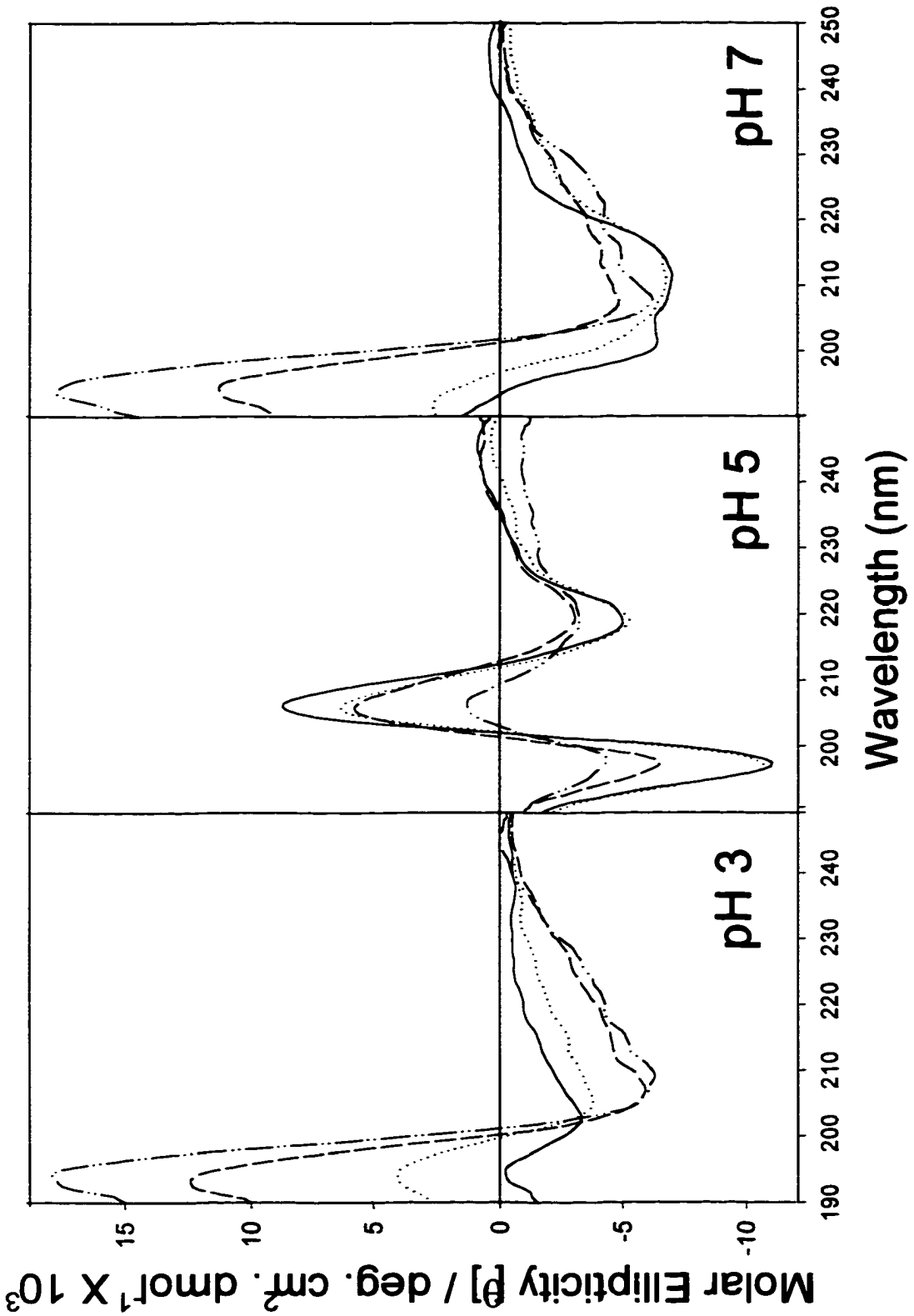

with increasing TFE concentration, both in the 208-230 nm region and in the positive peak at 195 nm.

At pH 5, TFE addition also produced a two state transition, as indicated by isodichroic points at 202, 212, and 227 nm, although the curve at 60% TFE deviates slightly from the isodichroic point at 212nm. The negative band at 217 nm in the central panel of Figure 13 is characteristic of β-structure. As the TFE concentration rises, this band shifts slightly to longer wavelength, and at high TFE, the ellipticity becomes somewhat less positive near 210 nm, showing a negative shoulder at about 212 nm. The α-helix has its characteristic bands at 208-210 nm and 222 nm. The TFE induced shift is thus in the helical direction.

The pair of oppositely signed bands at about 197 and 206 nm are almost certainly an effect of the aromatic side chains. They are due largely to the two tyrosines in peptide I, as the phenylalanines contribute but weakly to the CD even in the far UV (Kahn 1979; Woody and Dunker 1996). Overlap of the strong positive band at 206 nm with the negatively signed helix band which is normally near 208 nm both reduces the apparent intensity of the helix band and shifts its apparent position to longer wavelength, thus producing the 212 nm shoulder in high TFE instead of a band at 208 nm.

The aromatic bands are strong at low TFE and weaken as the TFE concentration rises. In the β-conformation shown in the model in Figure 12, the two tyrosines are on the same side of the sheet and are close enough for strong coupling between their transitions. The pair of bands at low TFE, in fact, looks like an exciton couple (Kahn 1979; Woody and Dunker 1996). As the number of molecules in the β-conformation falls, this coupling is lost irrespective of whether the molecules become helical or

unordered, since in the helical form they will point away from one another, which reduces their spectroscopic interaction. Thus the data describe a shift from a population of molecules many of which are relatively ordered in a way which allows strong aromatic side chain coupling toward forms which do not. These results, including the negative band at 217 nm, are consistent with the idea that the partially ordered structure at low TFE is β–sheet, while the population at high TFE contains both disordered molecules and molecules which are partly helical (Yang et al., 1994; Wang et al., 1995).

Similar trends toward helical structure are seen in the spectra at pH 7, but the absence of a clear isodichroic point indicates that more than two conformational forms are involved.

Unlike peptide I, peptide II, derived from domain III of the protein, had similar CD spectra at pH values between 2 and 10, so only the results at pH 5 are shown in Figure 14. Increasing TFE concentrations produced isodichroic points at 215 nm and 238 nm, indicating a two state transition. The transition in this case resembled that of peptide I at pH 3 in that the curve without TFE is a typical random coil spectrum with a negative peak at 200 nm (Woody 1985; Yang et al., 1986). Addition of TFE yielded clear negative peaks at 208 and 222-225 nm and a positive one at 192 nm, implying a switch from random to α-helix.

Figure 14. Effect of TFE on Far-UV CD of Peptide II. Spectra were measured in 10 mM sodium phosphate at pH from 2 to 10 in ——, 10% TFE; ·····, 20 % TFE; – – –, 40 % TFE or – · · – · ·, 60 % TFE. Since spectra at all pH values were similar, only the curves at pH 5 are shown. **Inset:** molar ellipticity at 222mn *vs* the concentration of TFE.

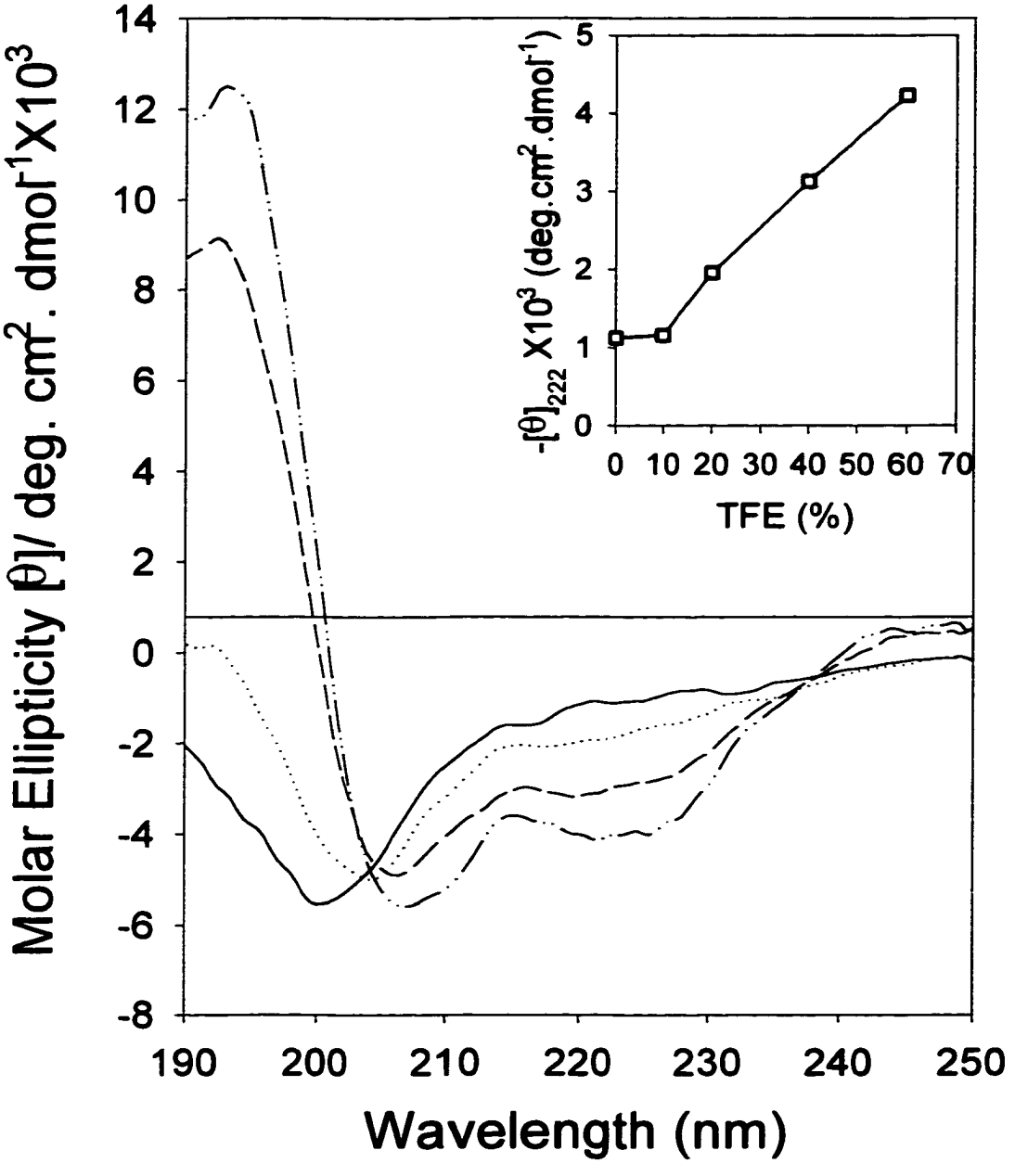

Discussion

Reversible Conformational Switching of α-Agglutinin: α-Agglutinin$^{20-351}$ shows reversible conformational switching from native all-β to partial α-helix when environmental conditions change moderately (Figures 8-10), and such switching has also been seen in two peptides derived from the sequence of the protein (Figures. 12-14). These peptides showed conformational switching in the presence of TFE, which can stabilize either helix or sheet conformation by potentiating local interactions (Toniolo et al., 1979; Lu et al., 1984; Lau et al., 1984; Martenson et al., 1985; Sonnichsen et al., 1992; Yang et al., 1994; Wang et al., 1995; Shiraki et al., 1995; Hamada et al., 1995; Najbar et al., 1997). The two tested sequences are among nine segments of 4 to 14 residues that have significantly higher potential to form α-helices than β-strands by both the Chou-Fasman and the Garnier-Robson algorithms (Chou and Fasman 1974; Garnier et al., 1978).

Peptide I, from the C strand-turn-C' strand region of domain II, had both coil to helix and β-strand to helix transitions, depending on the pH and TFE concentration. To our knowledge, such a dual transition has not been previously reported in an isolated peptide derived from a protein sequence, although similar behavior was seen in model peptides (Yang et al., 1994; Wang et al., 1995; Zhang and Rich 1997). The basis for these interactions are the interplay of local and non-local interactions.

Role of Charge Interactions: The pH dependence of the conformational shift of peptide I shows the importance of charge interactions. In both peptide I and the native protein, the side chains of Glu residues at protein positions 144, 146, and 148 will protrude to the same (exterior) side of a β-strand (Grigorescu et al., in preparation). These

residues alternate with residues expected to pack into the hydrophobic core of the domain (Figure 12). At pH 5.5, partial neutralization of these Glu residues would reduce repulsive interactions among them. On the other hand, full ionization at pH > 7 would destabilize the strand. Moreover, ionization of Glu^{148} might stabilize α-helix formation, because it could form a salt bridge with Lys^{151} in the next turn of a potential helix. It should also be noted that the negatively charged amino acids occur toward the amino end of the peptide, while the two lysines occur toward the carboxyl end. They are thus positioned to stabilize a helix dipole.

Similar arguments point to stabilization of β-strands at pH 5.5 and of α-helices at neutral pH in the vicinity of Asp^{63}, Glu^{93}, Asp^{266}, Asp^{271} and Glu^{295} (not shown). With exception of Glu^{93}, all of these potentially helical sequences are in regions which homology modeling indicates have β-loop-β conformations (Lipke et al., 1995; Grigorescu et al., in preparation). Indeed, those regions predicted to be α-helical at pH 8.5 by at least three of four criteria [Chou-Fasman (Chou and Fasman 1974), Garnier–Robson (Garnier et al., 1978), hydrophobic moment (Eisenberg et al., 1984), and charge interactions] account for 17% of the residues in α-agglutinin$^{20-351}$. The CD spectra at this pH value are consistent with a helical content of about 18% (Figure 8).

At pH values well below the optimum for agglutination activity, full protonation of the acidic residues would eliminate charge repulsion, and, as with polyglutamic acid at low pH, would allow the helical propensities to emerge.

Thus although the peptide I sequence can be consistent with a β-structure, its helical propensities are strong enough to assert themselves in the absence of countervailing tertiary interactions, and it is these interactions in the protein which are

weakened by pH and temperature, while local interactions are potentiated in the peptides by TFE.

Role of the Binding Regions and the Physical Constraints: A similar argument applies to peptide II, which is among the regions of α-agglutinin with high helical potential that are also implicated in ligand binding. For example: the E-F loop of domain III is a well-characterized component of the binding site for the ligand a-agglutinin and includes His^{292}, which is required for activity and protected by binding to ligands (Cappellaro et al., 1991; de Nobel et al., 1996). Peptide II, based on this region, showed high helical content at all tested pH values in the presence of TFE (Figure 14). This region has a β-loop-β structure in the molecules in the Ig superfamily and is presumably similar in α-agglutinin (Williams and Barclay 1988; Williams et al., 1989; Chen et al., 1995, Lipke et al., 1995; Grigorescu et al., in preparation). Therefore, physical constraints from neighboring regions and non-local interactions must be essential to determine the conformation of the model peptide in the native protein. Another example of such stabilization by the peptide backbone is from the CD study of Arg-C digestion. Cleavage of the backbone between Lys^{154} and Ser^{155} in the region of peptide I slightly increased helical content (not shown). Similarly, the disulfides must constrain part of the protein to all β-conformation because reduction leads to an increase of helical content to about 7%, the equivalent of about 20 residues (Figure 11). This constraint is in addition to the conventional function of disulfides in stabilizing the hydrophobic core of the Ig domains, including α-agglutinin (Amzel and Poljak 1979; Manning and Woody 1987; Williams et al., 1989; Baldwin et al., 1993; Chen et al., 1995, Lipke et al., 1995; Grigorescu et al., in

preparation). A similar shift may also occur in the region of the peptides when the solution conditions are changed.

A Basis for Low pH Stability: Some aspects of the stability of α-agglutinin were different from other members of Ig superfamily. For example, α-agglutinin was labile to high pH and unusually stable to acid (Figure 8). Such stabilization at low pH might be induced by strengthened inter-strand hydrogen bonds (Worobec et al., 1988; Yang et al., 1994; Molinari et al., 1996). The conformational stability at pH 3.5 (Figure 8) implies that the pH 4.0 threshold for agglutination activity was due to protonation of one or more amino acid residues critical for binding, an interpretation consistent with the rapid recovery of activity upon resuspension at pH 5.5. The acid stability of α-agglutinin may relate to its acidic nature: α-agglutinin$^{20\text{-}351}$ has a theoretical isoelectric point at pH 3.98, making it anionic at pH 5.5. In contrast, other members of the Ig superfamily have basic isoelectric points and are cationic (4 to 12 net positive charges) near the physiological pH. The pI of α-agglutinin reflects a paucity of basic residues in the sequence rather than an abundance of acidic residues relative to other members of the Ig superfamily (not shown). The deficiency in cationic groups would cause more severe charge repulsion at neutral pH and less instability at low pH.

Mechanism of the Conformational Switching: Conformational switching of α-Agglutinin was reversible at pH values between 1.5 and 8.5 and temperatures below 55°C, conditions in which the inactivation was also reversible (Figures 8-10). The energy difference between β and α structure must be small to enable the switching. In each case of reversible switching, however, there was retention of a large amount of β-sheet, which might serve as a "core" to nucleate refolding of the rest of the protein (Ptitsyn et al.,

1979; Jennings et al., 1991; Baldwin 1994; Kuwajima et al., 1996; Browne et al., 1997). The denaturation of α-agglutinin under more severe conditions might be due to the destruction of the core, with hydrogen bonds to solvent replacing inter-strand bonds (Privalov and Tsalkova 1979; Caflisch and Karplus 1994; Menendez et al., 1995). As a specific example, the β-sheet content was retained even after Arg-C cleavage at Lys^{154} in domain II (not shown), and as mentioned above, the digested fragments were only separable if the pH was raised to 7.8. This implies that charge interactions can destabilize the core of this region in domain II (Chen et al., 1995; Grigorescu et al., in preparation).

Importance of Conformational Switching: Conformational changes in proteins play important biological roles. For instance, dramatic transitions from non-helical to helical structures in viral fusion proteins are essential in promoting fusion of the virus and the target cell membranes (Carr and Kim 1993; Bullough et al., 1994; Chan et al., 1997; Weissenhorn et al., 1997). Helix to β-strand switching in the amyloid and prion proteins appears to be involved in diseases such as scrapie, bovine spongiform encephalitis and possibly Creutzfeld-Jacob and Alzheimer's diseases (Prusiner 1991).

In the hemagglutinin (Bullough et al., 1994) and HIV (Chan et al., 1997) proteins the changes are irreversible, being triggered in the former case by the low pH of the endosome during endocytosis and in the latter by interaction with CD4. In the intact amyloid and prion proteins (Prusiner 1991) the changes are also essentially irreversible under biological conditions, the β-forms aggregating *in vivo* and *in vitro* to form plaques and fibrils, although a large peptide from the prion protein undergoes a reversible transition (Jackson et al., 1999). Like hemagglutinin, the amyloid switch is triggered by lowered pH, while the prion conversion appears to involve both low pH and reduction of

a disulfide. In all four of these, the protein sequences that are involved have strong propensities for the secondary structures adopted after conversion, propensities which are overridden by tertiary interactions in the preconversion forms. When environmental conditions weaken long range effects, local interactions come to the fore and drive the conformational transitions. α-Agglutinin is similar in that low and high pH relax long range constraints, allowing the underlying local propensity, in this case for α-helix, to manifest itself.

Where α-agglutinin differs from these is that pH values both below and above the optimum for activity produce the changes and that the changes are reversible under biologically relevant conditions. The yeast protein must be able to survive changes in extracellular pH and temperature yet return to the native state when conditions are right. In all the examples cited, the strong propensity to form a specific secondary structure is overridden by interactions in the native molecule.

These proteins behave in a manner opposite to the dimeric yeast repressor protein Matα2p (Tan and Richmond 1998) and Minor and Kim's "chameleon" sequence (Minor and Kim 1996). Matα2p contains an eight amino acid sequence in the DNA-binding region that forms a β-strand in one monomer and an α-helix in the other monomer (Tan and Richmond 1998). The chameleon sequence is an eleven residue peptide which is α-helical when it is in one region of its protein and in a strand-turn-strand conformation when it is in another. In these cases, the local secondary structure propensities are ambiguous (not shown), and the long range interactions of the tertiary context determine the conformation.

In summary, α-agglutinin has unusual solution properties in that it shows reversible inactivation and formation of α-helical regions when brought to pH values either above or below the optimum for activity but within the range at which the cells survive. The helical propensity is in compliance with sequence-based secondary structure predictions. It should be pointed out that these prediction methods are based mostly on structures of proteins at neutral pH. In a protein active at acidic pH, other structures (β-sheets) are often stable and native. These structures may be identified by a combination of secondary structure prediction algorithms in conjunction with simple local sequence-based rules of charge interaction (Dalal et al., 1997).

Chapter III

Characterization of the Interaction of Cell Adhesion Molecules, α-Agglutinin and a-Agglutinins, in Sexual Agglutination

Introduction

Interaction of ^{125}I-α-agglutinin to a-agglutinin on **a** cells was previously studied by Terrance et al. (Terrance et al., 1987). ^{125}I-α-Agglutinin showed specific interaction to a-agglutinin. Terrance et al. made the hypothesis that the binding has two states, the weak and the tight state. The weak state refers to a reversible and cold sensitive interaction, and the tight state refers to an irreversible interaction (Lipke et al., 1987). The ^{125}I-α-agglutinin Terrance et al. used, however, was a mixture of partially purified proteins with some protein fragments having unclear binding activity. k_{off}, the dissociation rate constant and k_{on}, association rate constant could not be determined.

In this chapter, in order to explore the existence of two-state interaction of agglutination and its dependence on cold temperature, highly purified α-agglutinin was radioactively labeled, and its binding to a-agglutinin on intact **a** cells at both cold and room temperature was examined. BIAcore instrumentation was applied in order to explore detailed kinetics of the agglutination in real time. The BIAcore system allows a quantitative analysis of molecular interactions in real time by using surface plasmon resonance ("SPR"), which detects changes in optical properties at the surface of a thin gold film on a glass support (Johnsson et al., 1991, Mckeithan 1995, Alam et al., 1996, Corr et al., 1996). Purified Aga2p, the binding subunit of a-agglutinin, was immobilized on the sensor surface and its interaction to α-agglutinin flowing over the sensor surface was examined. The conformation of α-agglutinin was studied using Circular Dichroism (CD) at conditions mimicking binding.

The agglutinins bound to each other with high affinity, and a very slow dissociation rate was shown from both isotopic labeling and "SPR" studies. Our CD data

suggested that the interaction of the agglutinins with high affinity and a slow dissociation rate was related to conformational changes of the proteins. A model of ligand-binding induced conformational changes of the agglutinins was developed. It is similar to the induced-fit model of the interaction of substrates and enzymes. The hydrophobic effect appeared to be involved in driving the high affinity interaction between the agglutinins. Conformational changes of the agglutinins induced by binding enhance the interaction of the proteins.

Materials and Methods

Material: The following reagents were obtained from Sigma Chemical Company, St. Louis, Mo: Cycloheximide, p-chloromercuribenzoic acid (PCMB), α-methylmannoside. Protein standards and Bio-Gel P-60, Bio-Gel P-100 were purchased from Bio-Rad. Restriction enzymes were from New England Biolabs. Endoglycosidase H were from Boehringer Mannheim. All the Biacore experiments were performed on BIACORE X (Biacore AB, Uppsala, Sweden). The BIAcore X instrument and reagents for the interaction analysis including the sensor chip (C_1 sensor chip), N-hydroxysuccinimide (NHS), N-ethyl-N'-(3-dimethylaminopropyl)-carbodiimide hydrochloride (EDC), 1M ethanolamine, pH 8.5, were obtained from Pharmacia Biosensor AB (Uppsala, Sweden).

Strains: *S. cerevisiae* haploid strains were obtained from Yeast Genetics Stock Center, Berkeley, Calif. Wild type strains X2180-1A (*MAT*a *SUC2 mal mel gal2 CUP1*) and X2180-1B (*MAT*α *SUC2 mal mel gal2 CUP1*) were used for routine assays (Terrance and Lipke 1981).

Purification of Aga2p: W303 diploid cells containing pYEpPGK-AGA2 constitutively expresses Aga2p under the control of PGK prompter. Cells were grown in synthetic medium with minus uracil to 4 X 10^7 /ml and harvested. Cell culture supernatant was then collected and concentrated roughly 10-fold through a Millipore filter with a 10 kDa molecular weight cutoff. Concentrated supernatant was further dialyzed against 20 mM sodium acetate, pH 5.5, 1 mM EDTA, lyophilized, and resuspended in the same buffer with 10% (Vol/vol) glycerol. Aga2p was purified by Shen using a Bio-Gel P-60 size exclusion column equilibrated in 20 mM sodium acetate, pH 5.5.

Aga2p is highly glycosylated with an apparent molecular weight of 30 kDa on Coomassie Blue stained SDS-PAGE (Figure15).

Purification of α-agglutinin: α-Agglutinin$^{20-351}$ was purified from cell culture supernatant (4 Liters) of yeast strain Lα21 (*MATα ade*2-1 *his*3-11,15 *leu*2-3,112 *trp*1-1 *ura*3-1 *can*1-100 *agα*1-3) containing pPGK-AGα1^{351}. A DEAE-Sephadex A-25 column and a Bio-Gel P-60 size exclusion column were used for the purification (Detail procedure see Chapter II). α-Agglutinin$^{20-351}$ has an apparent molecular weight of 45 kDa on Coomassie Blue stained SDS-PAGE and is of 99% purity by scanning densitometry (Molecular Dynamics) (Figure 15).

Polyacryamide gel electrophoresis: The protein samples were electrophoresed in SDS or non-SDS polyacrylamide gels (10% as running gel and 4% as stacking gel) and stained by Coomassie brilliant blue (Bio-Rad laboratories).

Anti-α-agglutinin Preparation: Anti-α-agglutinin was produced by injecting purified protein (100 μg twice) in Hunter's Titemax into the rabbit and the sera of rabbits were then collected after the injection. Anti-α-agglutinin was adsorbed against **a** cells, which was grown in minimal medium (YNB). The cells were first washed with 50 mM Tris buffer pH 7.4, 150 mM NaCl twice and then heat killed at 60°C for 2 hours before the absorption. The absorption of anti-α-agglutinin took place at 4°C twice for a total of 12 hours and was retrieved by centrifugation, and stored at -20°C.

Separation of α-agglutinin Aggregates and Immunodetection by Western Blotting: The purified α-agglutinin sample taken out from -20°C freezer was thawed and run through Bio-Gel P-100 column. 100mM sodium acetate pH 5.5 was used as the running buffer. The samples collected from the column were electrophoresed in 10%

Figure 15. SDS-PAGE Analysis of α-Agglutinin and Aga2p. Protein samples were electrophoresed in SDS on a 10% polyacrylamide mini-gel, and the gel was stained with Coomassie Blue. Lane 1: Low molecular weight standards (Bio-Rad) were as follows: phosphorylase b, 97,400; bovine serum albumin, 66,200; ovalbumin 45,000; carbonic anhydrase, 31,000; soybean trypsin inhibitor, 21,500; lysozyme 14,400; Lane 2: Aga2p: glycosylated protein with apparent molecular weight of 33 kDa.; Lane 3: α-agglutinin: glycosylated protein with apparent molecular weight of 45 kDa; Lane 4-7: BSA: 1 to 8 μg. a-Agglutinin is highly glycosylated and diffuses out of Coomassie Blue stained gels. Therefore, the a-agglutinin band is light.

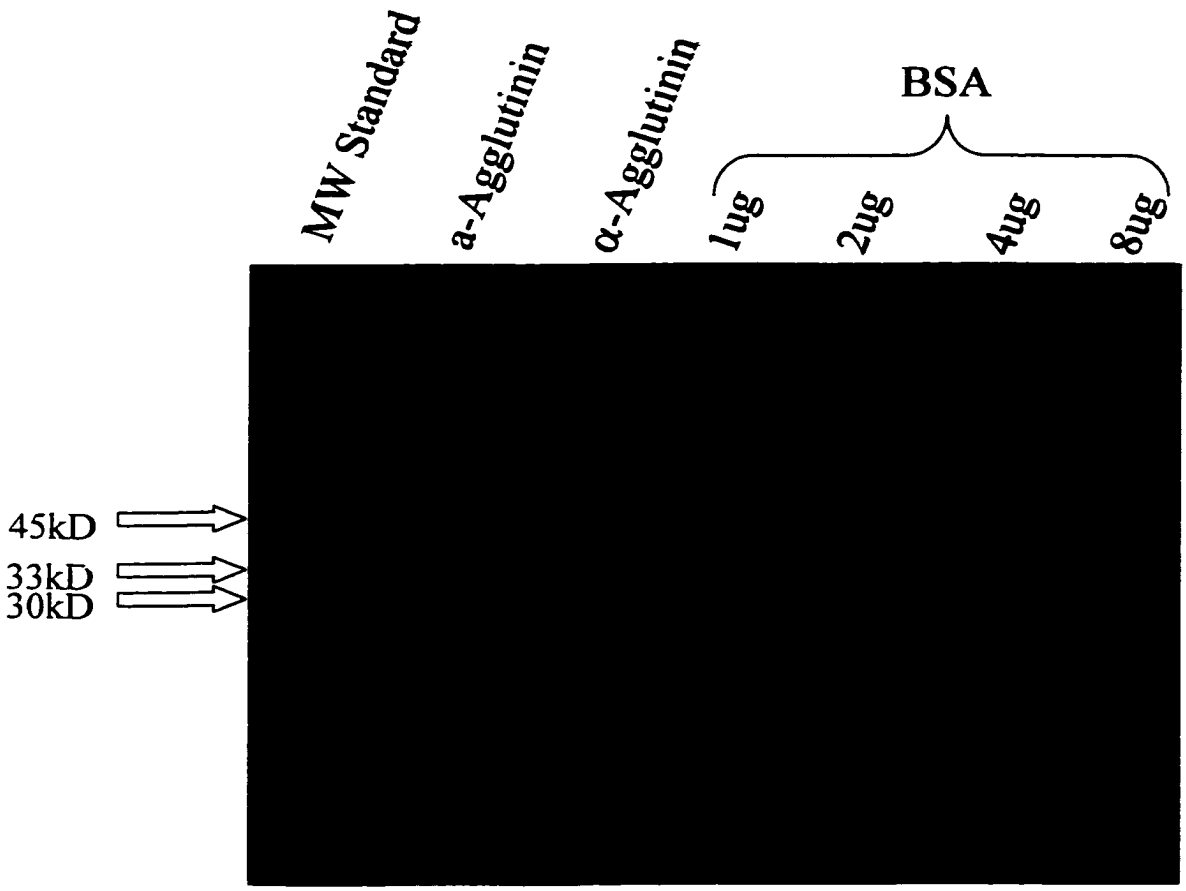

non-SDS and SDS polyacrylamide gels and then transferred to nitrocellulose membrane by electrophoresis. The blot was first incubated in 10mM Tris and 140mM NaCl pH 7.4 (buffer B) with 3% gelatin for 30 minutes followed by incubation of anti-α-agglutinin (1:500) for 1 hour. Afterwards, the blot was washed and incubated in anti-rabbit IgG peroxidase conjugate (1:1000) in B buffer with 1% gelatin for 1 hour. The blot was then washed and visualized in the mixture of 4-chloro-1-naphthol in 10 ml of cold methanol and 3% hydrogen-peroxide in 50 ml of buffer B. The sample containing no aggregates was used for BIAcore studies.

BIAcore usage: The kinetic studies of a-agglutinin and α-agglutinin using "SPR": The detection of the BIAcore instrument is based on the changes in the refractive index due to association of an analyte to the immobilized ligand or due to the dissociation of the formed complex. The resulting signal is proportional to the amount of protein bound with 1000 resonance units (RUs) corresponding to 1 ng/mm^2 (Johnsson et al., 1991). The flat carboxymethylated surface of the C_1 sensor chip was first cleaned by 10 µl 0.1M Glycine-NaOH and activated by 35 µl 0.4 M EDC/ 0.1M NHS (1/1) mixture at a flow rate of 5 µl /min. Then, 25 µl of a-agglutinin (5 µg/ml) in 100 mM phosphate buffer was injected onto the surface at a flow rate of 5 µl/min, twice. The remaining unreacted NHS-ester groups were blocked (deactivated) by injection of 25 µl 1M ethanolamine-HCl, pH 8.5, and the surface was further blocked by injecting 25 µl of 100 ug/ml bovine serum albumin (BSA), twice. The flow rate for blocking was 5 µl /min. The immobilization run was performed in HBS buffer (10mM Hepes and 150 mM NaCl, pH 7.4).

The instrument was primed three times after switching the buffer from HBS to MES buffer (10mM MES and 150mM NaCl, pH 5.9). The surface was then blocked by injection of BSA after switching the buffer, twice. After that, the association and subsequent dissociation was measured by the injection of 100μl aliquots of α-agglutinin with different concentrations at flow rate of 20 μl/min over the sensor surface and washed with delay time of 300 seconds. MES buffer was used as the running buffer for the binding interaction of a-agglutinin and α-agglutinin. The sensor surface was regenerated by injection of 100 μl of 4 M magnesium chloride ($MgCl_2$). Two temperatures, 10°C and 20°C were used for studying the kinetics of the binding between the two proteins.

"SPR" detects changes in refractive index close to the sensor surface. The refractive index change resulting from analyte bound to the ligand on the surface is monitored continuously, and the binding curve is directly visualized on a computer screen (Karlsson et al., 1991, Johnsson et al., 1991). Data analysis can be performed using BIA evaluation 3.0 software package (Pharmacia Biosensor AB), which allows non-linear fits of the experimental data to the standard. The association rate constant (k_{on}) and the dissociation rate constant (k_{off}) can be obtained from curve fitting. And the affinity constant K_D can be calculated from the equation: $K_D = k_{off} / k_{on}$.

Isotopic labeling of α-agglutinin by ^{125}I-Bolton Hunter reagent: Purified α-agglutinin (0.1mg/ml) was dialyzed against 200 mM sodium phosphate buffer, pH 8.5 overnight. 20μg of protein reacted with 250uCi of ^{125}I-Bolton-Hunter reagent (New England Nuclear Corp.) for 3 hours at 0°C. The reaction mixture was then diluted 20-fold in the reaction buffer (100 mM sodium acetate, pH 5.5, 1 μM $CaCl_2$ and 1 μM $MnSO_4$).

The diluted sample was then applied to a 1ml pre-packed lentil lectin-agarose column, which was pre-equilibrated with reaction buffer. The protein was eluted by 1M α-methylmannoside and 500 mM sodium chloride in 100 mM sodium acetate, pH 5.5. The labeled α-agglutinin was stored at 4°C in the eluting buffer supplemented with 10% glycerol and 1mg/ml Bovine Serum Albumin (BSA).

Concentration Determination of ^{125}I-α-agglutinin: ^{125}I-α-Agglutinin of 5μl and different amount of unlabeled α-agglutinin were incubated with 2 X 10^6 **a** cells or α-cells in 200 μl total volume on the rotary shaker at 200 rpm for 90 minutes. 10 μl ^{125}I-α-Agglutinin was used to incubate with 2 X 10^6 **a** and α cells to obtain the maximum binding capability of 2 X 10^6 **a** cells to α-agglutinin. After incubation, the cells with bound ^{125}I-α-agglutinin were washed and counted by a Compugamma 1282 Gamma Counter (LKB Wallac Inc). The concentration of ^{125}I-α-agglutinin was calculated from the unlabeled α-agglutinin with known concentration. The binding of ^{125}I-α-agglutinin to a-agglutinin could be competitively inhibited by addition of unlabeled α-agglutinin and at 50 % inhibition point, ^{125}I-α-agglutinin and unlabeled α-agglutinin have equal concentration (Berson et al., 1956; Berson and Yalow 1958).

Binding of ^{125}I-α-agglutinin to a cells: Various concentrations of ^{125}I-α-agglutinin were incubated with 2 X 10^6 **a** cells in a total volume of 250μl on rotary shaker at 200 rpm at 25°C or 0°C for 90 minutes, the time required to reach equilibrium. The buffer used for this study was 100 mM sodium acetate, pH 5.5, supplemented with 1mg / ml BSA, 1μg / ml cycloheximide, and 1uM PCMB (protease inhibitor). The inclusion of PCMB is provided in order to stabilize the agglutinability of the protein (Terrance et al.,

1987). After the incubation, **a** cells with bound α-agglutinin were centrifuged, the supernatants were aspirated and the cells were then washed three times. The bound ^{125}I-α-agglutinin on both **a** cells and α cells were counted in an Universal Gamma Counter: Compugamma 1282 (LKB Wallac Inc). The specific binding was determined as the difference in the binding to **a** and α cells under identical conditions since nonspecific binding was similar in **a** cells and α cells and was neither saturable nor competable (Terrance et al., 1987). Equilibrium constants were determined from Scatchard plot analysis of the binding.

Dissociation of ^{125}I-α-agglutinin from the complexes of ^{125}I-α-agglutinin and a cells: ^{125}I-α-Agglutinin, 5 μl, was incubated with three sets of **a** or α cells (2 X 10^6) in a total volume of 250μl on rotary shaker at 200 rpm for 90 minutes. Cells with bound ^{125}I-α-agglutinin were washed and count. Except the first set of cells, the other two sets of cells was re-suspended in 500 μl buffer and further incubated on rotary shaker at 200 rpm/min for another 17.5 hours and 65 hours, respectively. The cells were then washed and counted. Counts of α cells were subtracted as non-specific binding.

Peptide Synthesis: A peptide containing C-terminal 10 residues of Aga2p was synthesized by the solid phase method using fluorenylmethoxycarbonyl (Fmoc) chemistry on an Applied Biosystems automated model 432A peptide (Detail procedure see: Chapter II).

Agglutination Assay: *Saccharomyces cerevisiae* wild-type haploid strains X2180-1A (*MAT**a** SUC2 mal mel gal2 CUP1*) and X2180-1B (*MATα SUC2 mal mel gal2 CUP1*), were used for the bioassays (Detail Procedure see: Chapter II).

Circular Dichroism (CD) Spectroscopy: Far-UV CD spectra were recorded on a Jasco J-710 spectropolarimeter equipped with a thermo-regulated cell holder with 0.05 cm path length (HELLMA). Each spectrum represents the average of 10 spectra taken at 0.5nm intervals from 250 to 200 nm. The CD data presented here were analyzed by the self-consistent method (SELCON) program (Sreerama and Woody 1993; Sreerama and Woody 1994) (Details see: Chapter II).

Results

Kinetic parameters represent important characteristcs of molecular interaction in understanding the mechanism of molecular recognition. Communications of cell adhesion molecules in higher eucaryotic organism is intriguing. In this chapter, sexual agglutination in yeast, the simplest model of cell adhesion in eucaryotic system, was used to characterize the interaction of cell adhesion molecules, a-agglutinin and α-agglutinin.

Terrance et al. have proposed that the binding of α-agglutinin to a-agglutinin on intact **a** cells having two states (Terrance et al., 1987). The weak state refers to an interaction dissociable by washing with bound and free agglutinin in kinetic equilibrium, and the tight state refers to the interaction non-dissociable by washing, with the bound agglutinin removable only by disruptive reagents, such as high pH or detergents (Lipke et al., 1987). A better defined system needs to be used to confirm if there are indeed two-state interactions; to obtain the values of kinetic constants, k_{off}, the dissociation rate constant, and k_{on}, the association rate; to unveil the basis of reduction of agglutination at cold temperature; and to explore the mechanism of the adhesion between the agglutinins. Isotopic labeling using highly purified proteins, surface plasmon resonance ("SPR"), and CD studies were applied to resolve the above addressed questions.

Characterization of the interaction of the agglutinins using isotopic labeling: Highly purified α-agglutinin (Figure 15) was labeled with ^{125}I Bolton-Hunter reagent and the direct interaction of ^{125}I-α-agglutinin to intact **a** cells was measured. As shown in Figure 16, the concentration of ^{125}I-labeled α-agglutinin was obtained by isotope dilution (Berson et al., 1956; Berson and Yalow 1958) from the concentration of known unlabeled α-agglutinin by their competitive binding to **a** cells. Since both labeled and non-labeled

α-agglutinin can bind to **a** cells equally, at lower concentration of unlabeled α-agglutinin, there was more ^{125}I-α-agglutinin bound. However, there was less ^{125}I-α-agglutinin bound at higher concentration of unlabeled α-agglutinin. At the midpoint of the curve in Figure 16, the interaction of labeled and non-labeled α-agglutinin to **a** cells was equal and the labeled and non-labeled α-agglutinin had equal concentration. Since 0.192 μl of 0.1 μg/μl (2.72 μM) non-labeled α-agglutinin is equivalent to 5μl of ^{125}I-α-agglutinin, the concentration of ^{125}I-α-agglutinin was therefore calculated to be 0.0038 μg /μl (0.104 μM).

In order to obtain an accurate equilibrium constant, ^{125}I-α-agglutinin was incubated with 2 X 10^6 **a** cells for 90 minutes at both 25°C and 0°C. As indicated in Figure 17, the binding at 25°C and 0°C showed only slight differences in the dose-response saturation level. When the protein concentration reached 5 nM or higher, the binding became saturated. The inset of Figure 17 shows Scatchard plots of the binding, displaying a K_D of 6.34 X 10^{-10} M at 0°C and K_D of 8.6 X 10^{-10} M at 25°C. There were about 7.5 X 10^4 α-agglutinin/cell and there are no obvious weak interactions observed at either temperature. Therefore, the weak interaction seen in previous studies by Terrance et al. in 1987 might be due to some fragments of α-agglutinin, which had partial adhesive activity and lower binding affinity (Terrance et al., 1987).

The dissociation rate constant was measured by extending the dissociation time over 3 days. Three sets of samples were used. In each set, **a** cells and ^{125}I-α-agglutinin in triplicate were incubated for 90 minutes and **a** cells bound with radioactive labeled ^{125}I-α-agglutinin were centrifuged and washed with reaction buffer. The first sets of **a** cells bound with ^{125}I-α-agglutinin were counted directly after washing. The other two sets of **a**

Figure 16. Concentration Determination of ^{125}I-α-Agglutinin. Increasing amounts of unlabeled α-agglutinin and 5 μl of ^{125}I-α-agglutinin were incubated with $2X10^6$ **a** or α cells at 25°C for 90 minutes. After washing, **a** Cells and α cells bound with ^{125}I-α-agglutinin were counted by gamma counter. α Cells with ^{125}I-α-agglutinin bound were used to estimate non-specific interactions. Error bars represent the range for triplicate samples. The midpoint labeled on the graph is the point where labeled and unlabeled proteins had equal ability in binding to **a** cells.

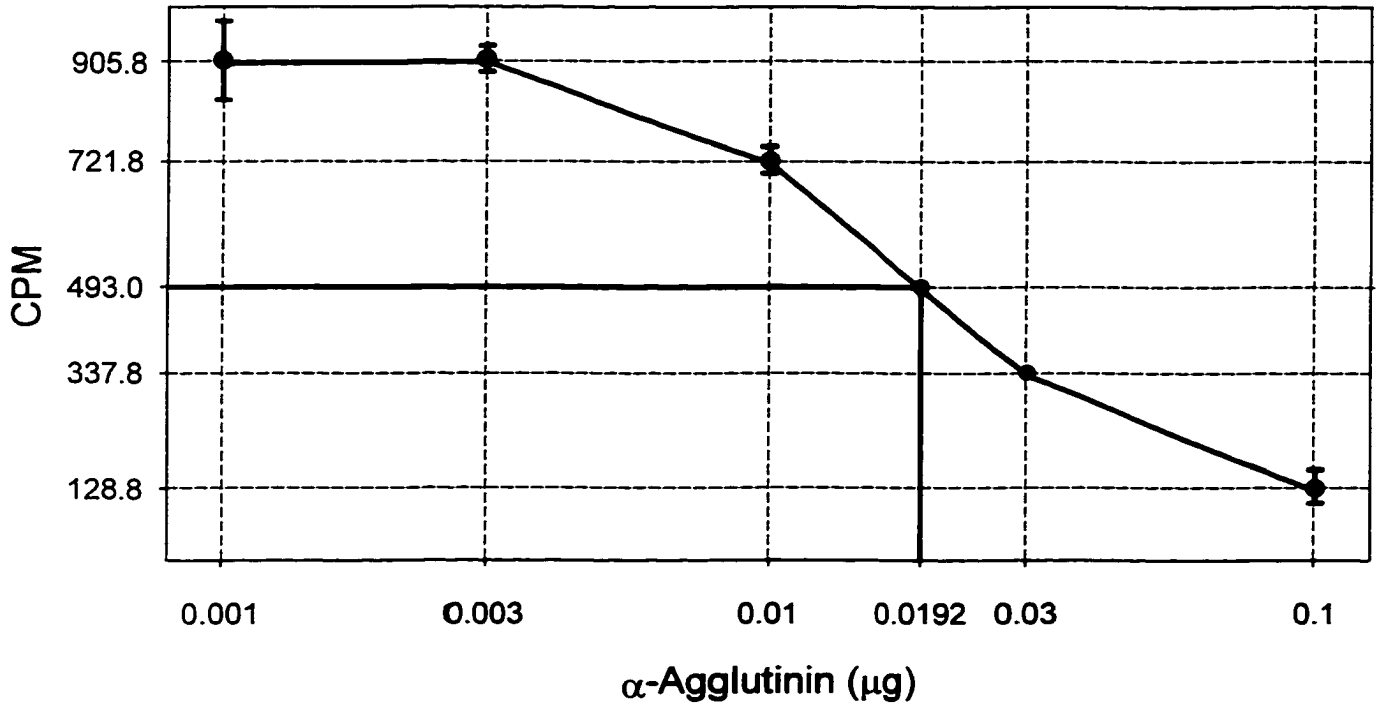

Figure 17. The Interaction of Purified ^{125}I-α-Agglutinin with a Cells at 25°C and 0°C. Increasing concentrations of ^{125}I-α-agglutinin were incubated with 2X10^6 **a** cells or α cells for 90 minutes at 25°C and 0°C. After thorough washing, **a** Cells and α cells with bound ^{125}I-α-agglutinin were counted by gamma counter. α Cells with ^{125}I-α-agglutinin bound were used for estimation of non-specific interactions. After subtracting the nonspecific binding, specific interactions of bound ^{125}I-α-agglutinin on **a** cells were plotted at 25°C (—●—) and 0°C (—▲—). Error bars represent the range for triplicate samples. Inset: data were plotted by the method of Scatchard for calculating equilibrium constant.

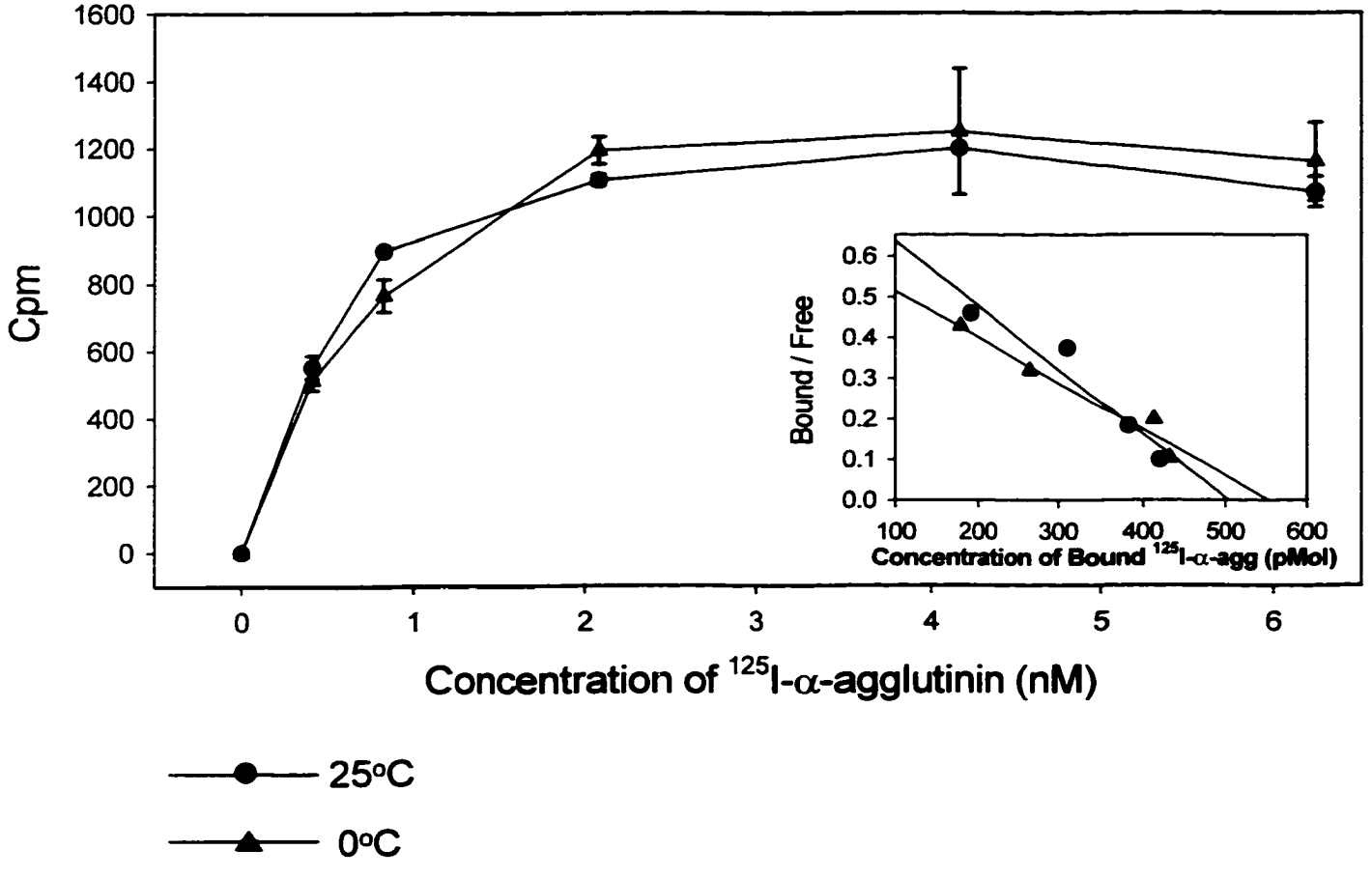

cells bound with ^{125}I-α-agglutinin were re-suspended in 500 μl binding buffer and incubated for another 17 hours and 65 hours, respectively. After incubation, a cells bound with ^{125}I-α-agglutinin were washed and counted. As shown in Figure 18, a slow dissociation rate with k_{off} of about 10^{-6} s^{-1} was calculated from the linear regression of the dissociation curve.

Characterization of the kinetics of the interaction between the agglutinins using surface plasmon resonance ("SPR"): From the experiments with radioactive-labeled α-agglutinin, low temperature was found to have little effect in the dose-response saturation level of the interaction. However, previous studies showed that low temperature does reduce the cellular agglutinability both in vivo and in vitro (Terrance and Lipke 1981, Yamaguchi 1982). Surface plasmon resonance ("SPR") was, therefore, used to obtain the dissociation rate constant (k_{off}), the association rate constant (k_{on}), and dissociation constant (K_D) and to detect the effect of low temperature on the interaction of the agglutinins in real time.

"SPR" has recently been applied for real time analysis in diverse biomolecular interactions including cell adhesion, signal transduction, protein/protein interaction, protein-DNA interaction and antibody/antigen interaction (Jonsson et al., 1991; Karlsson et al., 1991; McKeithan 1995; Alam et al., 1996; Corr et al., 1996).

"SPR" detects changes in the refractive index, which is proportional to the mass of the bound analyte on the surface (Karlsson 1994). Therefore, it is advantageous to immobilize the lower molecular reactant as the ligand and to use the larger molecular reactant as the analyte to increase the sensitivity of the system. Also, in order to limit mass transportation and to make sure the reaction reaches equilibrium within reasonable

Figure 18. Dissociation of ^{125}I-Agglutinin from $\underline{a}$ Cells Bound with ^{125}I-Agglutinin. ^{125}I-Agglutinin, 5 μl, was incubated with three sets of **a** or α cells (2×10^6) at 4°C for 90 minutes. The cells bound with ^{125}I-agglutinin were then washed and counted. The other two sets of cells bound with ^{125}I-agglutinin were re-suspended in the binding buffer and incubated for another 17.5 hrs and 65 hrs. The cells bound with ^{125}I-agglutinin were then washed and counted. After subtracting the non-specific counts obtained from α cells bound with ^{125}I-agglutinin, the counts of specifically bound ^{125}I-agglutinin on **a** cells vs time were graphed on a semi-log plot. The straight line in the graph is the linear regression of the interaction points. Error bars represent the range for triplicate samples.

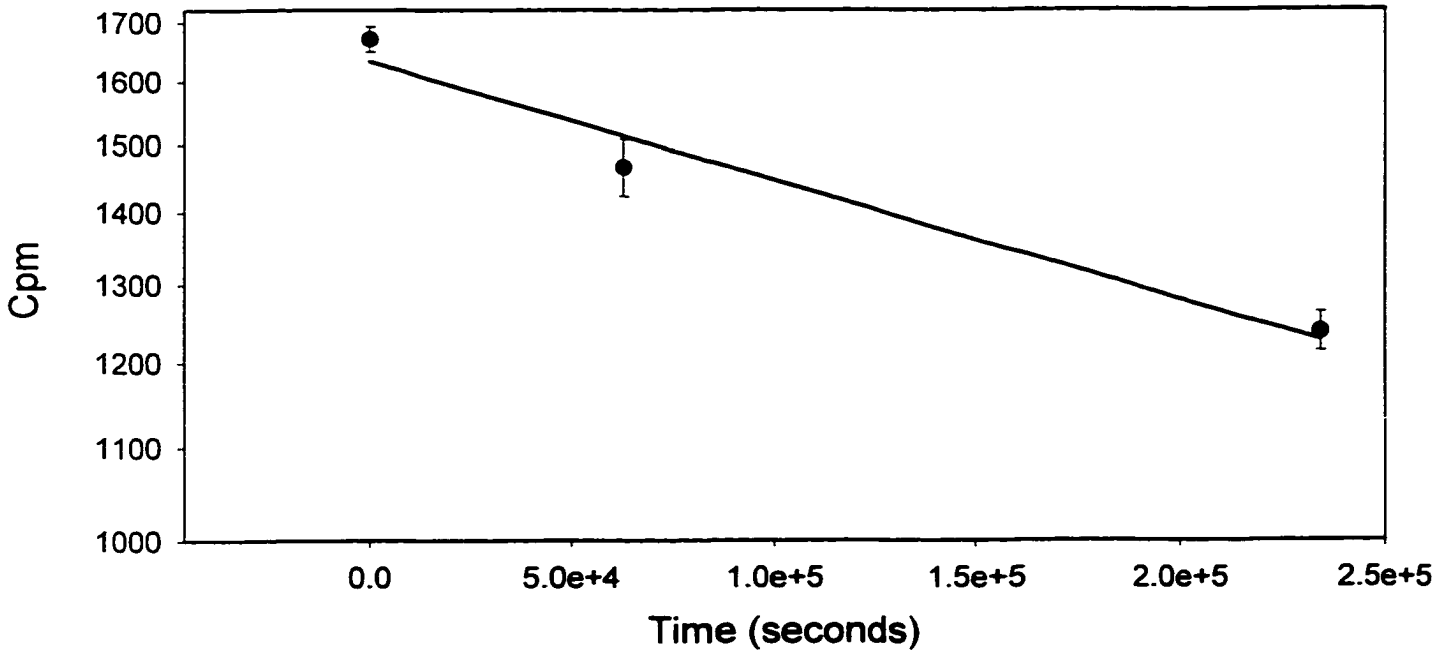

time limits, optimal conditions for the kinetic studies require a relatively low concentration of the protein on the surface.

In order to meet these conditions, Aga2p was immobilized on the sensor surface and the amount of α-agglutinin was adjusted so that the response (RU) of the binding would not be too high. "Sensorgrams" for the interaction of α-agglutinin with different concentrations to the immobilized a-agglutinin at 20°C and 10°C are shown in Figure 19 and 20. The dissociation rate constants and association constants at 20°C and 10°C were obtained by linear regression using SigmaPlot and curve fitting BIA evaluation software. Mean values derived from three concentration of α-agglutinin are summarized in Table I.

"SPR" sensorgrams of the interaction of the agglutinins at 20°C (Figure 19) showed a very slow dissociation rate, with k_{off} of 7.03 X 10^{-5} and a mono-phasic association rate, k_{on} of 4.61 ± 0.03 X 10^{4}. This value was obtained by curve fitting with residual of -0.05 to 0.07 which is within the valid range for curve fitting. The K_D of 1.55 ± 0.11X 10^{-9} at 20°C was calculated from k_{off} and k_{on}. At 10°C, sensorgrams of the interaction of the agglutinins were characterized by k_{off} of 5.42 X 10^{-5} (Figure 20) which is a little slower compared to that at higher temperature. A time dependent sigmoid-shaped association curve was observed. The initial rate was very slow with k_{on1} of 0.13 10^{0} ± 0.07 and was followed by a more rapid association rate of k_{on2} of 5.59 ± 0.4 X 10^{4}. These values gave residuals of -0.06 to 0.14 and -0.03 to 0.04, respectively. At 10°C, K_{D1} of 6.18 ± 3.49 X 10^{-4} and K_{D2} of 9.76 ± 0.68X 10^{-10} were calculated from k_{off} and k_{on}.

"SPR" data showed that the interactions of the agglutinins at both temperatures were characterized with high affinity interaction and very slow dissociation rate which

Figure 19. Sensorgram of the Binding of α-Agglutinin to Aga2p Immobilized on the Sensor Surface at 20°C. (A). Aga2p was coupled to a C1 pioneer chip through amine chemistry. Aliquots (100 μl) at various concentrations of α-agglutinin (31nM, 62nM, 125nM and 250nM) were then injected over the sensor chip at 20 μl /min in 10mM MES buffer + 150mM NaCl, pH 5.9. Sensorgrams of the interaction at 20°C were then recorded. (B). The dissociation data of the interaction at 20°C was exported into Sigmaplot, where ln (RU_{t1}-RU_{t0}) vs time was plotted. The dissociation rate constant, k_{off}, was calculated by linear regression, the line shown in the middle of the graph. (C). Calculation of the association rate constant. Mono-phasic association of the interaction was fitted with standard curves provided by BIAcore software 3.0. The association rate constant was then calculated by curve fitting with residues of -0.05 to 0.07, which is within the range of curve fitting.

A

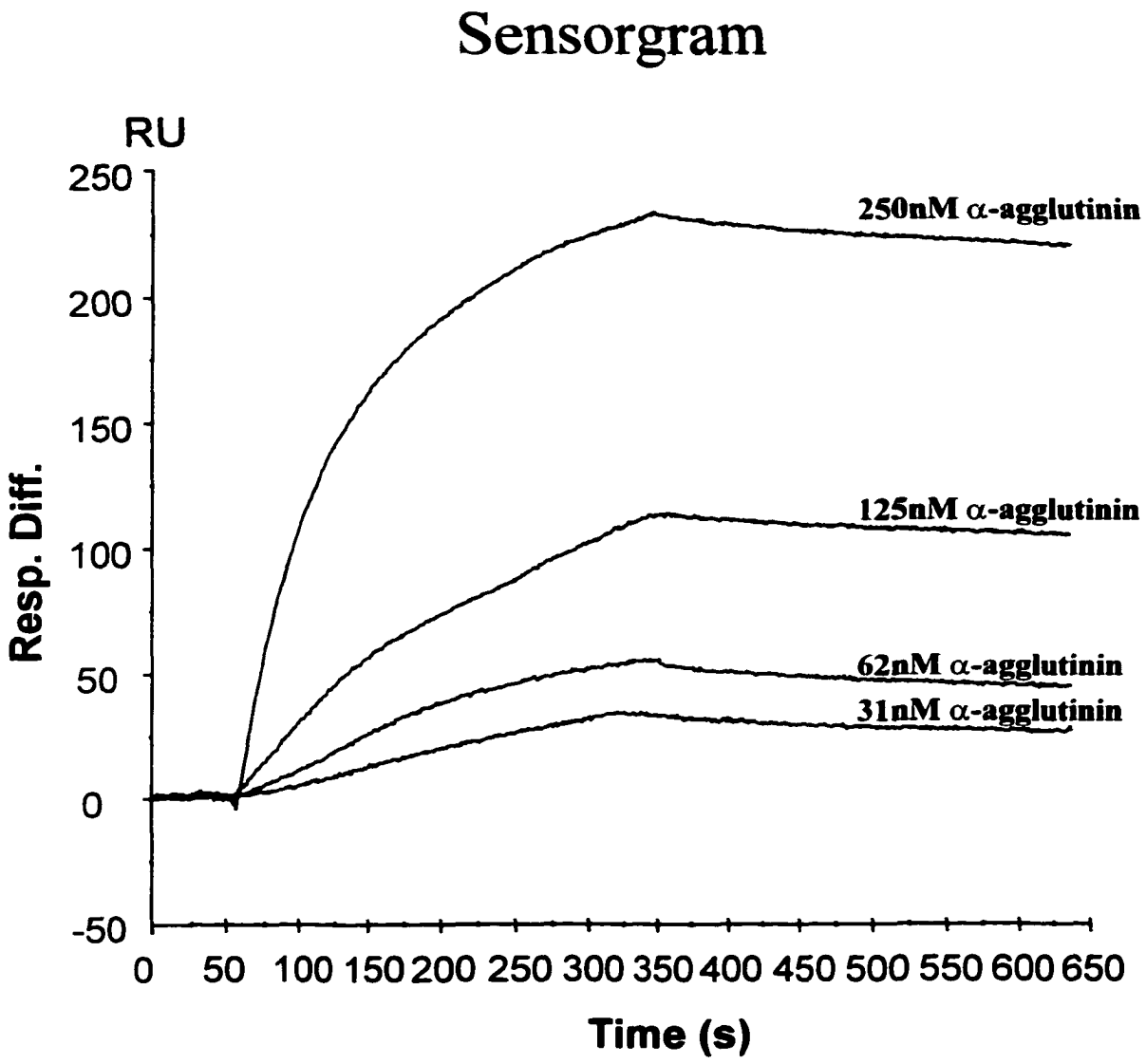

B

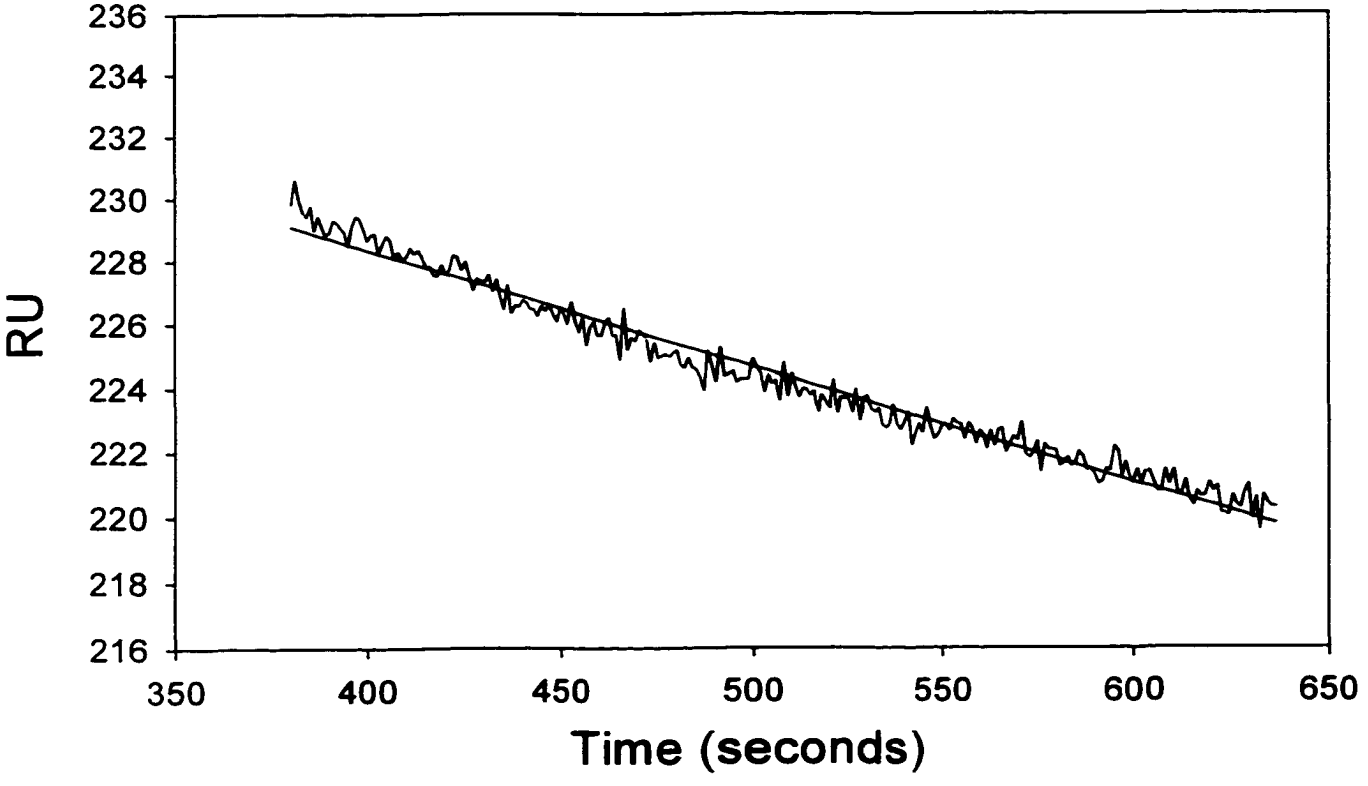

C

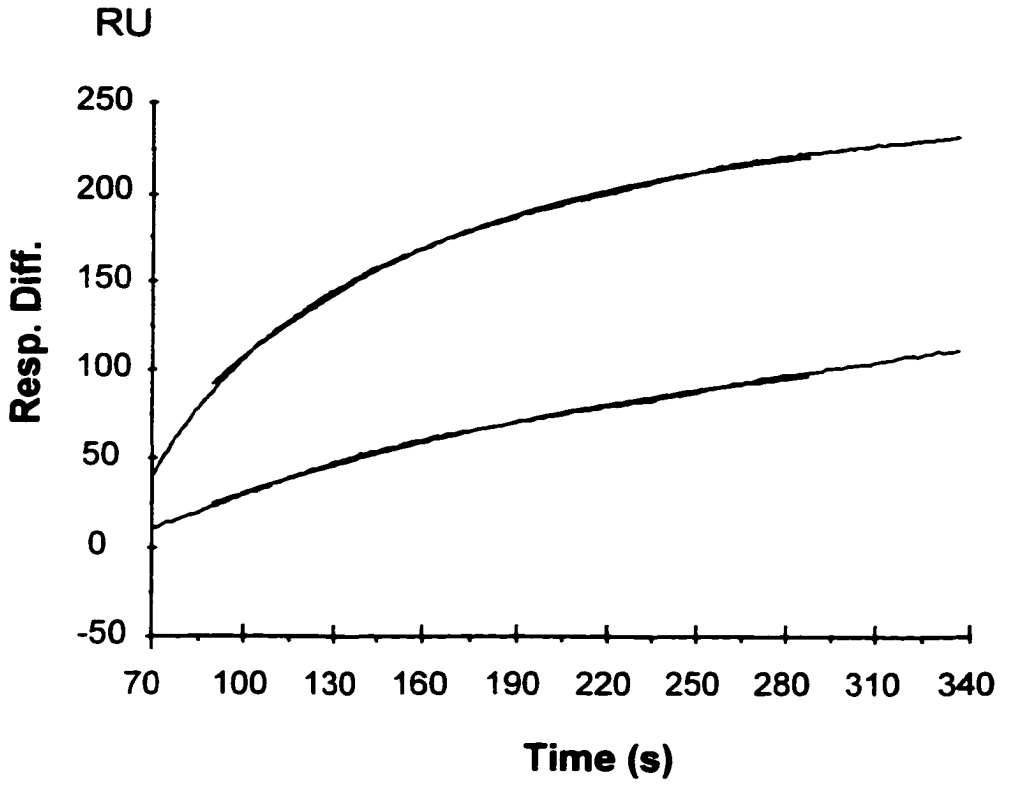

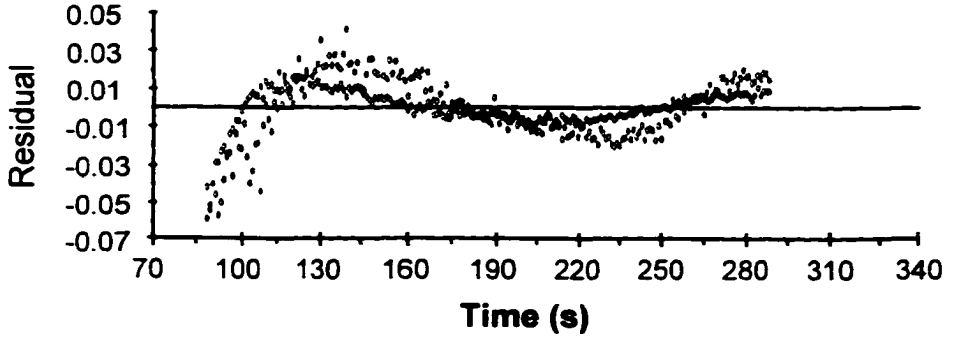

Figure 20. Sensorgram of the Binding of α-Agglutinin to Aga2p Immobilized on the Sensor Surface at 10°C. (A). Sensorgrams of the interaction of Aga2p with various concentrations (31nM, 62nM, 125nM and 250nM) of α-agglutinin to were recorded at 10°C. (B). Dissociation constant at 10°C was calculated using Sigmaplot as described in Figure 19. (C). Calculation of the association rate constant. Two distinct association phases were fitted with standard curves provided by BIAcore software 3.0, respectively. The association rate constants were calculated by the curve fitting with residues of -0.06 to 0.14 and -0.03 to 0.04, respectively, which are within the range of curve fitting.

A

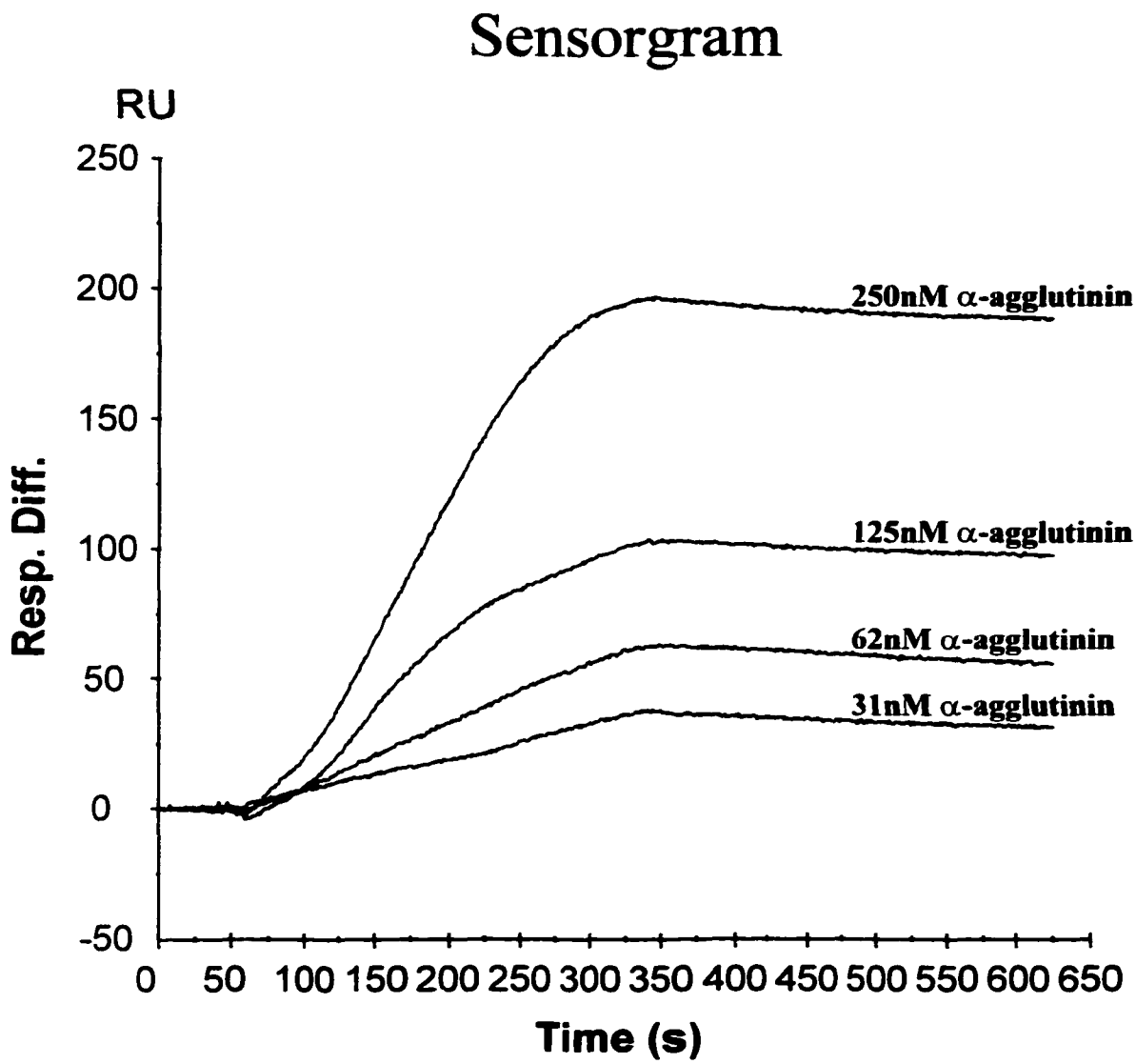

B

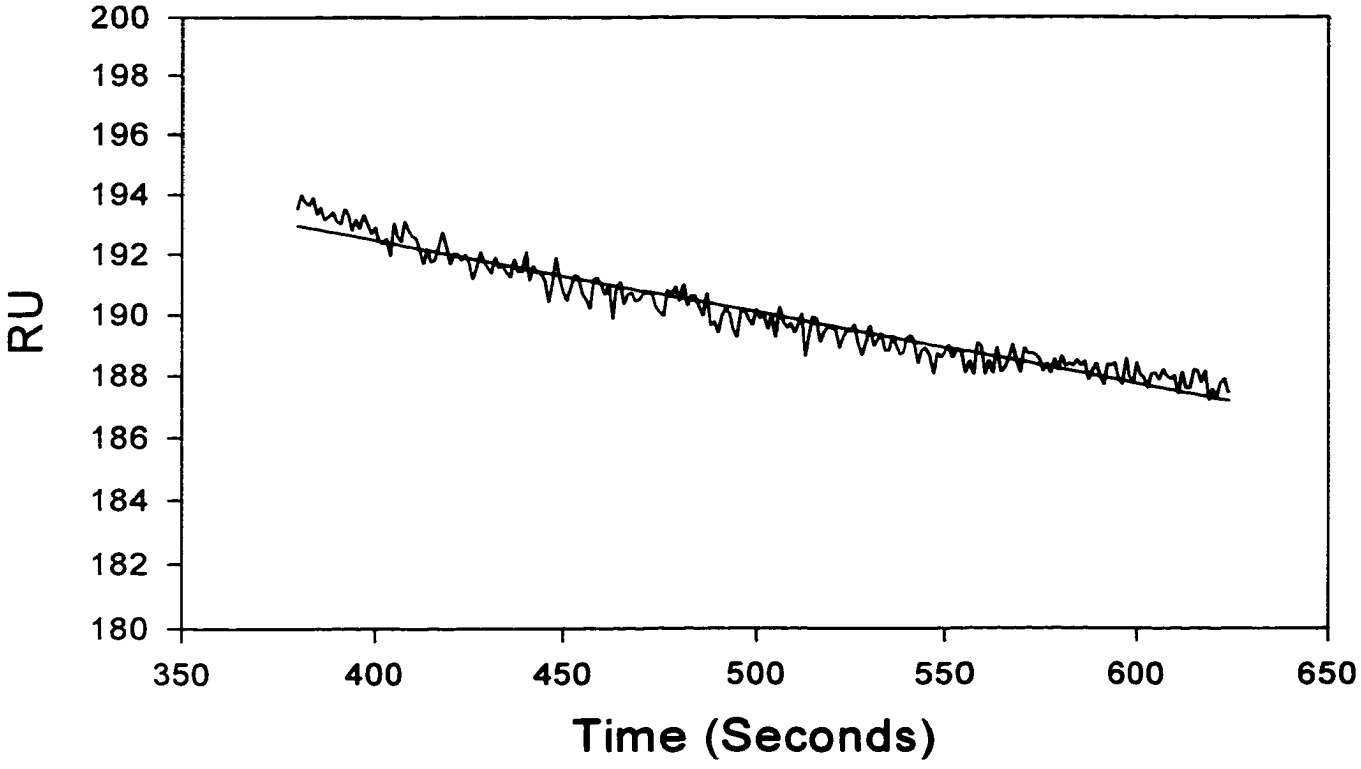

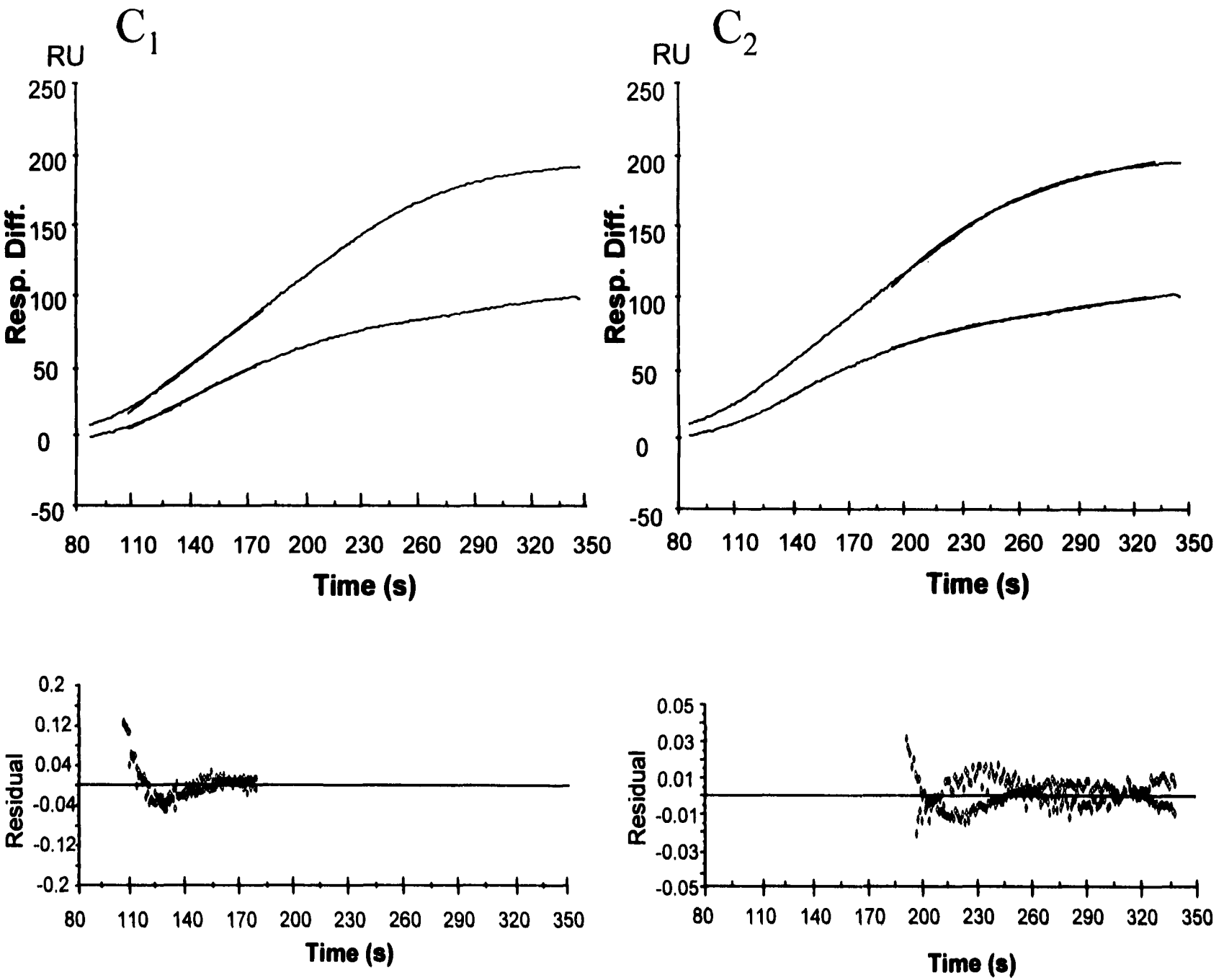

Table I: Summary of Kinetic Constants from SPR Studies

Rate Constant	20°C	10°C
Dissociation (k_{off}) (s^{-1})	7.03×10^{-5}	5.42×10^{-5}
Association (k_{on}) ($M^{-1}s^{-1}$)	$4.61 \pm 0.30 \times 10^{4}$	0.13 ± 0.07, $5.59 \pm 0.4 \times 10^{4}$
K_D (M)	$1.55 \pm 0.11 \times 10^{-9}$	$6.18 \pm 3.49 \times 10^{-4}$, $9.76 \pm 0.68 \times 10^{-10}$

were comparable to the results we obtained from the radioactive-labeling experiment described in the previous section. Interestingly, we also observed a second association rate at a lower temperature.

Elimination of protein aggregates: Protein aggregates may sometimes bind with high affinity and slow dissociation rates in geometric proportion to the number of the binding sites in the aggregates (Yurchenco and Cheng 1993; Kishore et al., 1998). In order to make sure that our results were not an artifact from protein aggregation, gel filtration was used to eliminate aggregated α-agglutinin with MW of 90,000 or higher. As shown in Figure 21, right after purification on Bio-Gel P-100, the sample of α-agglutinin (fraction # 11) with aggregates removed was immediately injected onto the sensor surface. As indicated in Figure 22, a faster dissociation rate characterized by k_{off} of 2.58 X 10^{-4}; a slightly faster association rate characterized by k_{on} of 5.61 ± 2.23 X 10^{4}; and K_D of 5.51 ± 2.19 X 10^{-9} were obtained after aggregates were removed. Our results demonstrated that the interaction of the agglutinins still occurred with high affinity and a slow dissociation rate even after the removal of aggregated proteins.

Conformational changes of the agglutinins induced by a-agglutinin peptide binding: Conformational changes of the proteins during binding could be the cause for this high affinity interaction. Because the agglutinins are highly glycosylated and the sugars interfere with protein crystallization and NMR studies, secondary structure of α-agglutinin under binding conditions was studied using circular dichroism.

A peptide containing the C-terminal 10 residues (GSPINTQYVF) of Aga2p is as functionally active as Aga2p (Cappellaro et al., 1994). We, therefore, synthesized this

Figure 21. Western-Blotting of non-SDS PAGE and SDS-PAGE of α-Agglutinin from Bio-Gel P-100 Column. α-Agglutinin samples collected from Bio-Gel P-100 column were electrophoresed on 10% non-SDS PAGE and 10% SDS PAGE mini-gel, and the proteins were transferred to nitrocellulose membrane by electrophoresis. The proteins were then detected by polyclonal anti-α-agglutinin. (A). non-SDS PAGE: Lane 1: Molecular Weight Standard; Lane2: fraction # 7; Lane3: fraction #9 and Lane4: fraction #11 and Lane5: fraction #13 (B). SDS PAGE: Lane1: Molecular Weight Standard; Lane 2: fraction #14, Lane 3: fraction #12; Lane4: fraction # 10; Lane 5: fraction #8.

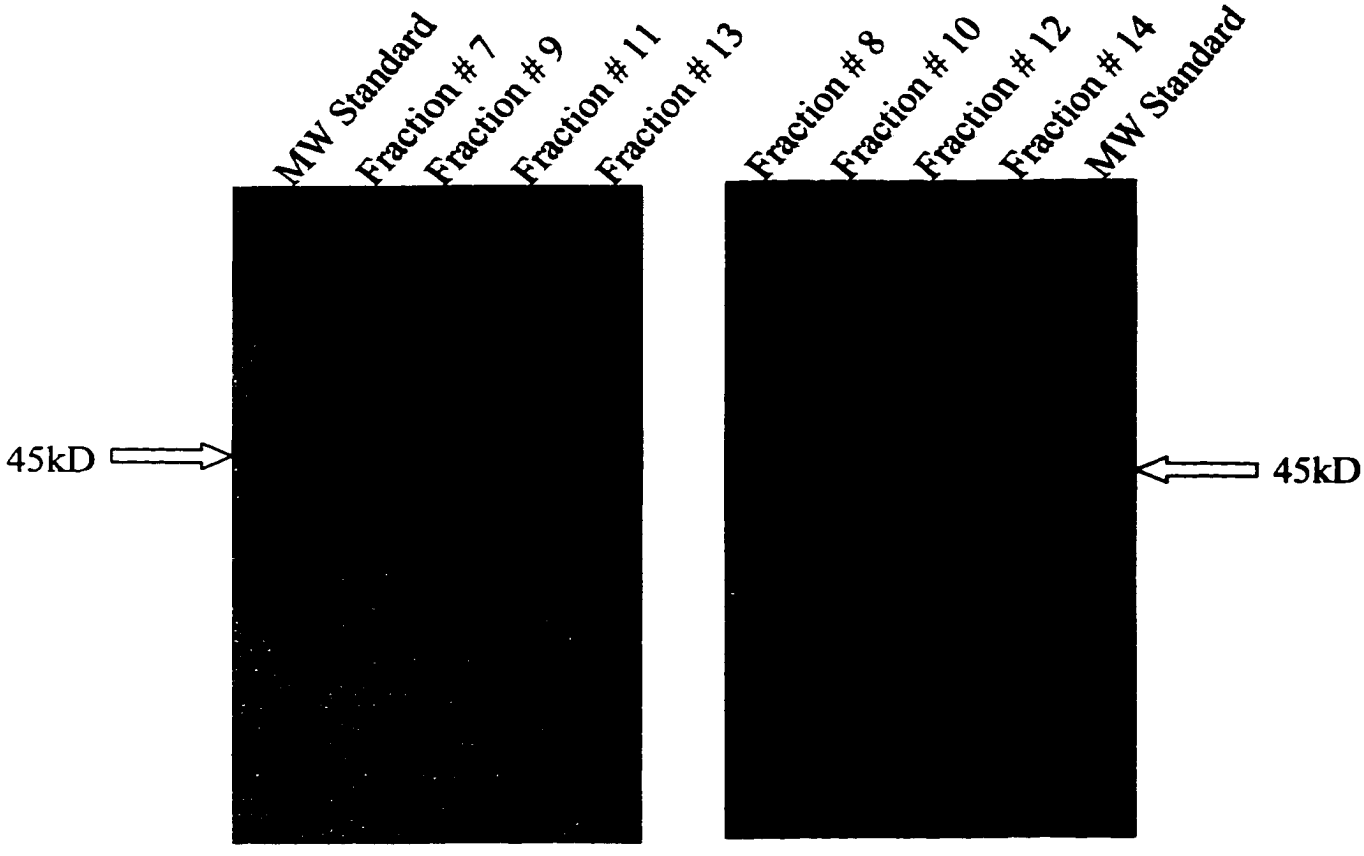

Figure 22. Sensorgram of the Binding of Aga2p to α-Agglutinin with Aggregates Removed at 20°C. (A). Immediately after the protein aggregates were removed using Bio-Gel p100 column, a sensorgram of the interaction of Aga2p immobilized with α-agglutinin at two concentrations (62nM, 125nM) was recorded at 20°C. (B). The dissociation rate constant was obtained using Sigmaplot as described in Figure 19. (C). Calculation of the association rate constant. The association rate constant was calculated by curve fitting as described in Figure 19 with residues of -0.12 to 0.12, which is within the range of curve fitting.

A

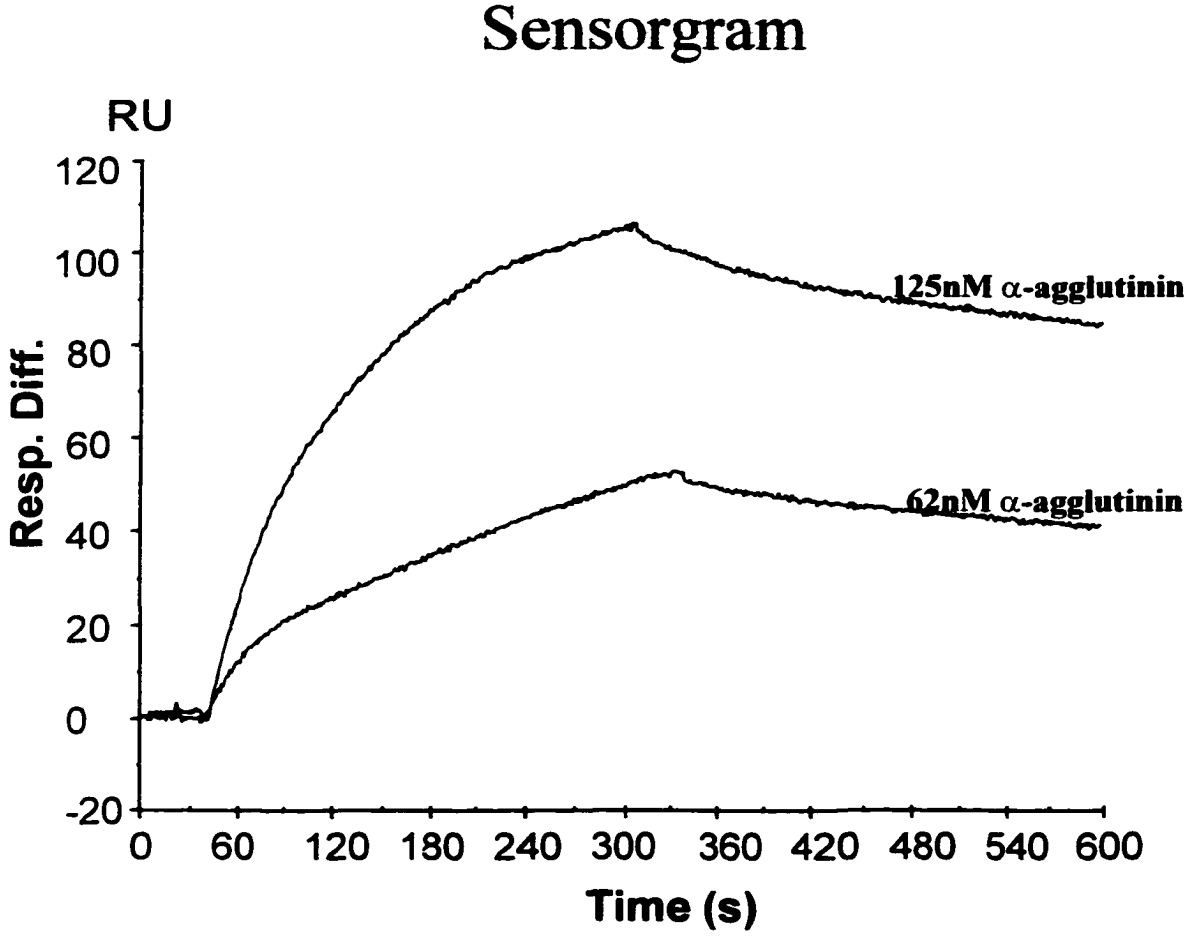

B

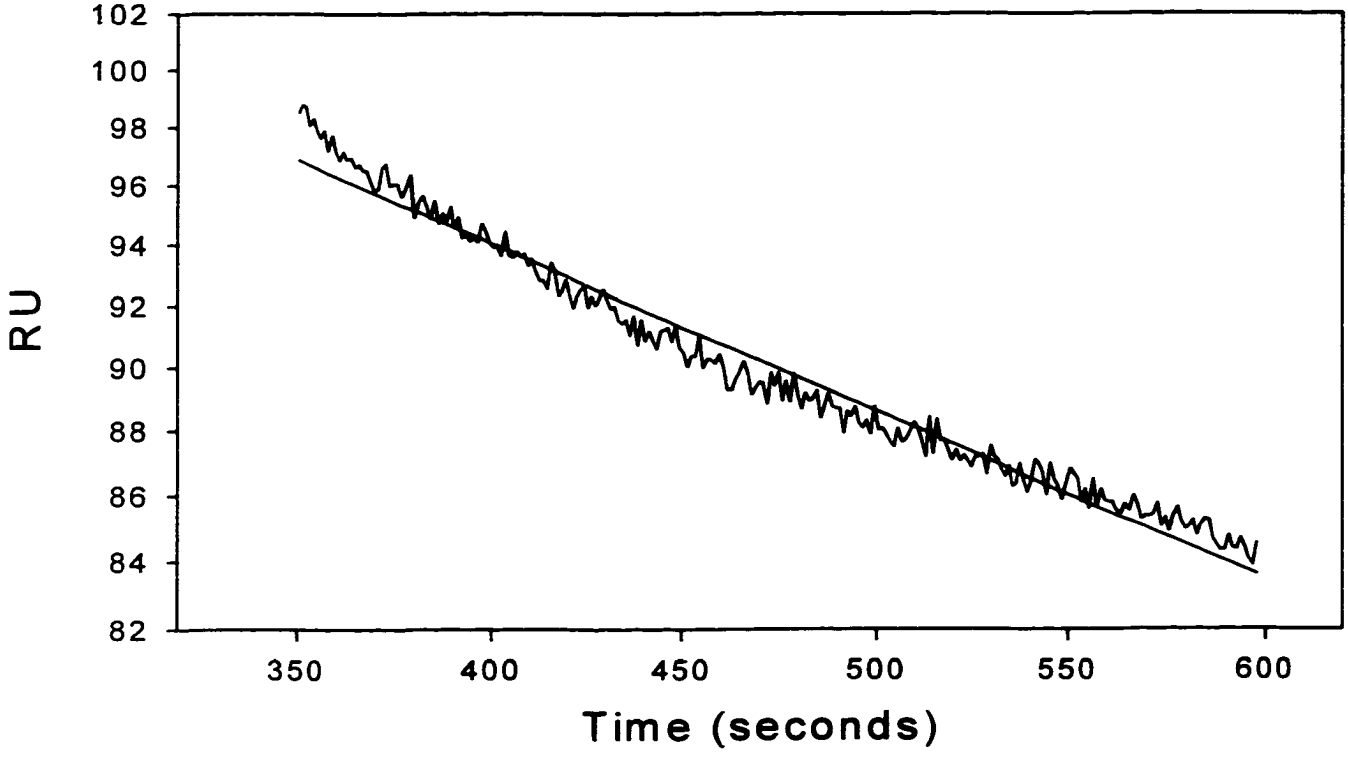

C

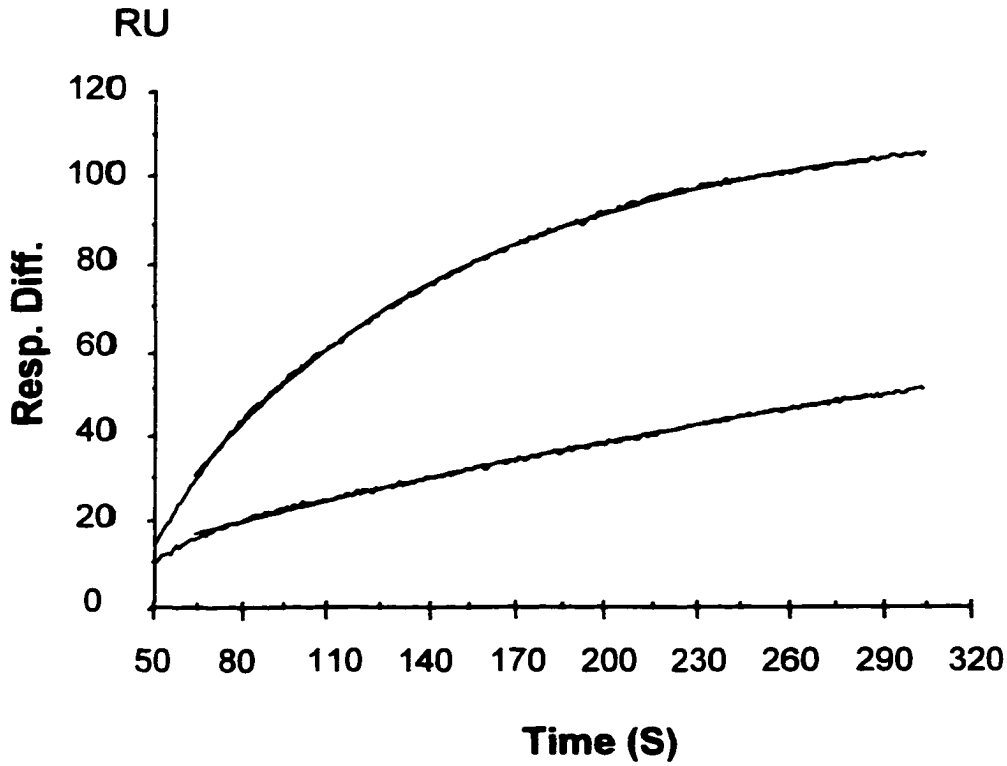

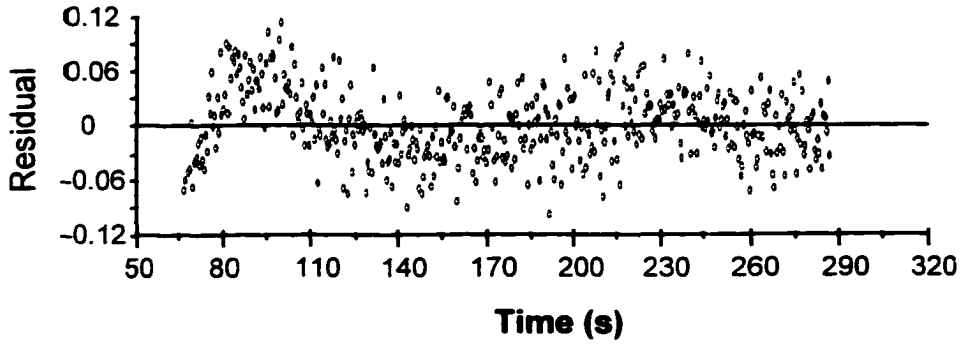

peptide and found that its specific activity of 2.6 X 10^{10} unit / Mol, which is 300 fold lower than intact a-agglutinin.

CD spectra of the complex of 5 X 10^{-6} α-agglutinin and 1 X 10^{-5} a-agglutinin peptide were measured after the complex was incubated in 10 mM sodium acetate, pH 5.5 at 25°C for 30 minutes (Figure 23). The CD spectrum of a-agglutinin peptide in 10 mM sodium acetate, pH 5.5 was then subtracted from that of the complex. As shown in Figure 23, after subtraction of the CD spectrum of a-agglutinin peptide, the complex showed differences in the CD spectrum compared to that of α-agglutinin. The spectrum of the complex still contained a principal negative magnitude band at 217 nm, which was similar to that of α-agglutinin. However, negative peak in the spectrum of the complex became narrower. The positive peak at low wavelength, especially lower than 207 nm, was strongly intensified, and there was an extra positive shoulder at wavelength of 225-234 nm. All these changes came either from secondary changes of α-agglutinin upon binding or a combination of secondary changes of both α-agglutinin and a-agglutinin peptide induced by binding. Secondary structure contents of β-sheets, α-helix, turn and others were analyzed by secondary structure analysis program, SELCON. The results are summarized in Table II. There was slight increase in each of the structured components, such as α helix, anti-parallel β sheet, parallel β sheet, and a decrease of random conformation from 38.6 % to 31.6 %. Although small, these changes are greater than the measured experimental errors. Therefore, This implies that some unstructured regions of a and α-agglutinin became more structured upon ligand binding.

Figure 23. Far-UV CD of α-Agglutinin Induced by Binding of a-Agglutinin Peptide. Far-UV CD spectra of α-agglutinin were measured at 25°C in 10mM sodium acetate buffer, pH 5.5 (——) and after incubating with a-agglutinin peptide for 30 minutes. Far-UV CD of α-agglutinin plus the changes of α-agglutinin and a-agglutinin peptide upon binding was obtained by subtracting CD of the complex of α-agglutinin and a-agglutinin peptide with CD of peptide alone (·····).

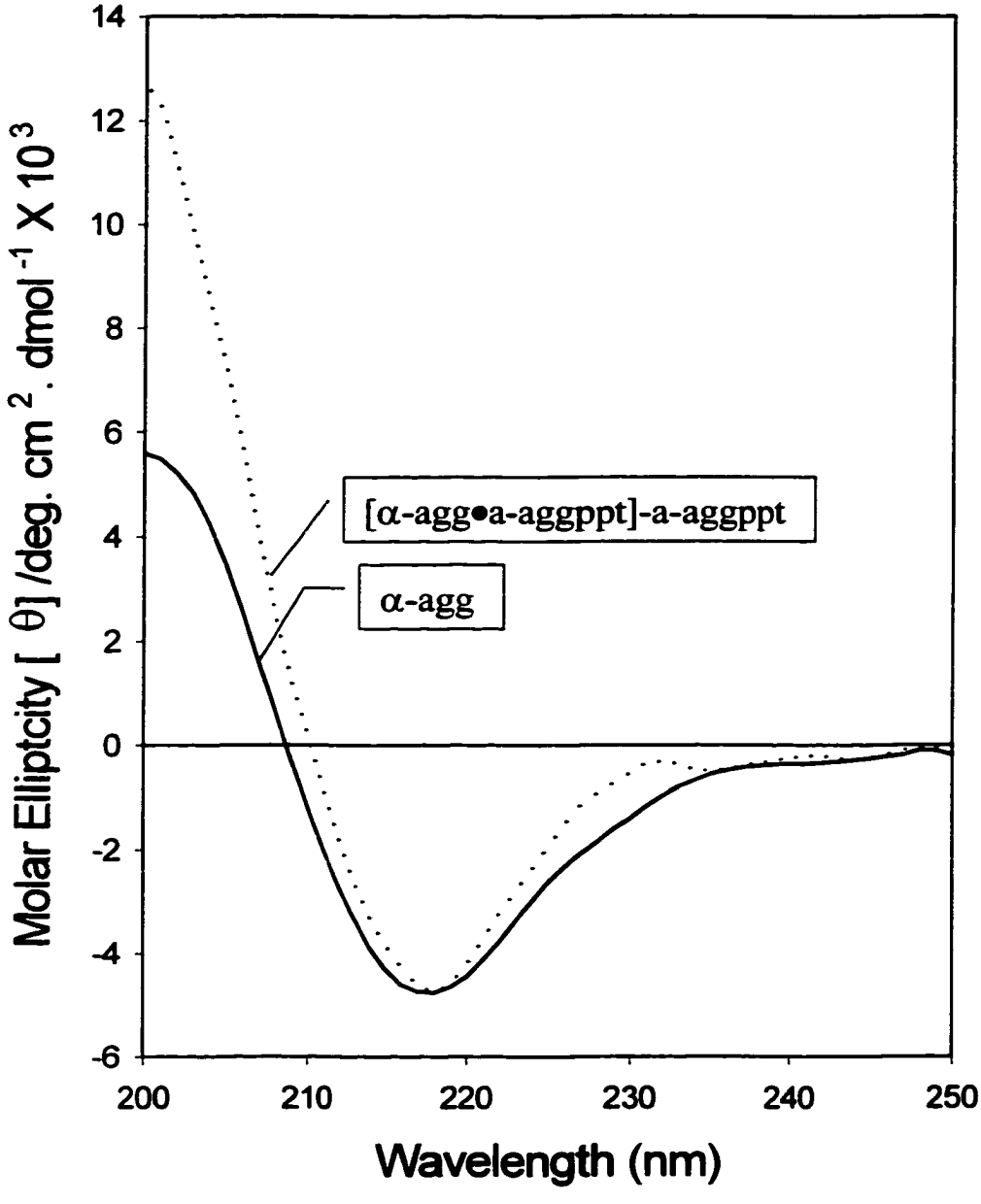

Table II: List of Secondary Structure contents of α-agglutinin and the complex of α-agglutinin and a-agglutinin peptide with peptide spectrum subtracted

Structure	α-Agglutinin		complex with subtraction of a-agglutinin peptide	
H	3.0 ± 2.6 %		4.3 ± 0.6 %	
A	39.1 ± 3.8 %	Total: 46.9 %	41.3 ± 2.4 %	Total: 52.9 %
P	7.8 ± 0.9 %		11.6 ± 0.8 %	
T	13.1 ± 1.6 %		11.1 ± 1.1 %	
O	38.6 ± 3.2 %		31.6 ± 2.9 %	

H, α-helix; A, antiparallel β-sheet; P, parallel β-sheet; T, turn; O, other structure.

Effect of cold temperature on the conformation of α-agglutinin: Far-UV CD spectra of α-agglutinin were measured and compared at 25°C and 0°C. As shown in Figure 24, CD spectra at both temperatures showed a major band at 217 nm, which was contributed by peptide chromophores in β-conformation. However, at 0°C, the magnitude of the negative band at 217 nm was intensified and broadened at lower wavelengths, indicating a possible increase of β sheet structure. In addition, at 0°C, there was an appearance of a positive shoulder at wavelength of 227-237nm. Secondary structure contents of sheets, helix, turn and others were analyzed by the secondary structure analysis program, SELCON. The results were summarized in Table III. The protein became more structured at a low temperature than at room temperature, especially in β sheet composition. For example, the total β sheet content was increased from 47.8 % to 54.4 % and the random structure dropped from 36.5 % to 26.1 %.

Combining the kinetic and CD data, our results indicated that similar degrees of conformational change were induced upon binding or by cold temperature.

Figure 24. Effect of Cold Temperature on Far-UV CD of α-Agglutinin. Far-UV CD spectra of α-agglutinin were measured in 10mM sodium acetate buffer, pH 5.5 at 25°C (——), and after incubation at 0°C for 20 minutes (·····).

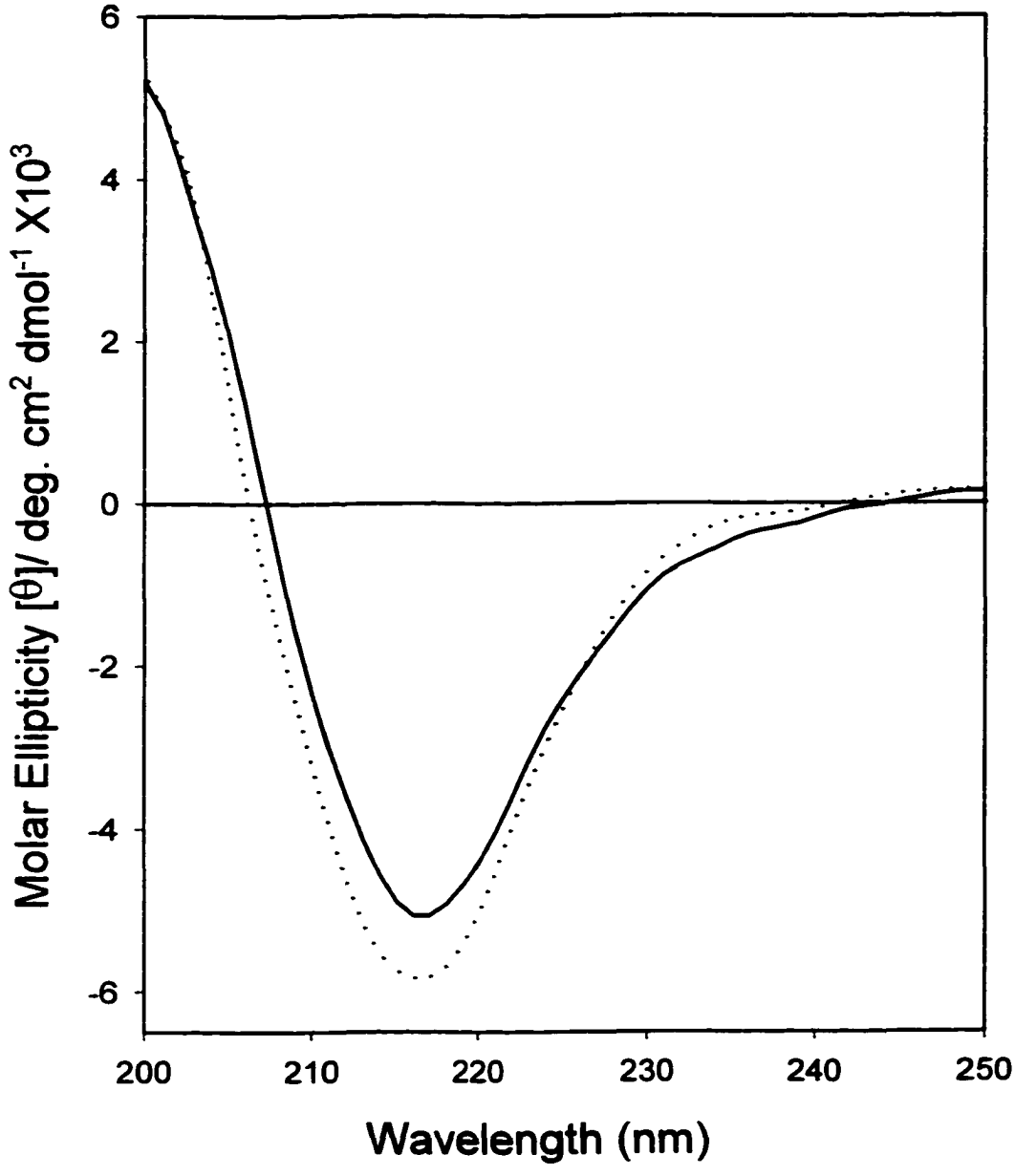

Table III: List of Secondary Structure Contents of α-agglutinin at 25 °C and 0 °C

Structure	25 °C		0 °C	
H	0.7 ± 3.0 %		4.0 ± 1.0 %	
A	41 ± 3.2 %	Total: 47.8 %	43.2 ± 2.5 %	Total: 54.4 %
P	6.8 ± 2.9 %		11.2 ± 1.6 %	
T	15.9 ± 1.0 %		15.5 ± 0.8 %	
O	36.5 ± 3.3 %		26.1 ± 2.6 %	

H, α-helix; A, antiparallel, β-sheet; P, parallel β-sheet; T, turn; O, other structure

Discussion

Characterization of the interaction between the agglutinins: Two approaches were described in this chapter to characterize the interaction of the agglutinins. Highly purified α-agglutinin was radioactively labeled with ^{125}I-Bolton-Hunter reagent and the interaction of α-agglutinin with a-agglutinin on intact **a** cells was studied. The equilibrium constants for the interaction were obtained by Scatchard analysis. Alternatively, biosensor technology "SPR" was used to monitor the interaction of the agglutinins in real time by immobilizing a-agglutinin on a sensor chip. "SPR" is a more informative technology, which enables us to obtain more precise association rate constant, dissociation rate constants, and affinity constant and also allows us to analyze the protein-protein interaction in a fast and reproducible way.

The results showed that the agglutinins adhered to each other with high affinity. The interaction were characterized by having K_D of 6.34 X 10^{-10} M at 0°C and K_D of 8.6 X 10^{-10} M at 25°C from the isotopic labeling; and having K_D of 1.55 ± 0.11 X 10^{-9} M at 20°C and K_{D1} of 6.18 ± 3.49X 10^{-4} M, K_{D2} of 9.76 ± 0.68X 10^{-10} M at 10°C from "SPR" studies. The interaction also had slow dissociation rate characterized by having k_{off}=7.03 X $10^{-5}s^{-1}$at 20°C and k_{off}=5.42 X 10^{-5} s^{-1} at 10°C from "SPR" studies and k_{off}=1.06 X 10^{-6} s^{-1} from the isotopic labeling experiment. The variation of k_{off} from "SPR" and the isotopic labeling studies most likely came from the difference in experimental conditions. The slower dissociation rate from the isotopic labeling experiment was probably due to the re-binding of α-agglutinin to the excess amount of a-agglutinin (7.5 X 10^4molecules / cell) on **a** cell surfaces. This concentration of receptors is above K_D for this assay; therefore, there should be significant rebinding and slower apparent K_D. The results from

"SPR" studies were more reliable since the amount of Aga2p immobilized on the sensor surface was limited for maximum binding and dissociated α-agglutinin was removed from the binding volume.

Our results demonstrated that the equilibrium constants appear to be within the same order of magnitude in both the isotopic labeling experiment and "SPR" studies. In terms of equilibrium constants from the isotopic labeling studies, the interaction of the agglutinins did not show a significant temperature dependency. However, real time observation from "SPR" studies showed a remarkable temperature dependent interaction, the association of the agglutinins at 10°C was characterized by a sigmoid-shaped curve with at least two distinct k_{on} in a time dependent manner. The dissociation rate at this temperature was a little slower comparing with that at 20°C. The use of "SPR", therefore, helps us to resolve the question about the basis of effect of cold temperature on reducing their binding ability in cellular level both in vivo and in vitro (Terrance and Lipke 1981, Yamaguchi et al., 1982).

The structural basis of the high affinity interactions: interactions of the proteins with high affinity are characterized by having K_D of 10^{-8} to 10^{-10} M. For example: antigen HIV core protein p24 antigen interacts with its monoclonal antibody CB-4/1 with K_D of 2 X 10^{-8} M (Glaser and Hausdorf 1996); immunoglobulin E binds to its receptor (FcεPI) expressed on mast cells and basophils with K_D of 2.6 X 10^{-10} in the development of allergic reaction (Henry et al., 1997); integrins such as $\alpha_v\beta_3$ and $\alpha_{IIb}\beta_3$ binds to their natural ligands and Arg-Gly-Asp (RDG)-containing peptides with K_D of 10^{-10} M in cell-cell adhesion (Barbas et al., 1993); platelet-derived growth factor (PDGF) binds to its binding ligand, α-platelet-derived growth factor receptor (α-PDGFR), with K_D of 7 X

10^{-9} M in promoting the growth of mesenchymal cells (Mahadevan et al., 1995); Tumor Necrosis Factor (OX40) binds to mouse T cells with K_D=2.4 X 10^{-10} M in cellular communication (Al-Shamkhani et al., 1997); proteinase, calpain, binds to proteinase-inhibitor, calpastatin, with K_D of 3.1 X 10^{-9} M (Yang et al., 1994); chaperon proteins Gro EL and Gro ES bind to their substrate proteins with K_D of 10^{-9} M in assisting the folding of proteins in the cells (Murai et al., 1995); and SH2 domains of Src and Lck binds to a variety of phosphopeptides with K_D of 3.7 X 10^{-9} M in intracellular signaling for signal transduction (Payne et al., 1993).

High affinity interactions are often related with conformational changes of the proteins upon ligand binding. The well-characterized examples are the interaction of antigen to antibody. For example, a structural rearrangement next to the helical binding site of a tobacco mosaic virus protein occurs during the high affinity interaction between the protein and its antibody (Altschuh et al., 1992). Slow conformational changes of HIV core protein p24 are involved in the high affinity interaction of the protein to its own monoclonal antibody (Glaser and Hausdorf 1996). Conformational changes of integrin $\alpha_{IIb}\beta_3$ (paltelet GPIIb-IIIa) triggered by binding of RDG sequences in fibrinogen generate a high affinity binding state of integrin (D'Souza et al., 1990; Du et al., 1991). Conformational changes of the cell adhesion protein thromborspondin (TSP) are induced by binding to the receptor CD36 (GPIIIb orGPIV) (Leung et al., 1992).

The characterization of the high affinity interaction of α-agglutinin with a-agglutinin suggests that conformational changes of the agglutinins might be involved upon binding. In order to demonstrate that the interaction of the agglutinins is indeed related to the conformational changes of the agglutinins, the CD spectrum of the protein

complex was studied under conditions mimicking binding. Small synthetic peptides containing the active binding site of the proteins can have similar function in inducing conformational changes upon binding in variant systems (Frelinger et al., 1990; Kieffer et al., 1991; Du et al., 1991; Leung et al., 1992; Yang et al., 1994).

There was a more structured conformation of α-agglutinin when it bound to a-agglutinin peptide. A more structured conformation, especially in β sheet composition was also discovered in the CD spectrum of α-agglutinin when the protein was incubated at cold temperature. A sigmoid shape of the association curve was observed in the real time interaction of the agglutinins at low temperature. This type of interaction has also been observed by Friguet et al. in the study of the interaction of antigen with antibody. They described such interaction as a multi-step association interaction and conformational rearrangement upon binding. An initial encounter of the components is believed to be responsible for inducing and stabilizing the second step interaction, a change due to conformational rearrangement (Friguet et al., 1989). Huber et al. have found similar characterization of the interaction in studying the binding of the platelet glycoprotein IIb-IIIa to fibrinogen by using "SPR". The platelet glycoprotein IIb-IIIa interacts with fibrinogen with low affinity and then changes into a more stable association with high affinity (Huber et al., 1995). Similar conformational change related two-phase association was also reported in the interaction of antigen HIVp24 with an antibody using "SPR" technology (Glaser and Haudorf, 1996). The binding of the agglutinins at cold temperature shows similar characteristics. This indicated that the interaction of the agglutinins was not a single step interaction, but requring structural rearrangement of the agglutinins upon binding.

Importance of Conformational Flexibility and Specificity of α-agglutinin: α-Agglutinin has a relatively flexible conformation as described in chapter III, and it was able to change its conformation reversibly from β-sheet to α-helix upon mild treatment such as pH ≤ 8.5 or temperature ≤ 55°C. The conformation of α-agglutinin became more helical when the protein was treated with higher pH, temperature or breakage of disulfide bonds, because parts of α-agglutinin have a high potential to form α-helix by secondary structural prediction based on its primary sequence.

In contrast, the conformation of α-agglutinin changed differently upon binding or incubation at cold temperature. More structured conformations were formed under these conditions.

A model of the interaction of the agglutinins at different temperatures: Molecular interactions could happen in successive steps, even though the final result and the overall binding constant are similar to a single step interaction (Burgen et al., 1975). A model of the interaction between the agglutinins was developed based on conformational changes of the initial binding site and the flexibility of the proteins under different conditions as shown below:

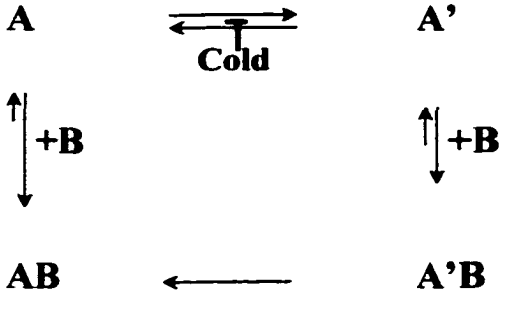

In this model, α-agglutinin can exist in either of two conformations "open" at room temperature (A) or "closed" at cold temperature (A'). The conformational change

of α-agglutinin between (A) and (A') is reversible. α-Agglutinin (A) binds to a-agglutinin (B) with high affinity at room temperature. α-Agglutinin (A') binds to a-agglutinin with low affinity due to the conformational constrains at low temperature. However, at low temperature, a conformational rearrangement from (A') to (A) occurs upon binding, which transforms the low affinity interaction into a high affinity interaction similar to the one at room temperature, and this is an irreversible process. A similar model can also be applied for a-agglutinin in order to bind to α-agglutinin.

Our "SPR" results at low temperature are consistent with the above model. The two-phase interaction at low temperature implies that the protein with two conformation "closed" and "open" may both be involved in the interaction and the proteins undergo conformational transition from "closed" to "open" form during the binding.

The above model of ligand-binding induced conformational changes of the agglutinins is similar to a form of the induced-fit model of interaction of substrate and enzyme, where the active site of the enzyme assumes a shape of complementary to substrate after it is bound (Koshland and Neet 1968). Induced fit has also been shown to have a key role in the structural alteration leading to antigen-antibody binding (Rini et al., 1992).

Involvement of hydrophobic complementation in high affinity interactions of the agglutinins: The surface-shape complementation of hydrophobic interfaces often results in high affinity interactions with high specificity (Creighton 1993). This type of interaction has been seen in antigen to antibody (Rini et al., 1992); chaperon proteins to their substrate proteins (Murai et al., 1995); Tumor Necrosis Factor (OX40) to T cells (Al-Shamkhani et al., 1997); intercellular adhesion molecules 1 (ICAM-1) to lymphocyte

function-associated molecule (LFA-1) (Dustin and Springer 1989); and SH2 domains of Src and Lck to phosphopeptides (Payne et al., 1993);

The high affinity interaction of the agglutinins also suggests the involvement of hydrophobic interactions in the interface of the proteins. The high affinity interaction resulting from hydrophobic interactions is compatible with the hydrophobic characteristics of conformation of the agglutinin. α-Agglutinin has three Ig domains stabilized by a hydrophobic core of each domains and hydrophobic interfaces of adjacent domains and C-terminal possible binding site of a-agglutinin is also hydrophobic (Lipke et al., 1995; Chen et al., 1995). In addition, CD study showed that a more organized conformation was formed in the protein complex upon ligand binding which imply that complementary interaction of proteins stabilized the conformation of the proteins.

Another sign of the involvement of hydrophobic interactions is that the interaction of the agglutinins was cold sensitive. As in α-agglutinin, cold temperature also induced β-structure formation in *Streptomyces subtilisin* inhibitor. *S. subtilisin* inhibitor is a dimeric protein consisting of two subunits, each of which contains a five-stranded β-sheet being associated through a hydrophobic interface (Konno et al., 1995). Low temperature reduces the hydrophobic interactions in *S. subtilisin* inhibitor, resulting in a low affinity interaction (Privalov et al., 1986; Konno et al., 1995). The conformational changes of α-agglutinin at cold temperature may also be functionally related, as cold temperature reduced agglutinability in the cellular level in vivo (Figure 20; 24).

This study presents a sucessful attempt to characterize interaction of the cell adhesion molecules, the agglutinins, and to measure the kinetic association and dissociation in real time. The combination of binding analyses and CD spectroscopy

enables us to establish the structural and functional relationship of the proteins in the binding reaction. The study of the interaction of the agglutinins not only reveals interesting aspects of the adhesion mechanism but also provides important information on the dynamic structure of the adhesive proteins. Our data have bearing also mechanism of cell adhesion / cell-cell recognition and cellular role of the proteins in other systems other than simple yeast sexual agglutination.

Chapter IV

Effect of Mutations on α-Agglutinin

Introduction

The initial purpose of this chapter is to investigate the effect of mutation on the secondary structure of α-agglutinin in order to confirm the 3-D models of α-agglutinin and to study how mutations affect kinetics of binding between the agglutinins. The mutations studied were located in domain III of α-agglutinin and were classified into two groups summarized in Table IV based on their binding ability to a-agglutinin. In this study, we discovered that two mutations that reduced the binding ability of α cells in vivo reduced the level of the proteins secreted. Moreover, the mutated α-agglutinin was more sensitive to protease digestion. However, the purified mutated α-agglutinin had similar structural and functional properties as that of the wild type protein. The results implied that such point mutations led to misfolding of the nascent α-agglutinin, so that the protein can not be secreted properly and is degraded in the ER. In addition, the misfolded α-agglutinin may also reduce the secretion of other proteins, because the total amount of the proteins secreted was also substantially reduced.

Table IV. Point Mutations Located in Domain III of α-Agglutinin vs their Binding Activity (de Nobel et al., 1996)

Putative Binding Sites			**Control**	
E-F Loop	**A-B Loop**	**Post G Strand**	**C-C'**	**C'-C"**
100 fold reduction of activity His 292 Leu His 292 Arg	100 fold reduction of activity Tyr 216 Ser Tyr 216 Asp	15 to 60 fold reduction of activity Tyr 322 Phe Tyr 322 Cys Tyr 322 Ala	Little reduction of activity Asp 253 Ala Val 254 Ala Thr 255 Ala	Little reduction of activity Asp 266 Asn Glu 267 Gln Lys 268 Gln
20 fold reduction of activity Leu 294 Ser Phe 296 Ser	10 fold reduction of activity Tyr 216 Val Asp 217 Asn			
Little reduction of activity Asp 291 Asn	Little reduction of activity Tyr 216 Phe Asp 215 Asn Asp 217 Ala	Little reduction of activity Gln 323 Leu Gly 324 Ala Arg 325 Gly		

Materials and Methods

Site-specific mutagenesis of residues within domain III of α-agglutinin$^{20-351}$: Plasmid YEpPGK-*AGα1*^{351} contains the N-terminal half of AGα1 under the control of the PGK promoter (Chen et al., 1995; de Nobel et al., 1996). The *Hin*d III *AGα1*^{351} fragment from YEpPGK-*AGα1* ^{351} is subcloned into M13mp19, and single-stranded DNA was used for oligonucleotide-directed mutagenesis by using the phosphorothioate method (Sayers et al., 1992; Olsen and Eckstein 1990). Most oligonucleotides used in the mutagenesis contained mixtures of two nucleotides (in either a 2:1 or 1:1 wild type:mutant ratio) at several positions, and gave rise to several different single mutations (de Nobel et al., 1996). After the mutagenesis reactions, the mutated regions were sequenced to determine the presence of mutations. The mutant *AGα1* ^{351} were sequenced completely to confirm that there were no additional mutations present (Primers: A12-5'GAGGGCGATGAATTCACATTA, G11-5'TGTACTGCTCAAAATGACCTG, T5-5'CGTTCAACTGGTTACGGTTCT and C471981-5'AATGATACCAATGCTGAC). The mutated *AGα1*^{351} gene were then subcloned into YEpPGK and transformed into α agα1:: LEU2 mutant.

Yeast transformation: E.coli strain HB101 was used for amplifying plasmids. α agα1:: LEU2 cells were grown in rich medium (YEPD) to mid-log phase, harvested and prepared for competent cells. Plasmids YEpPGK-AGα1^{351} and its mutants were then introduced into competent α agα1:: LEU2 cells by lithium acetate standard transformation procedure (Johnston 1993).

Purification of mutated α-agglutinins: Yeast strain Lα21 (*MATα ade*2-1 *his*3-11,15 *leu*2-3,112 *trp*1-1 *ura*3-1 *can*1-100 *agα*1-3) containing mutated pPGK-AGα1^{351}

constitutively expressed and secreted mutated α-agglutinin $^{20\text{-}351}$ with point mutations. Cell culture supernatant containing mutated α-agglutinin$^{20\text{-}351}$ was collected and concentrated through a Millipore filtration apparatus with a membrane having 30kDa molecular weight cutoff. Concentrated supernatant was then dialyzed and applied to DEAE-Sephadex A25 column. Partially purified mutated α-agglutinin$^{20\text{-}351}$ eluted from DEAE column was dialyzed, lyophilized, re-suspended, deglycosylated by endoglycosidase H. A Bio-Gel P-60 size exclusion column was used for further purification (Detail procedure see: Chapter II).

SDS-PAGE and Western Blotting: The protein samples were electrophoresed in 10% SDS-PAGE gels. The gels were either stained with Coomassie brilliant blue (Bio-Rad laboratories) or electro-transferred to Immobilion membrane (Millipore). The blots were then immuno-detected by anti-α-agglutinin (Detail procedure see: chapter III).

Purification of α-agglutinin using Con A Sephadex: Lα21 transformants containing pPGK-AGα1^{351} or pPGK-AGα1^{351} with point mutation were grown in 100 ml of medium to log phase with A_{660} = 0.6. Cells were centrifuged and cell supernatants were applied to Concanavalin A-Sepharose columns which were pre-equilibrated with 100mM sodium acetate buffer (pH 5.5), supplemented with 150 mM sodium chloride, 1 mM calcium chloride and 1mM maganese chloride. 1ml fractions were eluted with 1M α-methymannoside in 100 mM sodium acetate buffer (pH 5.5). α-Agglutinin or mutated α-agglutinins were then dialyzed against 100 mM sodium acetate buffer (pH 5.5) for 2 hours to remove α-methymannoside. The dialyzed samples were electrophoresed on 10 % SDS-PAGE gel and transferred to nitrocellulose membrane and immunoblotted by anti-α-agglutinin.

Construction of wild type and mutants pPGK-AGα1$^{351.6His}$: Two single-stranded oligonucleotides were synthesized and used as primers for construction of pPGK- AGα1$^{351.6His}$. Primer I: (*Hind* III *Xba* I ATG) 5'-CAA TTC AAG CTT CTA GAT TCA AA ATG TTC ACT 3'. Primer II (AGα1 351 6His stop *Bgl* II *Hind* III) 5' GCT GCT AAG CTT AGA TC TTA GTG ATG GTG ATG GTG ATG CGC ACT AGT GTT TAT3', Both primers contain *Hind* III sites (nucleotides with dotted underlined) outside the open reading frame. The 3' end primer II included sequences of 6 Histine (nucleotides with single underline), a stop codon (nucleotides with double underline) and nucleotide sequence corresponding to Ala 351 in the α-agglutinin protein sequence. The DNA fragments encoding α-agglutinin$^{20-351}$ and mutated α-agglutinin$^{20-351}$ with a point mutation in domain III were used as templates for a polymerase chain reaction (PCR). The mutated region at the C-terminal was sequenced to determine the addition of hexa Histidine. Since there is a single enzymatic digestion site located in domain III of AGα1^{351}, the orientation of the insertion was checked by digesting the plasmids with *Aat* II. AGα1$^{351.6His}$ and mutants were then sequenced completely to confirm that there were no additional mutations present. Three primers were used: C471981-5'AATGATACCAATGCTGAC; G11-5' TGT ACT GCT CAA AAT GAC CTG-3'; and A29-5' GAG AAG ATT GAT TAC GAC. AGα1$^{351.6His}$ and AGα1$^{351.6His}$ with point mutations were then subcloned into *Hind* III site of pYEpPGK and transformed into the agα1::Leu2 mutant.

Purification of His-tagged α-agglutinin and mutants: Lα21 transformants containing pPGK-AGα1$^{351.6His}$ and pPGK-AGα1$^{351.6His}$ with point mutations were grown to log phase. Cells were centrifuged, cell supernatants were collected and concentrated

and the pH of concentrated cell supernatants was adjusted to 5.5 by dialyzing against 30 mM sodium acetate. The samples were then treated with Endo H for 3 hours to remove N-glycosylated carbohydrate. After deglycosylation, the samples were dialyzed against PBS containing 10 mM imidazole (pH 7.4) and applied on a nickel column, pre-equilibrated with PBS (pH 7.4). 1ml fractions of His-tagged α-agglutinin and mutants were then eluted with 500 mM imidazole in PBS (pH 7.4). His-tagged α-Agglutinin or mutated α-agglutinins were then dialyzed against 30 mM sodium acetate buffer (pH 5.5) for 2 hours to remove imidazole. The dialyzed samples were electrophoresed on 10% SDS-PAGE gel and visualized by staining with Coomassie blue. The specific activity of His-α-agglutinin was examined by agglutination assay.

Agglutination assays: Haploid **a** and α cells were grown separately in minimal medium YNB at 30°C rotary shaker to 2×10^6 cells/ml ($OD_{660} = 0.3$). His-tagged α-agglutinin and mutants were assayed after incubating with **a** cells on a rotary shaker at 30°C for 90 minutes. The activities of the proteins were assayed by their ability to mask the binding sites on the surface of **a** cells (Detail procedure see: chapter II).

Interaction of His-tagged-α-agglutinin and its mutants to a-agglutinin on the surface of a cells: Unlabeled His-α-agglutinin (wild) and His-α-agglutinin with point mutaions with increasing amounts and 1 μl of ^{125}I-α-agglutinin were incubated with 2 X 10^6 **a** cells or α cells in 200 μl total volume on the rotary shaker at 200rpm/min for 90 minutes at 25°C. **a** and α cells with bound ^{125}I-α-agglutinin were washed and counted by Gamma Counter Compugamma 1282 (LKB Wallac Inc). Since the non-specific binding sites on the surface of **a** and a cells are the same (Terrance et al., 1987), the counts of α cells bound with I^{125}-α-agglutinin was used as control and subtracted.

Results

The effects of environmental condition on the conformation of α-agglutinin were discussed in chapter II. Characterization of the interaction of α-agglutinin and a-agglutinin using isotopic labeling and SPR analysis and IV was described in chapter III. The goal of this chapter was to study the effect of two mutations on the conformational and functional behavior of α-agglutinin.

Effect of mutation on the secretion of α-agglutinin: de Nobel et al. tested the effect of point mutations in domain III of α-agglutinin on the agglutinabilities of mutant cells and cell culture supernatants. The mutants were classified into two groups, based on their binding abilities. As indicated in Table IV, the experimental group is composed of mutations in residues located in the putative binding site, such as His 292, Leu 294, Tyr 216, Tyr 322 and others, located in the E-F loop, A-B loop and post-G strand. Mutations in these residues reduce the binding ability 10-100 fold. The control group consists of mutations in residues in C-C', C'-C" and some residues in the E-F loop, A-B loop and post-G strand. Mutations in these residues, however, have no effect on the binding activity.

Mutated α-agglutinin has to be purified in order to detect the effect of mutation on its structure and function. The first mutant we used was His 292 Leu, since chemical modification or mutation at this residue reduced the agglutination ability in vivo about 100 fold. A similar procedure as the one used for the purification of the wild type α-agglutinin was used (For details see: chapter II). Comparing the chromatogram of material from wild type and mutant, the area of first peak normally collected for further purification of α-agglutinin was decreased about 25 fold. The total amount of proteins

secreted from the mutant strain (His 292 Leu) was, therefore, substantially reduced by the mutation. Since the second peak on chromatograms (Figure 25A) also contains α-agglutinin by western blotting (data not shown), the samples from both peaks of the chromatograms were pooled together and lyophilized. In order to compare the ratio of α-agglutinin in the total amount of the proteins after mutation, the OD_{280} of both mutant and wild type samples were adjusted to the same level. After the samples were deglycosylated with Endo H, SDS-PAGE of both samples were stained by Coomassie blue and compared. As shown in Figure 25B, the mutation on α-agglutinin reduced the percentage of α-agglutinin in the total amount of proteins secreted as well.

The samples were further purified using Gel P-60 column. As indicated in Figure 26, fractions 51 to 54 collected from Gel P-60 column of both wild and His 292 Leu were immunoblotted by anti-α-agglutinin. There was more 30 kD fragment of α-agglutinin produced in the mutant strains (His 292 Leu). The 30 kD fragment is an inactive form of α-agglutinin, which has also been obtained by Arg-C proteolytic digestion (Chen et al., 1995). Therefore, this mutation increased the sensitivity of the protein to protease. In addition, the size of major band of mutated α-agglutinin was about 40 kD, which is smaller compared to wild type α-agglutinin. There were only a little 45 kD band of mutated α-agglutinin, the same size of wild type α-agglutinin. The same procedure used for purifying wild type α-agglutinin failed to purify enough mutated α-agglutinin for further studies.

Purification of mutated α-agglutinin by Con A-Sephadex: Since α-agglutinin is highly O-glycosylated, a Con A-Sephadex column was used to purify mutated α-

Figure 25. Chromatography of α-Agglutinin and Mutant α-Agglutinin (His 292 Leu) by DEAE-Sephadex. Lα21 transformants containing pPGK-AGα1^{351} and pPGK-AGα1^{351} with point mutation (His 292 Leu) were grown in 8 liters of medium to stationary phase (2 X 10^7 cells/ml). Cells were harvested. The cell supernatants were concentrated and dialyzed overnight against 4 liters of 30 mM sodium acetate (pH5.5) at 4°C. The dialyzed materials were applied on DEAE-Sephadex columns (200-ml bed volume). The columns were washed and eluted with 300 mM sodium chloride in 30 mM sodium acetate (pH5.5) in 3 ml fractions. (A). Absorption at OD_{280} of each fraction was recorded and graphed vs fraction numbers. —●— , α-agglutinin (wild type), —▲— , α-agglutinin (His 292 Leu). (B). Fractions containing partially purified α-agglutinin (wild type) or α-agglutinin (His 292 Leu) in the peak regions of the graphs in (A) were pooled together and 20 μl of each samples were loaded in three lanes and electrophoresed on 10% SDS-PAGE gel and visualized by staining with Coomassie blue.

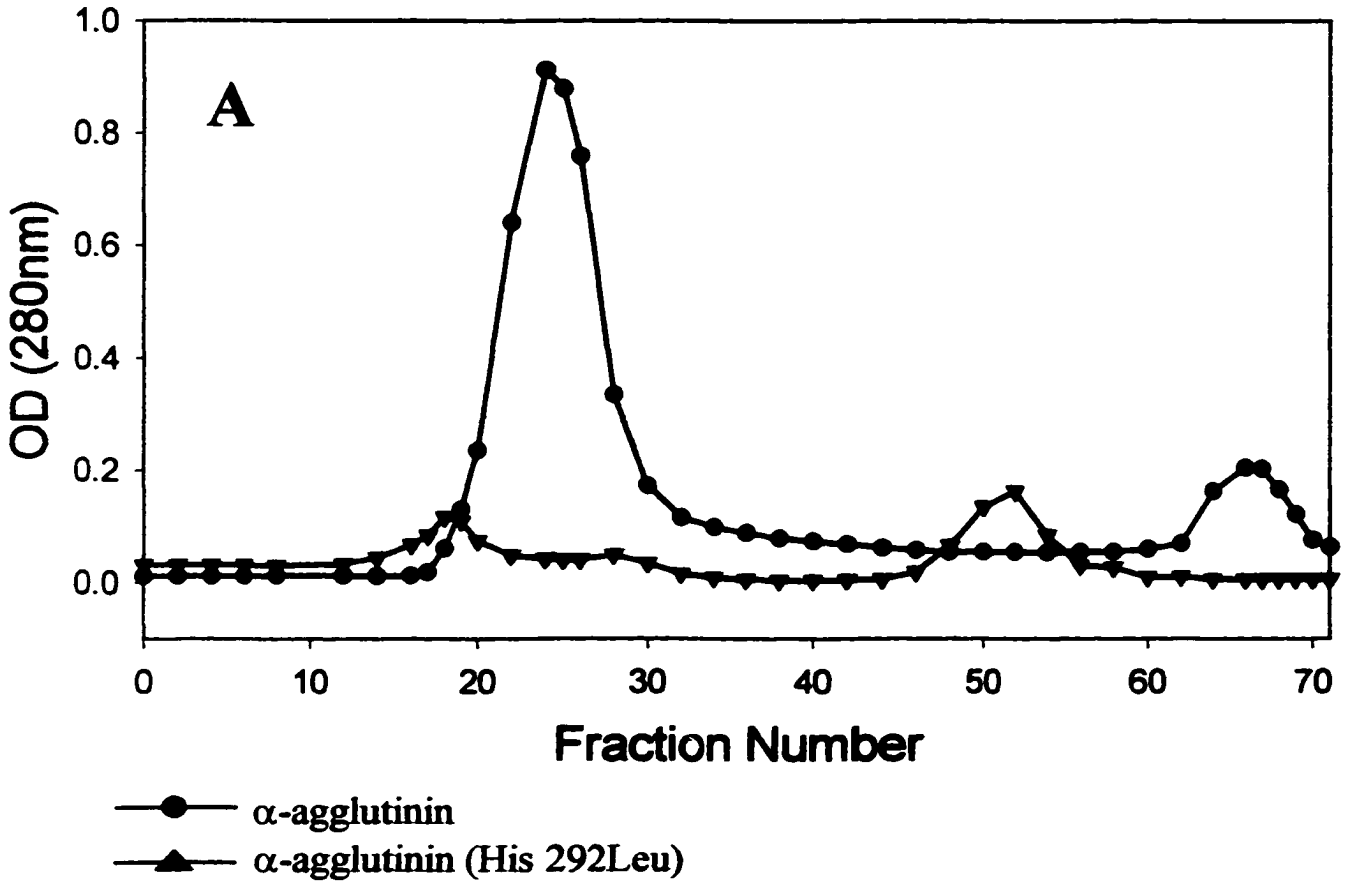

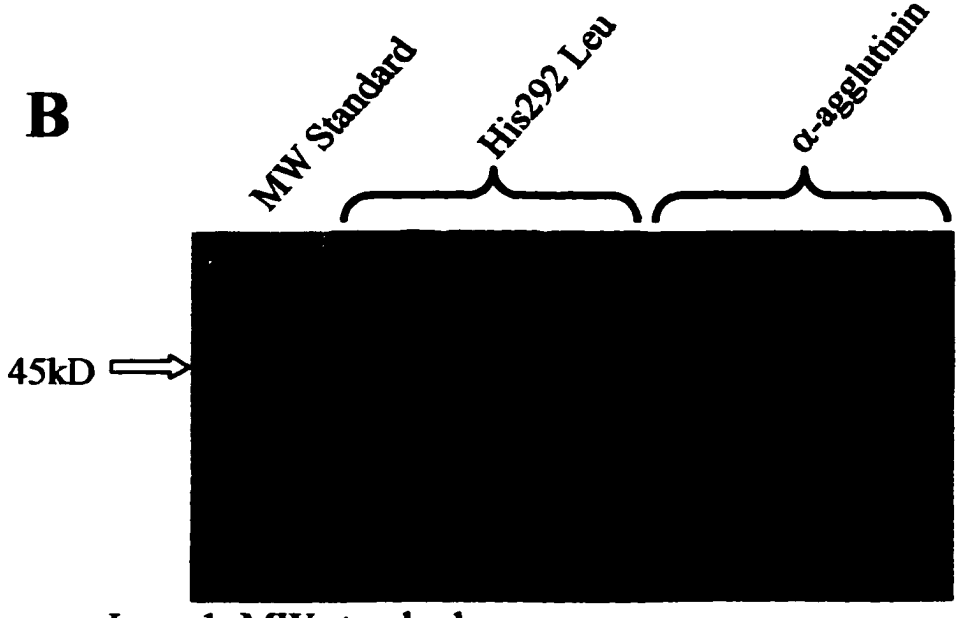

Lane 1: MW standard
Lanes 2-4: mutated α-agglutinin (His 292 Leu) from DEAE column
Lanes 5-7: wild type α-agglutinin from DEAE column

Figure 26. Western-Blotting of α-Agglutinin (Wild Type) and α-Agglutinin (His 292 Leu) after Bio-Gel P-60 Chromatography. Proteins collected from DEAE-Sephadex were lyophilized and re-suspended in 30 mM sodium acetate, pH 5.5, 0.01% SDS and 1 mM EDTA and partially deglycosylated by Endo H and loaded onto a Bio-Gel P-60 column pre-equilibrated in 30 mM sodium acetate. 300ml fractions were collected and electrophoresed on 10% SDS-PAGE gel and then transferred to nitrocellulose membrane by electrophoresis and analyzed by Western Blotting using anti-α-agglutinin.

Western Blotting

Lane 1: Molecular Weight Standard

Lanes 2, 4, 6, 8: Fractions 51-54 of wild type α-agglutinin

Lanes 3, 5, 7, 9: Fractions 51-54 of mutated α-agglutinin (His 292 to Leu)

Figure 27. Western Analysis of Partially Purified α-Agglutinin and α-Agglutinin (His 292 Leu) from Con A Sepharose Column. Lα21 transformants containing pPGK-AGα1^{351} and pPGK-AGα1^{351} with point mutation (His 292 Leu) were grown in 100ml of medium to log phase with OD_{660} of 0.6. Cells supernatants were applied to Concanavalin A-Sepharose columns which were pre-equilibrated with 100mM sodium acetate buffer (pH5.5), supplemented with 150mM sodium chloride, 1mM calcium chloride and 1mM manganese chloride. 1ml fractions were eluted with 1M α-methymannoside in the buffer above. α-Agglutinin and mutated α-agglutinin (His 292 Leu) fractions were then dialyzed against 30 mM sodium acetate buffer (pH5.5) for 2 hours to remove α-methymannoside. The dialyzed samples were electrophoresed on 10% SDS-PAGE gel and transferred to nitrocellulose membrane and immunoblotted by anti-α-agglutinin.

Western Blotting

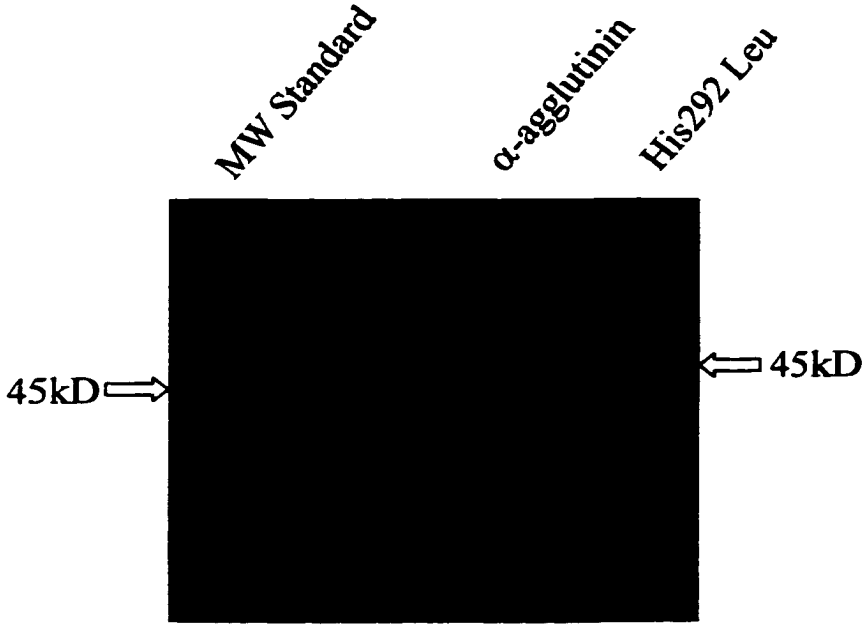

Lane 1: MW standard
Lane 3: wild type a-agglutinin from Con A column
Lane 4:mutated a-agglutinin from Con A column

agglutinin (His 292 Leu). As shown in Figure 27, there was much less 45 kD mutated α-agglutinin being purified from the column compared to that of the wild type. The protein fragment with molecular weight other than 45 kD, such as 40 kD and 30 kD fragments seen from previous purification did not appear. Either these fragments could not bind to the Con A column or could not be eluted from the column. We are, therefore, still unable to purify mutated α-agglutinin by this method.

Purification of His-tagged mutated α-agglutinin through a nickel column: In order to purify mutated α-agglutinin, YEpPGKAGα1^{351}.6His plasmid was constructed containing Histidine$_6$ in the C-terminal of *AGα1*^{351} (Figure 28A). AGα1^{351} and AGα1^{351} containing point mutations in domain III were used as templates in PCR reaction (Figure 28B). Two primers were used as for the PCR reaction (Figure 28B). Both primers and pYEpPGK have *Hin*d III cutting sites at the end. PCR products of AGα1^{351} and AGα1^{351} containing point mutations (Figure 28C) and plasmid YEp PGK were cut by *Hin*d III and ligated together. Since there is only one *Aa*t II cutting site located in domain III of AGα1^{351} (Figure 28D), the orientation of inserted DNA fragments were checked by *Aa*tII.

The addition of Histidine$_6$ in the C-terminal of α-agglutinin enabled us to purify wild type α-agglutinin in large quantity in a short period of time (Figure 29). For example, His-α-agglutinin, 0.5 mg, can be purified from 100ml culture supernatants (Figure 30A). In addition, the addition of His-tag to the C-terminal of α-agglutinin did not affect the binding activity of the protein (Figure 30B). Moreover, we can purify mutated α-agglutinins having same molecular weight as wild type (Figure 30A).

Figure 28. Diagram of Construction of pYEpPGK AGα1.6His and Its Mutants with Point Mutation in AGα1. (A). The shuttle vector pYEpPGK contains the pBR 322 AmpR, OriE (an E.coli replication origin), a yeast *URA*3 gene, yeast 2-μm replication origin and yeast phosphoglycerate kinase promoter and terminator. (B). DNA fragments encoded α-agglutinin$^{20\text{-}351}$ and mutated α-agglutinin$^{20\text{-}351}$ with point mutations in domain III were used as templates for a polymerase chain reaction (PCR). Two primers containing *Hind* III sites outside the open reading frame were used. The 3' end primer contained sequences of 6 Histine, a stop codon. (C). PCR products of AGα1 and AGα1 with point mutations were electrophoresed on 0.8 % agarose gel and detected by Et-Br (D). *Aat* II was used to check of insertion of DNA fragment. AGα1$^{351.6His}$ and its mutants were sequenced completely to confirm that there were no additional mutations present.

A

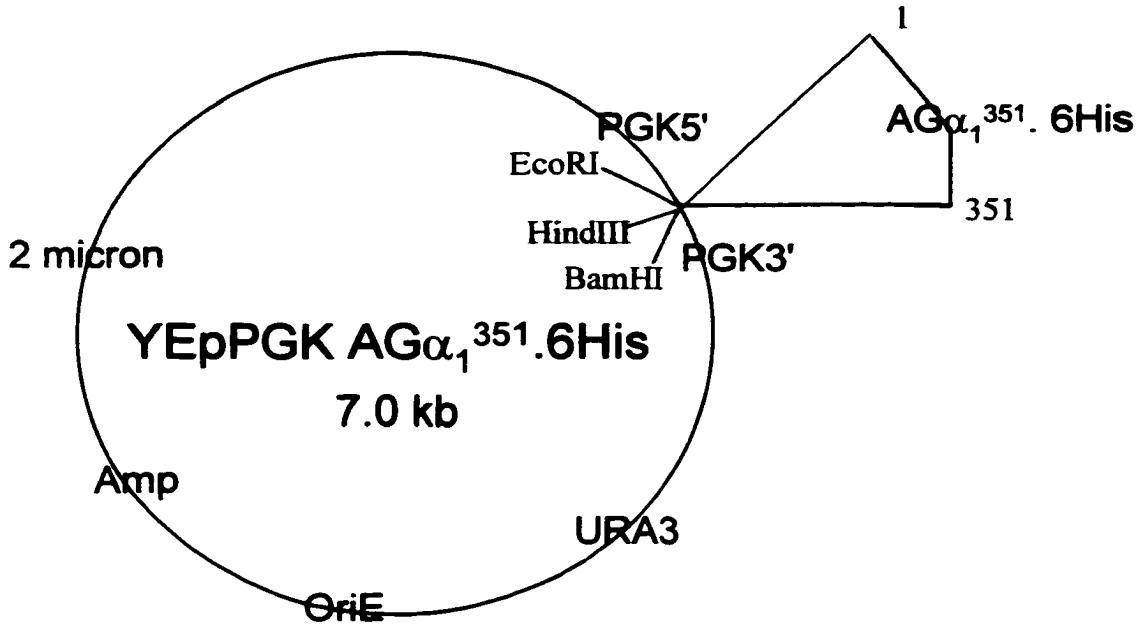

pYEpPGK AGα1 351.6His

B

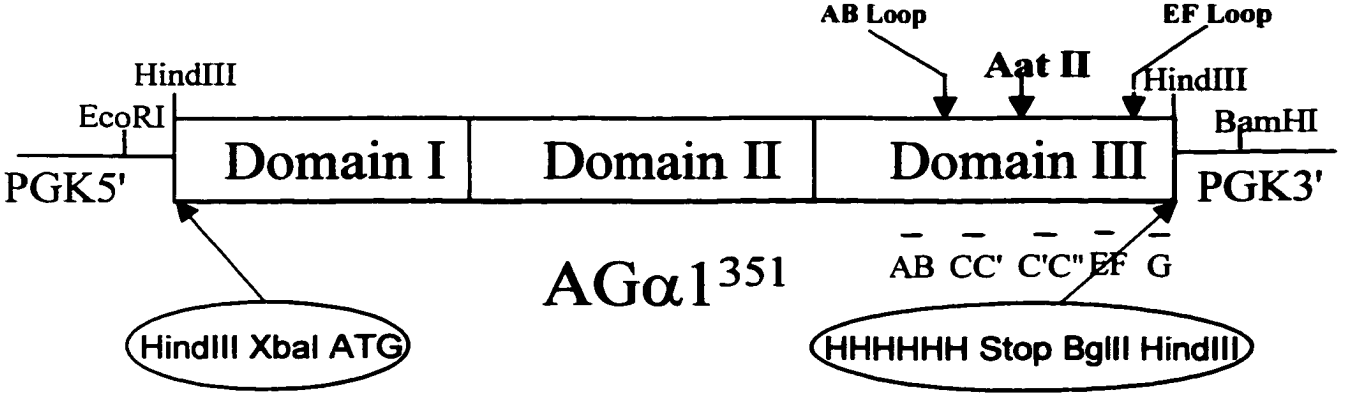

C

Lanes 1 and 16: 1 kb DNA standard

Lanes 2 to 15: PCR product of different His-tagged mutated AGα1^{351}

D

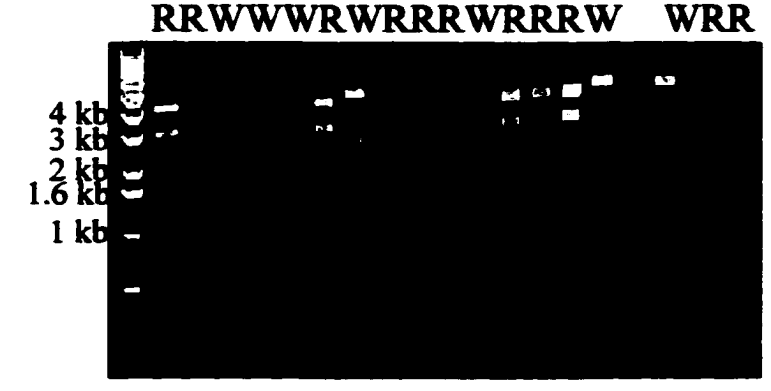

Lane 1: 1 kb DNA standard

Lane 2 to 20: mutated pYEpPGK AGα1^{351}.6His digested with AatII

R: insertion of DNA fragment with correct orientation

W: insertion of DNA fragment with wrong orientation

Figure 29. Purification Procedure of His-tagged α-Agglutinin and Its Mutants. Lα21 transformants containing pPGK-AGα1$^{351.6His}$ and pPGK-AGα1$^{351.6His}$ with point mutations were grown to log phase. After deglycosylation, the samples were purified using a nickel column, which selectively binds to hexa-histidine in the proteins.

Purification of His-Tagged α-Agglutinins

1). Sample Preparation

Grow transformed α cells to OD=0.6

⇩

Remove cell pellets by centrifugation

⇩

Treat cell supernatants with Endo H for 3 hours

⇩

Dialyze cell supernatant against PBS, pH7.4

2). Purification Procedure

Pack a nickel column

⇩

Equilibrate the nickel column with PBS, pH7.4 containing 10mM imidazole

⇩

Apply the sample

⇩

Wash the column with PBS, pH7.4

⇩

Elute His-tagged wild and mutant α-agglutinin with PBS, pH 7.4 containing 500mM imidazole

⇩

Collect the eluates in 1ml fraction

⇩

Dialyze the eluates against 30mM sodium acetate, pH 5.5

⇙ ⇘

Activity Assay SDS-PAGE

Figure 30. SDS-PAGE of His-tagged α-Agglutinin and His-Tagged Mutated α-Agglutinin (His 292 Leu). (A). His-tagged α-agglutinin and His-tagged mutated α-agglutinin (His 292 Leu) purified using procedure above in Figure 29 were electrophoresed on 10% SDS-PAGE gel and visualized by staining with Coomassie blue. Lane 1: Molecular weight standard; Lane 2: non-His-tagged wild type α-agglutinin purified using procedure as described in chapter III; Lane 3-4: fraction 1 and 2 of His-tagged wild type α-agglutinin purified using a nickel column; Lane 5-6: fraction 1 and 2 of His-tagged mutated α-agglutinin (His 292 Leu) purified using a nickel column. (B). The specific activity of His-tagged α-agglutinin was evaluated.

A

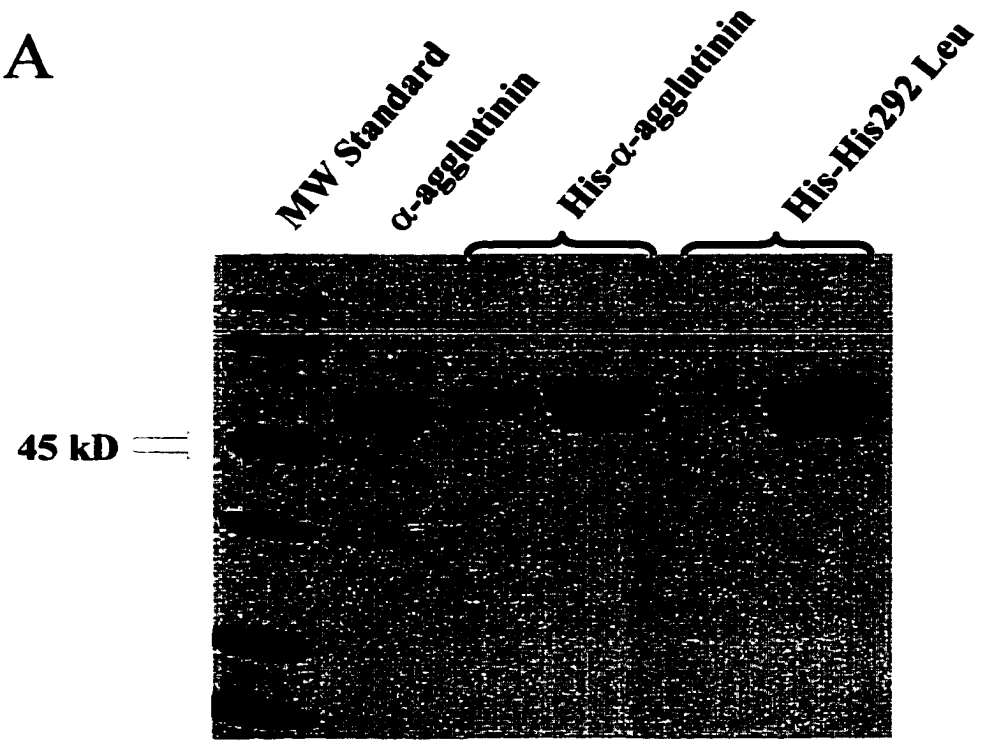

B

Comparison of Specific Activity

	Specific Activity
α-Agglutinin	$4.16*10^4$ -- $6.25 * 10^4$
His-Tagged α-Agglutinin	$4.72 * 10^4$

Effect of mutation on the structure and function of α-agglutinin: Culture supernatant, 5 liter, of mutated α-agglutinin (His292 Leu) were concentrated to 125 ml through a Millipore filtration apparatus with a membrane having 30 kDa molecular weight cutoff. We were able to purify about 1 mg of mutated α-agglutinin. The yield was about 25 fold lower than that of the wild type. Purified mutated α-agglutinin (His 292 Leu) with apparent molecular weight of 45 kD did not substantially change the CD of the protein. Also, purified mutated α-agglutinin (His 292 Leu) was fully active in an agglutination assay. Similar to his-α-agglutinin, mutated α-agglutinin can bind to a-agglutinin by competing with ^{125}I-α-agglutinin (Figure 31).

Since the addition of Histidine$_6$ in the C-terminal of mutated a-agglutinin (His 292 Leu) may compromise the loss of Histidine being mutated to Leucine, A second mutant strain (Phe 296 Ser) was then introduced to our study. His-α-agglutinin with point mutation Phe 296 Ser was purified using the procedure shown in Figure 29. As for mutated His-α-agglutinin (His 292 Leu), His-α-agglutinin with point mutation (Phe 296 Ser) not only had a similar CD spectrum to that of wild type, but was also active in binding to a-agglutinin by competing with ^{125}I-α-agglutinin (Figure 32).

By summary, two point mutations in α-agglutinin reduced the secretion of the protein in general and the ratio of α-agglutinin in the total proteins, corresponding to the reduction of agglutination ability of mutant strains in the cellular level. Also after mutation, the protein became more sensitive to proteolytic digestion, which resulted in formation of 30 kD and 40 kD fragments. The purified mutated α-agglutinin with apparent molecular weight of 45 kD, the same as that of wild type α-agglutinin, had similar functional properties as that of wild type.

Figure 31. Comparison of His-α-agglutinin (His 292 Leu) and His-α-agglutinin (wild type) by Binding Competition with ^{125}I-α-agglutinin. Increasing amounts of unlabeled His-α-agglutinin (His 292 Leu) or unlabeled His-α-agglutinin (wild type) were incubated with 1 µl of ^{125}I-α-agglutinin and 2 X 10^6 **a** cells at 25°C for 90 minutes. The Cells were then washed and counted by gamma counter. Error bars represent the range for triplicate samples. —●—, His-α-agglutinin (wild type), —▲—, His-α-agglutinin (His 292 Leu).

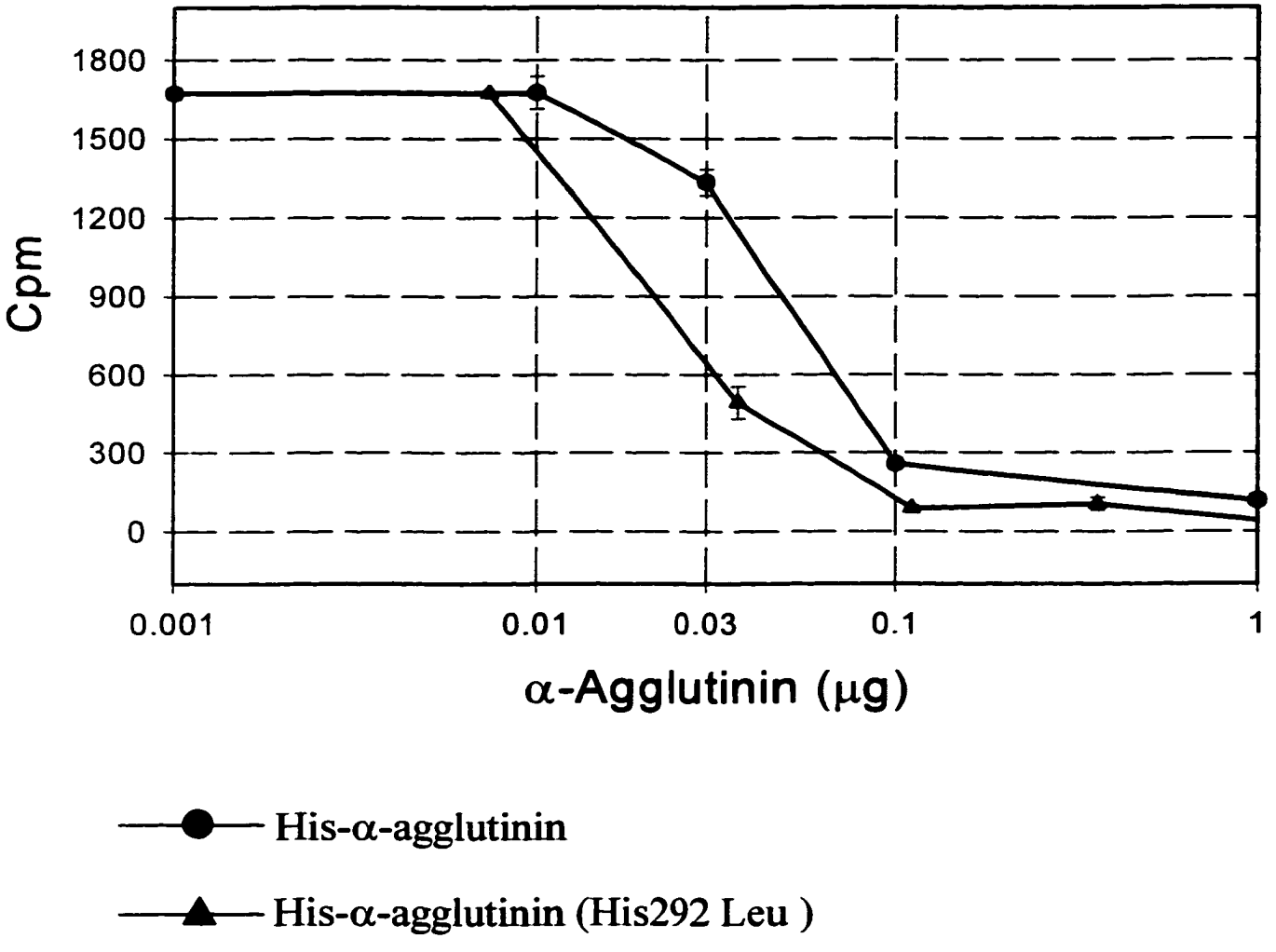

Figure 32. Comparison of His-α-agglutinin (Phe 296 Ser) and His-α-agglutinin (wild type) by Binding Competition with ^{125}I-α-Agglutinin. Increasing amounts of unlabeled His-α-agglutinin (Phe 296 Ser) or unlabeled His-α-agglutinin (wild type) with were incubated with 1 μl of ^{125}I-α-agglutinin and 2 X 10^6 **a** cells at 25°C for 90 minutes. The Cells were then washed and counted by gamma counter. Error bars represent the range for triplicate samples. —●—, His-α-agglutinin (wild type), —▲—, His-α-agglutinin (Phe 296 Ser).

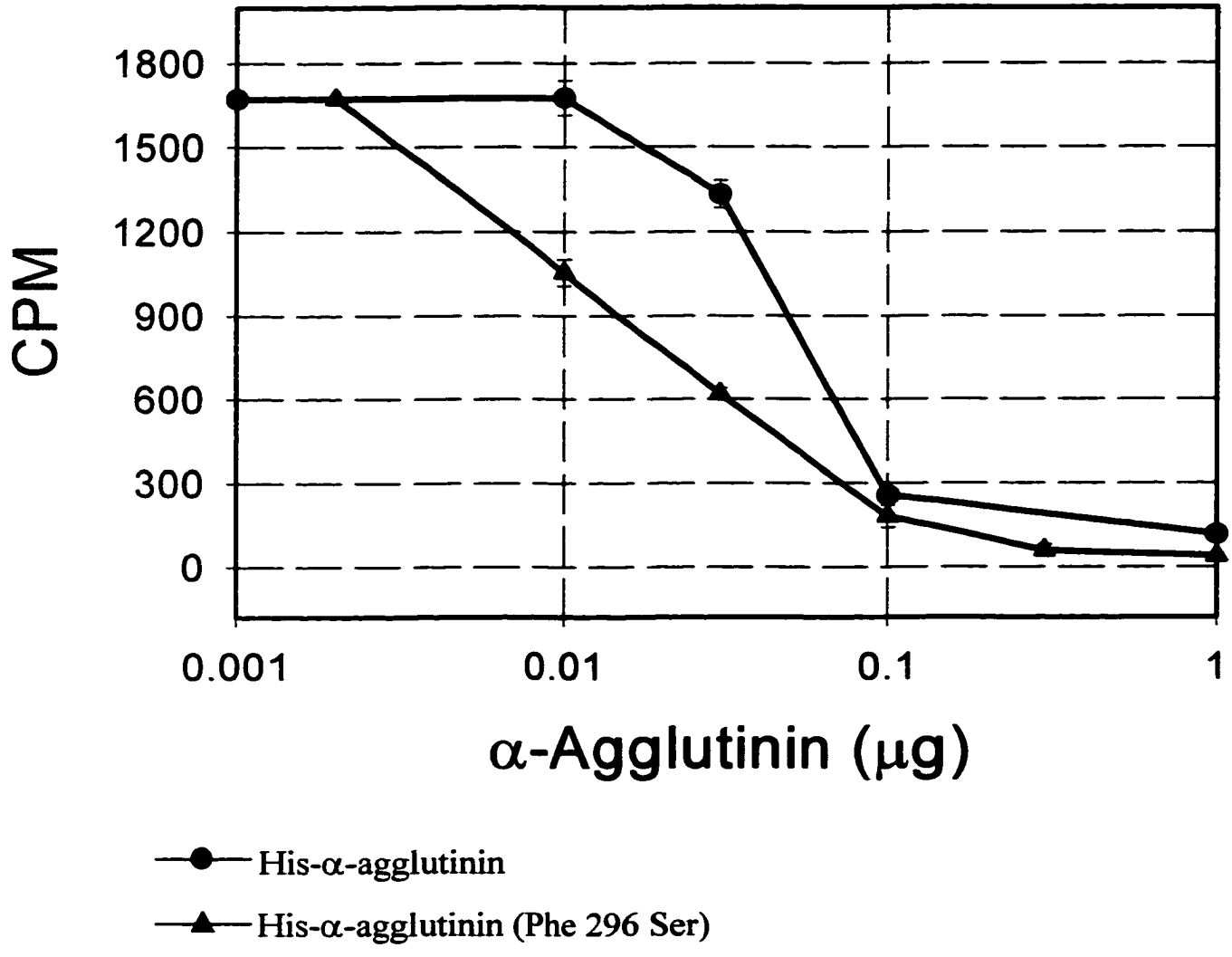

Discussion

Mutations in α-agglutinin reduced secretion of α-agglutinin and other proteins: de Nobel et al identified a putative binding site located in domain III of α-agglutinin by testing the agglutinability of the cell culture supernatants of mutant cells as well as intact mutant cells (de Nobel et al., 1996). Mutations of His 292 residue to leucine or arginine reduce binding activity more than 100 fold. Mutations in some residues located in close proximity to His 292, such as Y216, D217, L294, F296 reduced agglutinability about 10-100 fold. However, mutations in some residues located in distant regions such as: C-C' and C'-C" had no effect on the binding activity (Table IV) (de Nobel et al., 1996).

Our purpose is to examine how mutations affect the structure and function of the purified mutated α-agglutinins and to confirm and refine our structural model of domain III of α-agglutinin. The first mutant strain we start with was His 292 Leu, which is the core of the putative binding site (de Nobel et al., 1996). Purification of mutated α-agglutinin (His 292 Leu) was more difficult than that of wild type. Contradictory to de Nobel's results, we discovered that mutation of α-agglutinin (His 292 Leu) not only reduced the level of α-agglutinin secreted but also the level of the total amount proteins secreted (Figure 25 and 26). After addition of His-tag to the C-terminal of mutated α-agglutinin, mutated α-agglutinins were purified. Mutated α-agglutinins had the same structural and functional properties as that of wild type protein (Figure 31 and 32). Our data suggested that mutations in α-agglutinin did not change the structure or function of the protein. Instead, it reduced the secretion of the protein which might be correlated to

the reduction of the binding ability of culture supernatants of mutant cells or intact mutated cells de Nobel et al. had tested.

Degradation of α-agglutinin in the ER: Being a secretory protein, α-agglutinin is synthesized as an amino-terminally extended precursor which enters the endoplasmic reticulum (ER) and undergoes various modifications including proteolytic cleavages, formation of disulfide bonds, O-and N-glycosylation before it forms the mature protein (Lipke and Kurjan 1992).

The ER is the entrance of secretory proteins into the central vacuolar system. The ER is also the place where the secretory proteins acquire their mature tertiary and quaternary structures (Kopito 1997). Binding of molecular chaperones helps the nascent proteins to fold properly. However, misfolded proteins will remain associated with molecular chaperones and will be degraded in the ER by proteolytic digestion (Klausner and Sitia 1990; Hammond and Helenius 1995). Since α-agglutinin is also secreted via secretory pathway, the reduction of secretion of α-agglutinin by mutation (Figure 25-27) may also follow the above mechanism. After mutation, α-agglutinin was unable to obtain mature tertiary and quaternary structure in the ER and would be retarded in the ER and degraded. Therefore, the level of mutated α-agglutinin secreted would be reduced significantly. In addition, the misfolded α-agglutinin may also perturb the folding of other secretory proteins, therefore, the secretion of the other proteins.

Reduction of the stability of α-agglutinin by mutation. Efficiently produced proteins that are folded correctly are normally biologically active. However, mis-folded proteins are generally much more susceptible to degradation and inactive (Johnston 1993).

Mutation of α-agglutinin (His 292 Leu) may also reduce efficiency of producing correctly folded protein. There were a lot more 30 kD, and 40 kD fragments other than 45 kD protein were collected from Gel-60 column (Figure 26). However, even though all three proteins can interact with anti-α-agglutinin, neither 30 kD nor 40 kD fragments was seen from the purification using the Con A column. From the Con A columns, only a small amount of mutated α-agglutinin with molecular weight of 45 kD similar to that of wild type protein was able to be obtained. We, therefore, speculate that both 30 kD and 40 kD fragments may be the inactive proteolytic digestion forms of mis-folded mutated α-agglutinin.

Effect of mutation on agglutination: Purified mutated α-agglutinins (His 292 Leu, Phe 296 Ser) with the same molecular weight as that of wild type had similar functional activity to each other and to that of wild type. Mutations of α-agglutinin led to misfolding and protein degradation in the ER. Our results indicated that the reduction of the secretion level of α-agglutinin by point mutation was from misfolding of the protein.

Chapter V

Discussion and Future Work

A simple yeast cell adhesion system, sexual agglutination, was used in this work to study the conformational and functional properties of the cell adhesion molecule, α-agglutinin. Conformational flexibility and proper folding of α-agglutinin determined its functional properties.

Conformational flexibility of α-agglutinin enabled the reversible switching of parts of the protein from β-sheet to α-helix at pH values and temperatures in which protein inactivation was reversible (Figures 8-10). We have identified nine segments of 4 to 14 residues in α-agglutinin which have a higher potential to form α-helices than β-strands based on the secondary structure predictions (Figure 12). All of these potential helical sequences are in the regions having β-loop-β conformations in 3-D model of α-agglutinin (Lipke et al., 1995; Grigorescu et al., in preparation). Peptides derived from two of these regions showed similar conformational switching as that of the intact protein at different pH (Figures 13; 14).

A large amount of β-sheet conformation remained when α-agglutinin switched from β-sheet to α-helical conformational. However, with disruption of the "core" β-sheet under more severe conditions, such as higher pH, temperatures or DTT treatment, conformational changes of the protein became irreversible and the protein became inactive. The energy difference of formation of β and α structure must be small to enable the reversible switching. Retention of the "core" β-sheet conformation is probably essential in nucleating the refolding of the protein.

Results from study of a single point mutation suggested that conformational flexibility of α-agglutinin determined the secretion level of the protein. Only 4 % of α-agglutinin was able to be secreted after a point mutation His 292 to Leu. This result

implied that a large majority of the protein was misfolded and became too flexible to be secreted, and therefore, was retained in the ER. The results was consistent with de Nobel's results that the agglutinability of cell supernatants secreted from the mutant strain was reduced significantly, comparing to that from wild type cells (de Nobel et al., 1996).

Conformational flexibility of α-agglutinin also enabled rearrangements of the agglutinins to form more structured conformations upon ligand binding or induced by cold temperature. A CD study showed that random structure decreased from 38.6% to 31.6% upon binding (Table II). Kinetic studies of showing fast k_{on} and high affinity interaction of the agglutinins implied that conformation of α-agglutinin became more structured. The basis of this statement is that unstructured regions are normally not tightly packed and have high mobility, which can accelerate dynamic searching of binding ligand and, therefore, have fast k_{on}. Unstructured to structured conformational transitions enable alternative packing of binding partners, which lead to high affinity interactions (Dunker et al., 1998). A CD study of α-agglutinin at cold temperature showed that the random structures dropped from 36.5% to 26.1% and total β sheet conformation increased from 47.8% to 54.4% (Table III). Correlating to these conformational changes, kon was significantly reduced, probably because the more structured conformation at cold temperature reduced the flexibility of the protein and therefore, resulted in a slow kon and low affinity interaction.

Interestingly, in yeast *Candida albicans*, cell adhesion molecules in *ALS* family have significant sequence similarity to α-agglutinin, especially in the three Ig domain regions of the proteins (Figure 4). *C. albicans* is pathogenic in adhering on mammalian

epithelial cells. Little is known about the structure and function of the adhesion molecules in ALS family. More interestingly, Chou-Fasman secondary structure prediction shows *ALS* proteins not only having three similar Ig domain regions, but also similar potential regions to form helical structures (Figure 33). Therefore, conformational studies of α-agglutinin in this work could be a good model for investigating the structure and function of ALS proteins from *C. albicans*.

Figure 33. Chou-Fasman Secondary Structure Prediction of AGα1^{350} and ALS1. β-Sheet (——) and helical (••••••) potential of three Ig domains of AGα1^{350} and N-terminal 326 amino acids of ALS were predicted by Chou-Fasman and compared.

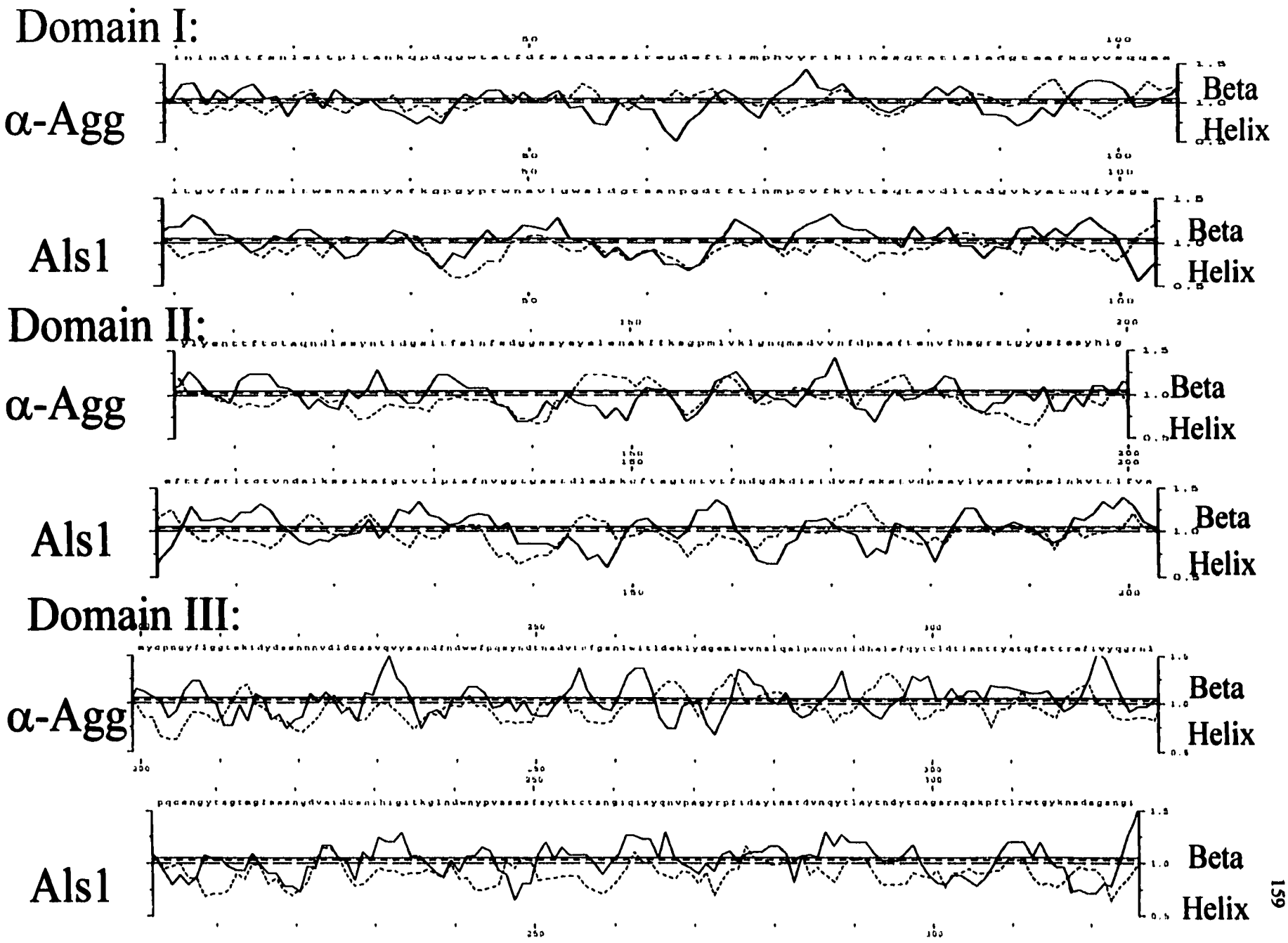

Appendix:

Table V: Summary of Dissociation Constants

	Temperature (°C)	K_D (M)
Isotopic Labeling	0	6.34×10^{-10}
	25	8.6×10^{-10}
SPR	10	$6.18 \pm 3.49 \times 10^{-4}$
		$9.76 \pm 0.68 \times 10^{-10}$
	20	$1.55 \pm 0.11 \times 10^{-9}$
SPR (after removal of aggregates)	20	$5.5 \pm 2.2 \times 10^{-9}$

Alam, S. M., Travers, P. J., Wung, J. L., Nasholds, W., and Redpath, S. 1996. T-cell-receptor affinity and thymocyte positive selection. *Nature* 381: 616-620.

Albelda, S. M., and Buck, C. A. 1990. Integrins and other cell adhesion molecules. *Faseb J* 4: 2868-2880.

Alon, R., Hammer, D. A., and Springer, T. A. 1995. Lifetime of the P-selectin-carbohydrate bond and its response to tensile force in hydrodynamic flow. *Nature* 374: 539-542.

Al-Shamkhani, A., Mallett, S., Brown, M. H., James, W., and Barclay, A. N. 1997. Affinity and kinetics of the interaction between soluble trimeric OX40 ligand, a member of the tumor necrosis factor superfamily, and its receptor OX40 on activated T cells. *J Biol Chem* 272: 5275-5282.

Altschuh, D., Dubs, M. C., Weiss, E., Zeder-Lutz, G., and Van Regenmortel, M. H. 1992. Determination of kinetic constants for the interaction between a monoclonal antibody and peptides using surface plasmon resonance. *Biochemistry* 31: 6298-6304.

Amzel, L. M., and Poljak, R. J. 1979. Three-dimensional structure of immunoglobulins. *Annu Rev Biochem* 48: 961-997.

Anderson, C. M., Zucker, F. H., and Steitz, T. A. 1979. Space-filling models of kinase clefts and conformation changes. *Science* 204: 375-380.

Baldwin, E. P., Hajiseyedjavadi, O., Baase, W. A., and Matthews, B. W. 1993. The role of backbone flexibility in the accommodation of variants that repack the core of T4 lysozyme. *Science* 262: 1715-1718.

Baldwin, R. L. 1994. Protein folding. Matching speed and stability. *Nature* 369: 183-184.

Barbas, C. F. d., Languino, L. R., and Smith, J. W. 1993. High-affinity self-reactive human antibodies by design and selection: targeting the integrin ligand binding site. *Proc Natl Acad Sci U S A* 90: 10003-10007.

Bass, S. H., Mulkerrin, M. G., and Wells, J. A. 1991. A systematic mutational analysis of hormone-binding determinants in the human growth hormone receptor. *Proc Natl Acad Sci U S A* 88: 4498-4502.

Berson, S. A., Yalow, R. S., Bauman, A., Rothschild, M. A., and Newerly, K. 1956. *J Clin Invest* 35:170-190.

Berson, S. A., and Yalow, R. S. *Advan Biol Med Phys* 6:349-430.

Betts, M. J., and Sternberg, M. J. 1999. An analysis of conformational changes on protein-protein association: implications for predictive docking. *Protein Eng* 12: 271-283.

Birchmeier, C., and Birchmeier, W. 1993. Molecular aspects of mesenchymal-epithelial interactions. *Annu Rev Cell Biol* 9: 511-540.

Bork, P., Holm, L., and Sander, C. 1994. The immunoglobulin fold. Structural classification, sequence patterns and common core. *J Mol Biol* 242: 309-320.

Browne, J. P., Strom, M., Martin, S. R., and Bayley, P. M. 1997. The role of beta-sheet interactions in domain stability, folding, and target recognition reactions of calmodulin. *Biochemistry* 36: 9550-9561.

Bullough, P. A., Hughson, F. M., Skehel, J. J., and Wiley, D. C. 1994. Structure of influenza haemagglutinin at the pH of membrane fusion. *Nature* 371: 37-43.

Burgen, A. S., Roberts, G. C., and Feeney, J. 1975. Binding of flexible ligands to macromolecules. *Nature* 253: 753-755.

Cabanas, C., and Hogg, N. 1993. Ligand intercellular adhesion molecule 1 has a necessary role in activation of integrin lymphocyte function-associated molecule 1. *Proc Natl Acad Sci U S A* 90: 5838-5842.

Caflisch, A., and Karplus, M. 1994. Molecular dynamics simulation of protein denaturation: solvation of the hydrophobic cores and secondary structure of barnase. *Proc Natl Acad Sci U S A* 91: 1746-1750.

Calderone, R. A., and Braun, P. C. 1991. Adherence and receptor relationships of *Candida albicans*. *Microbiol Rev* 55: 1-20.

Cappellaro, C., Baldermann, C., Rachel, R., and Tanner, W. 1994. Mating type-specific cell-cell recognition of *Saccharomyces cerevisiae*: cell wall attachment and active sites of a- and alpha-agglutinin. *Embo J* 13: 4737-4744.

Cappellaro, C., Hauser, K., Mrsa, V., Watzele, M., and Watzele, G. 1991. *Saccharomyces cerevisiae* a- and alpha-agglutinin: characterization of their molecular interaction. *Embo J* 10: 4081-4088.

Carr, C. M., and Kim, P. S. 1993. A spring-loaded mechanism for the conformational change of influenza hemagglutinin. *Cell* 73: 823-832.

Chaffin, W. L., Lopez-Ribot, J. L., Casanova, M., Gozalbo, D., and Martinez, J. P. 1998. Cell wall and secreted proteins of *Candida albicans*: identification, function, and expression. *Microbiol Mol Biol Rev* 62: 130-180.

Chan, D. C., Fass, D., Berger, J. M., and Kim, P. S. 1997. Core structure of gp41 from the HIV envelope glycoprotein. *Cell* 89: 263-273.

Chant, J., and Pringle, J. R. 1995. Patterns of bud-site selection in the yeast *Saccharomyces cerevisiae*. *J Cell Biol* 129: 751-765.

Chen, M. H., Shen, Z. M., Bobin, S., Kahn, P. C., and Lipke, P. N. 1995. Structure of *Saccharomyces cerevisiae* alpha-agglutinin. Evidence for a yeast cell wall protein with multiple immunoglobulin-like domains with atypical disulfides. *J Biol Chem* 270: 26168-26177.

Chou, P. Y., and Fasman, G. D. 1974. Conformational parameters for amino acids in helical, beta-sheet, and random coil regions calculated from proteins. *Biochemistry* 13: 211-222.

Clayton, L. K., Sieh, M., Pious, D. A., and Reinherz, E. L. 1989. Identification of human CD4 residues affecting class II MHC versus HIV- 1 gp120 binding. *Nature* 339: 548-551.

Colman, P. M., Laver, W. G., Varghese, J. N., Baker, A. T., and Tulloch, P. A. 1987. Three-dimensional structure of a complex of antibody with influenza virus neuraminidase. *Nature* 326: 358-363.

Corbin, V., Michelson, A. M., Abmayr, S. M., Neel, V., and Alcamo, E. 1991. A role for the Drosophila neurogenic genes in mesoderm differentiation. *Cell* 67: 311-323.

Creighton, T. E. 1993. *Proteins: structure and molecular properties.* W H Freeman, New York

Corr, M., Slanetz, A. E., Boyd, L. F., Jelonek, M. T., and Khilko, S. 1994. T cell receptor-MHC class I peptide interactions: affinity, kinetics, and specificity. *Science* 265: 946-949.

Cross, F., Hartwell, L. H., Jackson, C., and Konopka, J. B. 1988. Conjugation in *Saccharomyces cerevisiae*. *Annu Rev Cell Biol* 4: 429-457.

Dalal, S., Balasubramanian, S., and Regan, L. 1997. Transmuting alpha helices and beta sheets. *Fold Des* 2: 71-79.

Daughdrill, G. W., Chadsey, M. S., Karlinsey, J. E., Hughes, K. T., and Dahlquist, F. W. 1997. The C-terminal half of the anti-sigma factor, FlgM, becomes structured when bound to its target, sigma 28. *Nat Struct Biol* 4: 285-291.

de Nobel, H., Lipke, P. N., and Kurjan, J. 1996. Identification of a ligand-binding site in an immunoglobulin fold domain of the *Saccharomyces cerevisiae* adhesion protein alpha-agglutinin. *Mol Biol Cell* 7: 143-153.

de Nobel, H., Pike, J., Lipke, P. N., and Kurjan, J. 1995. Genetics of a-agglutunin function in *Saccharomyces cerevisiae*. *Mol Gen Genet* 247: 409-415.

Drubin, D. G., and Nelson, W. J. 1996. Origins of cell polarity. *Cell* 84: 335-44.

Du, X. P., Plow, E. F., Frelinger, A. L. d., TE, O. T., Loftus, J. C., and Ginsberg, M. H. 1991. Ligands "activate" integrin alpha IIb beta 3 (platelet GPIIb-IIIa). *Cell* 65: 409-416.

Dunker, A. K., Garner, E., Guilliot, S., Romero, P., and Albrecht, K. 1998. Protein disorder and the evolution of molecular recognition: theory, predictions and observations. *Pac Symp Biocomput*: 473-484.

Dustin, M. L., and Springer, T. A. 1989. T-cell receptor cross-linking transiently stimulates adhesiveness through LFA-1. *Nature* 341: 619-624.

Eisenberg, D., Weiss, R. M., and Terwilliger, T. C. 1984. The hydrophobic moment detects periodicity in protein hydrophobicity. *Proc Natl Acad Sci U S A* 81: 140-144.

Ekblom, P., and Timpl, R. 1996. Cell-to-cell contact and extracellular matrix. A multifaceted approach emerging. *Curr Opin Cell Biol* 8: 599-601.

Feher, V. A., and Cavanagh, J. 1999. Millisecond-timescale motions contribute to the function of the bacterial response regulator protein Spo0F. *Nature* 400: 289-293.

Fleury, S., Lamarre, D., Meloche, S., Ryu, S. E., and Cantin, C. 1991. Mutational analysis of the interaction between CD4 and class II MHC: class II antigens contact CD4 on a surface opposite the gp120-binding site. *Cell* 66: 1037-1049.

Frankel, A. D., and Kim, P. S. 1991. Modular structure of transcription factors: implications for gene regulation. *Cell* 65: 717-719.

Frelinger, A. L. d., Cohen, I., Plow, E. F., Smith, M. A., and Roberts, J. 1990. Selective inhibition of integrin function by antibodies specific for ligand-occupied receptor conformers. *J Biol Chem* 265: 6346-6352.

Friguet, B., Djavadi-Ohaniance, L., and Goldberg, M. E. 1989. Polypeptide-antibody binding mechanism: conformational adaptation investigated by equilibrium and kinetic analysis. *Res Immunol* 140: 355-376.

Fu, Y., Rieg, G., Fonzi, W. A., Belanger, P. H., Edwards, J. E., Jr., and Filler, S. G. 1998. Expression of the *Candida albicans* gene ALS1 in *Saccharomyces cerevisiae* induces adherence to endothelial and epithelial cells. *Infect Immun* 66: 1783-1786.

Garnier, J., Osguthorpe, D. J., and Robson, B. 1978. Analysis of the accuracy and implications of simple methods for predicting the secondary structure of globular proteins. *J Mol Biol* 120: 97-120.

Gaur, N. K., and Klotz, S. A. 1997. Expression, cloning, and characterization of a *Candida albicans* gene, ALA1, that confers adherence properties upon *Saccharomyces cerevisiae* for extracellular matrix proteins. *Infect Immun* 65: 5289-5294.

Gill, S. C., and von Hippel, P. H. 1989. Calculation of protein extinction coefficients from amino acid sequence data. *Anal Biochem* 182: 319-326.

Ginsberg, M. H., Du, X., and Plow, E. F. 1992. Inside-out integrin signalling. *Curr Opin Cell Biol* 4: 766-771.

Glaser, R. W., and Hausdorf, G. 1996. Binding kinetics of an antibody against HIV p24 core protein measured with real-time biomolecular interaction analysis suggest a slow conformational change in antigen p24. *J Immunol Methods* 189: 1-14.

Greenfield, N. J. 1996. Methods to estimate the conformation of proteins and polypeptides from circular dichroism data. *Anal Biochem* 235:1-10.

Grigorescu, A., Kakn, P. C., and Lipke, P. N. *Submitted for Publication.*

Guadagno, T. M., Ohtsubo, M., Roberts, J. M., and Assoian, R. K. 1993. A link between cyclin A expression and adhesion-dependent cell cycle progression. *Science* 262: 1572-1575.

Gumbiner, B. M. 1996. Cell adhesion: the molecular basis of tissue architecture and morphogenesis. *Cell* 84: 345-357.

Hamada, D., Kuroda, Y., Tanaka, T., and Goto, Y. 1995. High helical propensity of the peptide fragments derived from beta- lactoglobulin, a predominantly beta-sheet protein. *J Mol Biol* 254: 737-746.

Hammond, C., and Helenius, A. 1995. Quality control in the secretory pathway. *Curr Opin Cell Biol* 7: 523-529.

Hartwell, L. H., and Smith, D. 1985. Altered fidelity of mitotic chromosome transmission in cell cycle mutants of *S. cerevisiae*. *Genetics* 110: 381-395.

Hauser, K., and Tanner, W. 1989. Purification of the inducible alpha-agglutinin of *S. cerevisiae* and molecular cloning of the gene. *FEBS Lett* 255: 290-294.

Henry, A. J., Cook, J. P., McDonnell, J. M., Mackay, G. A., and Shi, J. 1997. Participation of the N-terminal region of Cepsilon3 in the binding of human IgE to its high-affinity receptor FcepsilonRI. *Biochemistry* 36: 15568-15578.

Herskowitz, I. 1988. Life cycle of the budding yeast *Saccharomyces cerevisiae. Microbiol Rev* 52: 536-553.

Herskowitz, I., and Herskowitz, I. 1989. A regulatory hierarchy for cell specialization in yeast Life cycle of the budding yeast *Saccharomyces cerevisiae. Nature* 342: 749-757.

Hoepelman, A. I., and Tuomanen, E. I. 1992. Consequences of microbial attachment: directing host cell functions with adhesions. *Infect Immun* 60: 1729-1733.

Holness, C. L., Bates, P. A., Little, A. J., Buckley, C. D., and McDowall, A. 1995. Analysis of the binding site on intercellular adhesion molecule 3 for the leukocyte integrin lymphocyte function-associated antigen 1. *J Biol Chem* 270: 877-884.

Hoyer, L. L., Payne, T. L., Bell, M., Myers, A. M., and Scherer, S. 1998. *Candida albicans* ALS3 and insights into the nature of the ALS gene family. *Curr Genet* 33: 451-459.

Hoyer, L. L., Scherer, S., Shatzman, A. R., and Livi, G. P. 1995. *Candida albicans* ALS1: domains related to a *Saccharomyces cerevisiae* sexual agglutinin separated by a repeating motif. *Mol Microbiol* 15: 39-54.

Huber, A. H., Wang, Y. M., Bieber, A. J., and Bjorkman, P. J. 1994. Crystal structure of tandem type III fibronectin domains from Drosophila neuroglian at 2.0 A. *Neuron* 12: 717-731.

Huber, W., Hurst, J., Schlatter, D., Barner, R., and Hubscher, J. 1995. Determination of kinetic constants for the interaction between the platelet glycoprotein IIb-IIIa and fibrinogen by means of surface plasmon resonance. *Eur J Biochem* 227: 647-656.

Humphries, M. J. 1996. Integrin activation: the link between ligand binding and signal transduction. *Curr Opin Cell Biol* 8: 632-640.

Ikemizu, S., Sparks, L. M., van der Merwe, P. A., Harlos, K., and Stuart, D. I. 1999. Crystal structure of the CD2-binding domain of CD58 (lymphocyte function-associated antigen 3) at 1.8-A resolution. *Proc Natl Acad Sci U S A* 96: 4289-4294.

Jackson, G. S., Hill, A. F., Joseph, C., Hosszu, L., and Power, A. 1999. Multiple folding pathways for heterologously expressed human prion protein. *Biochim Biophys Acta* 1431: 1-13.

Jansson, M., Hallen, D., Koho, H., Andersson, G., and Berghard, L. 1997. Characterization of ligand binding of a soluble human insulin-like growth factor I receptor variant suggests a ligand-induced conformational change. *J Biol Chem* 272: 8189-8197.

Jansson, M., Uhlen, M., Nilsson, B., Jansson, M., and Hallen, D. 1997. Structural changes in insulin-like growth factor (IGF) I mutant proteins affecting binding kinetic rates to IGF binding protein 1 and IGF-I receptor. *Biochemistry* 36: 4108-4117.

Jennings, P. A., Saalau-Bethell, S. M., Finn, B. E., Chen, X. W., and Matthews, C. R. 1991. Mutational analysis of protein folding mechanisms. *Methods Enzymol* 202: 113-126.

Johnsson, B., Lofas, S., and Lindquist, G. 1991. Immobilization of proteins to a carboxymethyldextran-modified gold surface for biospecific interaction analysis in surface plasmon resonance sensors. *Anal Biochem* 198: 268-277.

Johnston, J. R. *Molecular Genetics of Yeast.* 1993. Oxford University Press, New York

Jones, E. Y. 1996. Three-dimensional structure of cell adhesion molecules. *Curr Opin Cell Biol* 8: 602-608.

Jonsson, U., Fagerstam, L., Ivarsson, B., Johnsson, B., and Karlsson, R. 1991. Real-time biospecific interaction analysis using surface plasmon resonance and a sensor chip technology. *Biotechniques* 11: 620-627.

Juliano, R. L., and Haskill, S. 1993. Signal transduction from the extracellular matrix. *J Cell Biol* 120: 577-585.

Kahn, P. C. 1979. The interpretation of near-ultraviolet circular dichroism. *Methods Enzymol* 61: 339-378.

Kapteyn, J. C., Montijn, R. C., Vink, E., de la Cruz, J., and Llobell, A. 1996. Retention of *Saccharomyces cerevisiae* cell wall proteins through a phosphodiester-linked beta-1,3-/beta-1,6-glucan heteropolymer. *Glycobiology* 6: 337-345.

Karlsson, R., Karlsson, R., Michaelsson, A., and Mattsson, L. 1994. Real-time competitive kinetic analysis of interactions between low- molecular-weight ligands in solution and surface-immobilized receptors. *Anal Biochem* 221: 142-151.

Karlsson, R., Michaelsson, A., and Mattsson, L. 1991. Kinetic analysis of monoclonal antibody-antigen interactions with a new biosensor based analytical system. *J Immunol Methods* 145: 229-240.

Kieffer, N., Fitzgerald, L. A., Wolf, D., Cheresh, D. A., and Phillips, D. R. 1991. Adhesive properties of the beta 3 integrins: comparison of GP IIb-IIIa and the vitronectin receptor individually expressed in human melanoma cells. *J Cell Biol* 113: 451-461.

Kishore, U., Leigh, L. E. A., Eggleton, P., Strong, P., and Perdikoulis, M. V. 1998. Functional characterization of a recombinant form of the C-terminal, globular head region of the B-chain of human serum complement protein, C1q. *Biochem J* 333: 27-32.

Klausner, R. D., and Sitia, R. 1990. Protein degradation in the endoplasmic reticulum. *Cell* 62: 611-614.

Konno, T., Kataoka, M., Kamatari, Y., Kanaori, K., Nosaka, A., and Akasaka, K. 1995. Solution X-ray scattering analysis of cold- heat-, and urea-denatured states in a protein, Streptomyces subtilisin inhibitor. *J Mol Biol* 251: 95-103.

Kopito, R. R. 1997. ER quality control: the cytoplasmic connection. *Cell* 88: 427-30.

Koshland, D. E., Jr., and Neet, K. E. 1968. The catalytic and regulatory properties of enzymes. *Annu Rev Biochem* 37: 359-410.

Krammer, A., Lu, H., Isralewitz, B., Schulten, K., and Vogel, V. 1999. Forced unfolding of the fibronectin type III module reveals a tensile molecular recognition switch. *Proc Natl Acad Sci U S A* 96: 1351-1356.

Kron, S. J., Styles, C. A., and Fink, G. R. 1994. Symmetric cell division in pseudohyphae of the yeast *Saccharomyces cerevisiae*. *Mol Biol Cell* 5: 1003-1022.

Kuwajima, K., Yamaya, H., and Sugai, S. 1996. The burst-phase intermediate in the refolding of beta-lactoglobulin studied by stopped-flow circular dichroism and absorption spectroscopy. *J Mol Biol* 264: 806-822.

Kwong, P. D., Wyatt, R., Robinson, J., Sweet, R. W., Sodroski, J., and Hendrickson, W. A. 1998. Structure of an HIV gp120 envelope glycoprotein in complex with the CD4 receptor and a neutralizing human antibody. *Nature* 393: 648-659.

Larsen, T. A., Olson, A. J., and Goodsell, D. S. 1998. Morphology of protein-protein interfaces. *Structure* 6: 421-427.

Lau, S. Y., Taneja, A. K., and Hodges, R. S. 1984. Synthesis of a model protein of defined secondary and quaternary structure. Effect of chain length on the stabilization and formation of two-stranded alpha-helical coiled-coils. *J Biol Chem* 259: 13253-13261.

Leung, L. L., Li, W. X., McGregor, J. L., Albrecht, G., and Howard, R. J. 1992. CD36 peptides enhance or inhibit CD36-thrombospondin binding. A two- step process of ligand-receptor interaction. *J Biol Chem* 267: 18244-18250.

Lipke, P. N. 1996. Cell adhesion proteins in the nonvertebrate eukaryotes. *Prog Mol Subcell Biol* 17: 119-157.

Lipke, P. N., Chen, M. H., de Nobel, H., Kurjan, J., and Kahn, P. C. 1995. Homology modeling of an immunoglobulin-like domain in the *Saccharomyces cerevisiae* adhesion protein alpha-agglutinin. *Protein Sci* 4: 2168-2178.

Lipke, P. N., and Kurjan, J. 1992. Sexual agglutination in budding yeasts: structure, function, and regulation of adhesion glycoproteins. *Microbiol Rev* 56: 180-194.

Lipke, P. N., Terrance, K., and Wu, Y. S. 1987. Interaction of alpha-agglutinin with *Saccharomyces cerevisiae* a cells. *J Bacteriol* 169: 483-488.

Lipke, P. N., Wojciechowicz, D., and Kurjan, J. 1989. AG alpha 1 is the structural gene for the *Saccharomyces cerevisiae* alpha-agglutinin, a cell surface glycoprotein involved in cell-cell interactions during mating. *Mol Cell Biol* 9: 3155-3165.

Lu, C. F., Kurjan, J., and Lipke, P. N. 1994. A pathway for cell wall anchorage of *Saccharomyces cerevisiae* alpha- agglutinin. *Mol Cell Biol* 14: 4825-4833.

Lu, C. F., Montijn, R. C., Brown, J. L., Klis, F., and Kurjan, J. 1995. Glycosyl phosphatidylinositol-dependent cross-linking of alpha- agglutinin and beta 1,6-glucan in the *Saccharomyces cerevisiae* cell wall. *J Cell Biol* 128: 333-340.

Lu, Z. X., Fok, K. F., Erickson, B. W., and Hugli, T. E. 1984. Conformational analysis of COOH-terminal segments of human C3a. Evidence of ordered conformation in an active 21-residue peptide. *J Biol Chem* 259: 7367-7370.

Mahadevan, D., Yu, J. C., Saldanha, J. W., Thanki, N., and McPhie, P. 1995. Structural role of extracellular domain I of alpha-platelet-derived growth factor (PDGF) receptor for PDGF-AA and PDGF-BB binding. *J Biol Chem* 270: 27595-27600.

Main, A. L., Harvey, T. S., Baron, M., Boyd, J., and Campbell, I. D. 1992. The three-dimensional structure of the tenth type III module of fibronectin: an insight into RGD-mediated interactions. *Cell* 71: 671-678.

Manning, M. C., and Woody, R. W. 1987. Theoretical determination of the CD of proteins containing closely packed antiparallel beta-sheets. *Biopolymers* 26: 1731-1752.

Martenson, R. E., Park, J. Y., and Stone, A. L. 1985. Low-ultraviolet circular dichroism spectroscopy of sequential peptides 1-63, 64-95, 96-128, and 129-168 derived from myelin basic protein of rabbit. *Biochemistry* 24: 7689-7695.

McKeithan, T. W. 1995. Kinetic proofreading in T-cell receptor signal transduction. *Proc Natl Acad Sci U S A* 92: 5042-5046.

Menendez, M., Gasset, M., Laynez, J., Lopez-Zumel, C., and Usobiaga, P. 1995. Analysis of the structural organization and thermal stability of two spermadhesins. Calorimetric, circular dichroic and Fourier-transform infrared spectroscopic studies. *Eur J Biochem* 234: 887-896.

Minor, D. L., Jr., and Kim, P. S. 1996. Context-dependent secondary structure formation of a designed protein sequence. *Nature* 380: 730-734.

Molinari, H., Ragona, L., Varani, L., Musco, G., and Consonni, R. 1996. Partially folded structure of monomeric bovine beta-lactoglobulin. *FEBS Lett* 381: 237-243.

Moscona, A. A. 1957. The development in vitro of chimeric aggregates of dissociated embryonic chick and mouse cells. *Proc Natl Acad Sci USA* 43: 184-194.

Murai, N., Taguchi, H., and Yoshida, M. 1995. Kinetic analysis of interactions between GroEL and reduced alpha- lactalbumin. Effect of GroES and nucleotides. *J Biol Chem* 270: 19957-19963.

Nagar, B., Overduin, M., Ikura, M., and Rini, J. M. 1996. Structural basis of calcium-induced E-cadherin rigidification and dimerization. *Nature* 380: 360-364.

Najbar, L. V., Craik, D. J., Wade, J. D., Salvatore, D., and McLeish, M. J. 1997. Conformational analysis of LYS(11-36), a peptide derived from the beta- sheet region of T4 lysozyme, in TFE and SDS. *Biochemistry* 36: 11525-11533.

Nakagawa, Y., and Yanagishima, N. 1982. Changes in production of the mating-type-specific glycoproteins, agglutination substances in association with mating type interconversion in homothallic strains of the yeast, *Saccharomyces cerevisiae*. *Mol Gen Genet* 185: 207-210.

Nose, A., Tsuji, K., and Takeichi, M. 1990. Localization of specificity determining sites in cadherin cell adhesion molecules. *Cell* 61: 147-155.

Olsen, D. B., and Eckstein, F. 1990. High-efficiency oligonucleotide-directed plasmid mutagenesis. *Proc Natl Acad Sci U S A* 87: 1451-1455.

Orlean, P., Arnold, E., and Tanner, W. 1985. Apparent inhibition of glycoprotein synthesis by *S. cerevisiae* mating pheromones. *FEBS Lett* 184: 313-317.

Paudel, H. K., and Li, W. 1999. Heparin-induced conformational change in microtubule-associated protein Tau as detected by chemical cross-linking and phosphopeptide mapping. *J Biol Chem* 274: 8029-8038.

Payne, G., Shoelson, S. E., Gish, G. D., Pawson, T., and Walsh, C. T. 1993. Kinetics of p56lck and p60src Src homology 2 domain binding to tyrosine- phosphorylated peptides determined by a competition assay or surface plasmon resonance. *Proc Natl Acad Sci U S A* 90: 4902-4906.

Phillips, D. R., Charo, I. F., and Scarborough, R. M. 1991. GPIIb-IIIa: the responsive integrin. *Cell* 65: 359-362.

Picker, L. J., and Butcher, E. C. 1992. Physiological and molecular mechanisms of lymphocyte homing. *Annu Rev Immunol* 10: 561-591.

Politou, A. S., Gautel, M., Pfuhl, M., Labeit, S., and Pastore, A. 1994. Immunoglobulin-type domains of titin: same fold, different stability? *Biochemistry* 33: 4730-4737.

Pringle, J. R., Bi, E., Harkins, H. A., Zahner, J. E., and De Virgilio, C. 1995. Establishment of cell polarity in yeast. *Cold Spring Harb Symp Quant Biol* 60: 729-744.

Privalov, P. L., and Potekhin, S. A. 1986. Scanning microcalorimetry in studying temperature-induced changes in proteins. *Methods Enzymol* 131: 4-51.

Privalov, P. L., and Tsalkova, T. N. 1979. Micro- and macro-stabilities of globular proteins. *Nature* 280: 693-696.

Prusiner, S. B. 1991. Molecular biology of prion diseases. *Science* 252: 1515-1522.

Ptitsyn, O. B., and Finkelstein, A. V., Falk, P. 1979. Principal folding pathway and topology of all-beta proteins. *FEBS Lett* 101: 1-5.

Qu, A., and Leahy, D. J. 1995. Crystal structure of the I-domain from the CD11a/CD18 (LFA-1, alpha L beta 2) integrin. *Proc Natl Acad Sci U S A* 92: 10277-10281.

Ramamurthy, P., Hocking, A. M., and McQuillan, D. J. 1996. Recombinant decorin glycoforms. Purification and structure. *J Biol Chem* 271: 19578-19584.

Recny, M. A., Neidhardt, E. A., Sayre, P. H., Ciardelli, T. L., and Reinherz, E. L. 1990. Structural and functional characterization of the CD2 immunoadhesion domain. Evidence for inclusion of CD2 in an alpha-beta protein folding class. *J Biol Chem* 265: 8542-8549.

Rini, J. M., Schulze-Gahmen, U., and Wilson, I. A. 1992. Structural evidence for induced fit as a mechanism for antibody-antigen recognition. *Science* 255: 959-965.

Roy, A., Lu, C. F., Marykwas, D. L., Lipke, P. N., and Kurjan, J. 1991. The AGA1 product is involved in cell surface attachment of the *Saccharomyces cerevisiae* cell adhesion glycoprotein a-agglutinin. *Mol Cell Biol* 11: 4196-4206.

Ruoslahti, E., and Pierschbacher, M. D. 1987. New perspectives in cell adhesion: RGD and integrins. *Science* 238: 491-497.

Ruoslahti, E., and Reed, J. C. 1994. Anchorage dependence, integrins, and apoptosis. *Cell* 77: 477-478.

Sayers, J. R., Krekel, C., and Eckstein, F. 1992. Rapid high-efficiency site-directed mutagenesis by the phosphorothioate approach. *Biotechniques* 13: 592-596.

Sechi, S., Roller, P. P., Willette-Brown, J., and Kinet, J. P. 1996. A conformational rearrangement upon binding of IgE to its high affinity receptor. *J Biol Chem* 271: 19256-19263.

Shapiro, L., Fannon, A. M., and Kwong, P. D., Thompson, A., Lehmann, M. S. 1995. Structural basis of cell-cell adhesion by cadherins. *Nature* 374: 327-337.

Shapiro, L., Kwong, P. D., Fannon, A. M., Colman, D. R., and Hendrickson, W. A. 1995. Considerations on the folding topology and evolutionary origin of cadherin domains. *Proc Natl Acad Sci U S A* 92: 6793-6797.

Shiraki, K., Nishikawa, K., and Goto, Y. 1995. Trifluoroethanol-induced stabilization of the alpha-helical structure of beta-lactoglobulin: implication for non-hierarchical protein folding. *J Mol Biol* 245: 180-194.

Sonnichsen, F. D., Van Eyk, J. E., Hodges, R. S., and Sykes, B. D. 1992. Effect of trifluoroethanol on protein secondary structure: an NMR and CD study using a synthetic actin peptide. *Biochemistry* 31: 8790-8798.

Spolar, R. S., and Record, M. T., Jr. 1994. Coupling of local folding to site-specific binding of proteins to DNA. *Science* 263: 777-784.

Sprague, G. F., Jr., Jensen, R., and Herskowitz, I. 1983. Control of yeast cell type by the mating type locus: positive regulation of the alpha-specific STE3 gene by the MAT alpha 1 product. *Cell* 32: 409-415.

Springer, T. A. 1990. Adhesion receptors of the immune system. *Nature* 346: 425-434.

Sreerama, N., and Woody, R. W. 1993. A self-consistent method for the analysis of protein secondary structure from circular dichroism. *Anal Biochem* 209: 32-44.

Sreerama, N., and Woody, R. W. 1994. Protein secondary structure from circular dichroism spectroscopy. Combining variable selection principle and cluster analysis with neural network, ridge regression and self-consistent methods. *J Mol Biol* 242: 497-507.

Stetler-Stevenson, W. G., Aznavoorian, S., Liotta, L. A., Birchmeier, C., and Birchmeier, W. 1993. Tumor cell interactions with the extracellular matrix during invasion and metastasis. *Annu Rev Cell Biol* 9: 541-573.

Takeichi, M. 1991. Cadherin cell adhesion receptors as a morphogenetic regulator. *Science* 251: 1451-1455.

Tan, S., and Richmond, T. J. 1998. Crystal structure of the yeast MATalpha2/MCM1/DNA ternary complex. *Nature* 391: 660-666.

Terrance, K., and Lipke, P. N. 1981. Sexual agglutination in *Saccharomyces cerevisiae*. *J Bacteriol* 148: 889-896.

Toniolo, C., Bonora, G. M., Marchiori, F., Borin, G., and Filippi, B. 1979. Protamines. II. Circular dichroism study of the three main components of clupeine. *Biochim Biophys Acta* 576: 429-439.

van Berkel, M. A., Caro, L. H., Montijn, R. C., and Klis, F. M. 1994. Glucosylation of chimeric proteins in the cell wall of *Saccharomyces cerevisiae*. *FEBS Lett* 349: 135-138.

van der Merwe, P. A., and Barclay, A. N. 1996. Analysis of cell-adhesion molecule interactions using surface plasmon resonance. *Curr Opin Immunol* 8: 257-261.

van't Wout, J., Burnette, W. N., Mar, V. L., Rozdzinski, E., Wright, S. D., and Tuomanen, E. I. 1992. Role of carbohydrate recognition domains of pertussis toxin in adherence of Bordetella pertussis to human macrophages. *Infect Immun* 60: 3303-3308.

Vaughn, D. E., and Bjorkman, P. J. 1996. The (Greek) key to structures of neural adhesion molecules. *Neuron* 16: 261-273.

Wang, J., Hodges, R. S., and Sykes, B. D. 1995. Effect of trifluoroethanol on the solution structure and flexibility of desmopressin: a two-dimensional NMR study. *Int J Pept Protein Res* 46: 547.

Wang, J. H., Smolyar, A., Tan, K., Liu, J. H., and Kim, M. 1999. Structure of a heterophilic adhesion complex between the human CD2 and CD58 (LFA-3) counterreceptors. *Cell* 97: 791-803.

Wassarman, P. M. 1999. Mammalian fertilization: molecular aspects of gamete adhesion, exocytosis, and fusion. *Cell* 96: 175-183.

Weinreb, P. H., Zhen, W., Poon, A. W., Conway, K. A., and Lansbury, P. T., Jr. 1996. NACP, a protein implicated in Alzheimer's disease and learning, is natively unfolded. *Biochemistry* 35: 13709-13715.

Weissenhorn, W., Dessen, A., Harrison, S. C., Skehel, J. J., and Wiley, D. C. 1997. Atomic structure of the ectodomain from HIV-1 gp41. *Nature* 387: 426-430.

Williams, A. F., and Barclay, A. N. 1988. The immunoglobulin superfamily--domains for cell surface recognition. *Annu Rev Immunol* 6: 381-405.

Williams, A. F., Davis, S. J., He, Q., and Barclay, A. N. 1989. Structural diversity in domains of the immunoglobulin superfamily. *Cold Spring Harb Symp Quant Biol* 54 Pt 2: 637-647.

Wilson, H. V. 1907. Coalescence and regeneration in sponges. *J Exp Zool* 5: 245-253.

Wojciechowicz, D., and Lipke, P. N. 1989. Alpha-agglutinin expression in *Saccharomyces cerevisiae*. *Biochem Biophys Res Commun* 161: 46-51.

Wojciechowicz, D. 1990. The immunological and molecular characterization of alpha-agglutinin from *Saccharomyces cerevisiae*. Ph. D. Thesis. City University of New York.

Wojciechowicz, D., Lu, C. F., Kurjan, J., and Lipke, P. N. 1993. Cell surface anchorage and ligand-binding domains of the *Saccharomyces cerevisiae* cell adhesion protein alpha-agglutinin, a member of the immunoglobulin superfamily. *Mol Cell Biol* 13: 2554-2563.

Woody, R. W. 1985. *Peptides* 7, 15-114.

Woody, R. W., and Dunker, A. K. 1996. *In Circular Dichroism and the Conformational Analysis of Biomolecules* (Fasman, G.D. ed) pp 109-157, Plenum Press, New York.

Worobec, E. A., Martin, N. L., McCubbin, W. D., Kay, C. M., and Brayer, G. D., Hancock, R. E. 1988. Large-scale purification and biochemical characterization of crystallization-grade porin protein P from Pseudomonas aeruginosa. *Biochim Biophys Acta* 939: 366-374.

Yamaguchi, M., Yoshida, K., and Yanagishima, N. 1982. Isolation and partial characterization of cytoplasmic alpha agglutination substance in the yeast *Saccharomyces cerevisiae*. *FEBS Lett* 139: 125-129.

Yamaguchi, M., Yoshida, K., and Yanagishima, N. 1984. *Mol Gen Genet* 194: 24-30.

Yang, H. Q., Ma, H., Takano, E., Hatanaka, M., and Maki, M. 1994. Analysis of calcium-dependent interaction between amino-terminal conserved region of calpastatin functional domain and calmodulin-like domain of mu-calpain large subunit. *J Biol Chem* 269: 18977-18984.

Yang, J. J., Artis, D. R., and Van Wart, H. E. 1994. Differential effect of halide anions on the hydrolysis of different dansyl substrates by thermolysin. *Biochemistry* 33: 6516-6523.

Yang, J. J., Pikeathly, M., and Radford, S. E. 1994. Far-UV circular dichroism reveals a conformational switch in a peptide fragment from the beta-sheet of hen lysozyme. *Biochemistry* 33: 7345-7353.

Yang, J. T., Wu, C. S., and Martinez, H. M. 1986. Calculation of protein conformation from circular dichroism. *Methods Enzymol* 130: 208-269.

Yurchenco, P. D., and Cheng, Y. S. 1993. Self-assembly and calcium-binding sites in laminin. A three-arm interaction model. *J Biol Chem* 268: 17286-17299.

Zhang, M., Tanaka, T., and Ikura, M. 1995. Calcium-induced conformational transition revealed by the solution structure of apo calmodulin. *Nat Struct Biol* 2:758-767.

Zhang, S., and Rich, A. 1997. Direct conversion of an oligopeptide from a beta-sheet to an alpha- helix: a model for amyloid formation. *Proc Natl Acad Sci U S A* 94: 23-28.